Iron-Enhanced Mitigation of Viruses in Drinking Water

Joseph Aiden Heffron
Marquette University

IRON-ENHANCED MITIGATION OF VIRUSES IN DRINKING WATER

by

Joseph Heffron

A Dissertation submitted to the Faculty of the Graduate School,
Marquette University,
in Partial Fulfillment of the Requirements for
the Degree of Doctor of Philosophy

Milwaukee, WI

May 2019

ABSTRACT
IRON-ENHANCED MITIGATION OF VIRUSES IN DRINKING WATER

Joseph Heffron

Marquette University, 2019

Waterborne viruses are ubiquitous in the environment and present a global threat to public health. Previous research has suggested that iron-based water treatment has promise as a low-cost, non-toxic means of virus mitigation. In particular, zero-valent and ferrous iron have shown evidence of inactivating bacteria and viruses. The purpose of this research was to elucidate the relationship between iron oxidation and virus inactivation and determine if iron-based inactivation can enhance two water treatment processes, electrocoagulation and electrooxidation, for virus mitigation.

This research first investigated bacteriophage inactivation due to ferrous oxidation in batch tests using ferrous chloride salt. Ferrous iron oxidation correlated to bacteriophage inactivation, indicating that viruses can be inactivated as well as physically removed by ferrous iron coagulation. Greater inactivation was associated with both a higher ferrous iron dose and a slower rate of iron oxidation.

Next, the importance of ferrous oxidation was determined for virus mitigation via iron electrocoagulation. Ferrous-based inactivation was an important fate of viruses in iron electrocoagulation. However, some bacteriophages showed far greater inactivation than human viruses. Physical removal was the dominant fate under most conditions for the three mammalian viruses tested, as well as bacteriophage ΦX174. This result casts doubt on the appropriateness of using common bacteriophages for research into iron-based water treatment technologies. However, most viruses did demonstrate some inactivation at low pH (pH 6).

Finally, an electrocoagulation-electrooxidation treatment train was investigated to capitalize on the strengths of iron electrocoagulation. At typical coagulation doses (<30 mg/L Fe), ferrous iron did not enhance electrooxidation with boron-doped diamond electrodes. Nevertheless, the electrocoagulation-electrooxidation treatment train was beneficial in model surface waters, though electrocoagulation alone achieved equal or better mitigation in model groundwaters. The electrocoagulation-electrooxidation system also outperformed conventional treatment (ferric salt coagulant and free chlorine disinfection) in model groundwaters.

ACKNOWLEDGEMENTS

Joseph Heffron

Firstly, I would like to thank my advisor, Dr. Brooke Mayer, for guiding me through the process of academic research. Throughout my time at Marquette, Dr. Mayer has smiled patiently though my abrupt reversals in research direction, frequent despair, and drafts so rough they did not merit the name “draft.” I also thank Dr. Patrick McNamara, who has been an invaluable mentor in pursuing an academic career and provided much-needed support and faith in trying times. Thanks go to Dr. Daniel Zitomer for taking time out of his many duties as Department Chair to be part of my dissertation committee. Many thanks are also due Dr. Than Huong Nguyen of the University of Illinois at Urbana-Champaign for graciously agreeing to be part of my committee at no small inconvenience.

I thank Brad McDermid for his innumerable diligent hours in the lab as well as his valuable observations and intellectual contributions. Thanks also go to fellow graduate researchers Emily Maher and Donald Ryan, with whom I have co-authored papers on electrocoagulation. I am also grateful to Stephen Hornbeck for his assistance in the laboratory, as well as fellow environmental microbiology labmates (in order of appearance) Vinny Martino, Dr. Kyana Young, Kyra Ochsner and William Lynn. The rest of Dr. Mayer’s lab group also helped me greatly over the years by providing feedback on papers and presentations. Thanks also go to Ms. Chen Li and A.O. Smith for introducing me to electrocoagulation and supplying the initial materials to begin research.

Financial support for this research came from diverse sources. Partial funding for objectives 1 and 2 were provided by the National Science Foundation, Grant # 1433003. Objective 3 was partially funded by a gift from the Lafferty Family Foundation. I also would like to thank the Richard W. Jobling Foundation for a research assistantship (2017-2018) and the Arthur J. Schmitt Foundation for a fellowship (2018-2019), as well as Tom Marek and Carrianne Hayslett for administering those awards.

Most importantly, I thank my family for their unwavering support. I truly could not have achieved this degree without the emotional, financial and alimentary assistance of my parents, John and Sue Heffron. Above all, I owe this achievement to my wonderful, beloved wife, Sierra Starner-Heffron, who not only put up with terrible hours and an often-preoccupied husband, but also consented to have a child with this farcical man.

TABLE OF CONTENTS

LIST OF TABLES

LIST OF FIGURES

1. EXECUTIVE SUMMARY

Waterborne viruses are persistent and ubiquitous human pathogens. Because waterborne viruses remain stable in the environment, consumption of fecal-contaminated drinking water is an important route of transmission.[1–4] Though waterborne viruses are susceptible to typical drinking water processes,[5,6] the majority of drinking water outbreaks in the United States (US) arise in groundwater sources which may lack disinfection and/or physical separation processes.[4] In the five most recent years of National Outbreak Reporting System (NORS) data (2013 – 2017), viruses accounted for 11 drinking water outbreaks in the US, affecting over 450 people. Over half of these outbreaks occurred in private/individual water systems.[7] However, waterborne viruses are likely responsible for many outbreaks that go unreported or are of unknown etiology.[4]

This research investigated the role of iron oxidation in water treatment to enhance virus mitigation. Iron electrocoagulation (EC), a technology using zero-valent iron to generate coagulant *in situ*, was evaluated as an application of iron-enhanced mitigation. The central hypothesis guiding this research was that ferrous iron oxidation enhances disinfection, and that ferrous-based inactivation can significantly impact the fate of viruses in electrochemical water treatment. Few studies[8–10] have raised the potential of iron-based disinfection. The mechanisms of virus removal by EC are likewise poorly understood. Virus inactivation using aluminum electrodes has been demonstrated in the presence of chloride ions; however, inactivation was due to evolution of free chlorine, and long contact times were required.[11] Virus inactivation has been hypothesized to occur in iron EC,[12] though a rigorous investigation of the importance of inactivation in iron EC is lacking. Oxidation of Fe^{II} to Fe^{III} can be promoted using a polishing treatment process such as electrooxidation (EO) in what is referred to here as “iron-enhanced oxidation.” EO also serves as a disinfection step, and previous studies of iron-catalyzed oxidation

suggest that the combination of ferrous ions and other oxidants could be synergistic. To the author's knowledge, iron-enhanced disinfection has not previously been tested for viruses, nor has the proposed sequential EC-EO treatment train.

Existing research of virus mitigation by EC or ferrous iron disinfection,[8,9,11–14] all focuses on a single bacteriophage surrogate (MS2). Though widely accepted as a surrogate virus for filtration processes, MS2 may be more susceptible to disinfection than other possible bacteriophage surrogates for human viruses of interest.[15] In addition, limited variation in water constituents has been tested for these technologies. This research evaluated iron-based mitigation not only for multiple bacteriophages, but also human viruses, and in a wide range of water matrices.

This research comprised three objectives:

1) Establish the relationship between ferrous iron and bacteriophage inactivation

The relationship between ferrous iron and bacteriophage inactivation was investigated using bacteriophages MS2 and P22 as model viruses. To determine this relationship, ferrous chloride was added to batch reactors under a variety of conditions to control the dose and oxidation conditions. The hypothesis for this objective was that bacteriophage inactivation would increase with both a greater dose of oxidized iron and a slower rate of ferrous iron decay. Therefore, both the extent and the rate of iron oxidation were altered to determine the impact on bacteriophage inactivation. Bacteriophage inactivation was then related to a model of ferrous oxidation kinetics. The results for this objective are presented in Chapter 3.

2) Determine the mechanisms of virus mitigation and suitability of bacteriophages as surrogates in drinking water treatment by iron electrocoagulation

Irreversible and reversible reduction in bacteriophage concentrations during EC

treatment were compared to determine the degree to which inactivation impacts virus mitigation in varying water matrices. The hypothesis for this objective was that, since EC depends on an iron oxidation reaction, ferrous-based inactivation would be a significant mechanism of virus mitigation. Four bacteriophages (fr, MS2, P22 and ΦX174) were compared to three viruses of interest (adenovirus 4, echovirus 12, and feline calicivirus) to identify appropriate surrogates for iron-based water treatment research. To determine the mechanisms of virus mitigation, EC was compared to chemical coagulation using $FeCl_3$ and $FeCl_2$, as well as sorption to flocs pre-formed by EC and inactivation via EO with inert titanium electrodes. The results for this objective are presented in Chapter 4.

3) Evaluate sequential electrocoagulation-electrooxidation for virus mitigation

The potential synergy between iron oxidation and conventional disinfection processes was investigated using a sequential EC – EO treatment system. The combination of iron coagulation and oxidation was hypothesized to be synergistic for two possible reasons: 1) coagulation removes oxidant scavengers (*e.g.,* natural organic matter) prior to oxidation, and/or 2) the addition of ferrous iron catalyzes oxidation reactions. Bacteriophages MS2 and ΦX174 were used for this objective, in addition to human echovirus 12 to evaluate the suitability of the bacteriophage surrogates. The results for this objective are presented in Chapter 5.

In addition to the brief introductions in Chapters 3 -5, an in-depth review of the literature relevant to virus mitigation via coagulation and iron oxidation is provided in Chapter 2.

1.1. References

1. Kocwa-Haluch R. Waterborne Enteroviruses as a Hazard for Human Health. *Polish J*

Environ Stud. 2001;10(6):485-487.

2. Abbaszadegan M, Lechevallier M, Gerba CP. Occurrence of Viruses in US Groundwaters. *J Am Water Works Assoc*. 2003;95(9):107-120.

3. Bosch A, Pintó RM, Abad FX. Survival and Transport of Enteric Viruses in the Environment. *Viruses in foods*. 2003;(Springer US):151-187. doi:10.1007/0-387-29251-9_6

4. Xagoraraki I, Yin Z, Svambayev Z. Fate of Viruses in Water Systems. *J Environ Eng*. 2014;140(7):040140201-18. doi:10.1061/(ASCE)EE.1943-7870.0000827

5. World Health Organization, ed. *WHO Guidelines for Drinking-Water Quality.* 4th ed. Geneva: World Health Organization; 2011. doi:10.1016/S1462-0758(00)00006-6

6. Centers for Disease Control and Prevention. Effect of chlorination on inactivating selected pathogens. http://www.cdc.gov/safewater/effectiveness-on-pathogens.html. Published 2012. Accessed January 1, 2015.

7. Centers for Disease Control and Prevention. National Outbreak Reporting System. https://wwwn.cdc.gov/norsdashboard/. Published 2018.

8. Kim JY, Lee C, Sedlak DL, Yoon J, Nelson KL. Inactivation of MS2 coliphage by Fenton's reagent. *Water Res*. 2010;44(8):2647-2653. doi:10.1016/j.watres.2010.01.025

9. Kim JY, Lee C, Love DC, Sedlak DL, Yoon J, Nelson KL. Inactivation of MS2 coliphage by ferrous ion and zero-valent iron nanoparticles. *Environ Sci Technol*. 2011;45(16):6978-6984. doi:10.1021/es201345y

10. Delaire C, Van Genuchten CM, Nelson KL, Amrose SE, Gadgil AJ. Escherichia coli attenuation by Fe electrocoagulation in synthetic Bengal groundwater: effect of pH and natural organic matter. *Environ Sci Technol*. 2015;49(16):9945-9953. doi:10.1021/acs.est.5b01696

11. Tanneru CT, Jothikumar N, Hill VR, Chellam S. Relative insignificance of virus inactivation during aluminum electrocoagulation of saline waters. *Environ Sci Technol*. 2014;48(24):14590-14598. doi:10.1021/es504381f

12. Tanneru CT, Chellam S. Mechanisms of virus control during iron electrocoagulation--microfiltration of surface water. *Water Res*. 2012;46(7):2111-2120. doi:10.1016/j.watres.2012.01.032

13. Zhu B, Clifford DA, Chellam S. Comparison of electrocoagulation and chemical coagulation pretreatment for enhanced virus removal using microfiltration membranes. *Water Res*. 2005;39(13):3098-3108. doi:10.1016/j.watres.2005.05.020

14. Tanneru CT, Chellam S. Sweep flocculation and adsorption of viruses on aluminum flocs during electrochemical treatment prior to surface water microfiltration. *Environ Sci Technol*. 2013;47:4612-4618.

15. Heffron J, Mayer BK. Virus mitigation by coagulation: recent discoveries and future directions. *Environ Sci Water Res Technol*. 2016;2(3):443-459. doi:10.1039/C6EW00060F

2. LITERATURE REVIEW: VIRUS MITIGATION BY COAGULATION

This work was previously published in part as:

Heffron, J.; Mayer, B. K. Virus Mitigation by Coagulation: Recent Discoveries and Future Directions. Environ. Sci. Water Res. Technol. 2016, 2 (3), 443–459.

2.1. Introduction

Waterborne viruses account for an estimated 30 to 40% of infectious diarrhea in the U.S.[1] Associated with both acute gastric and respiratory diseases and chronic conditions,[2] some viruses can persist several months in the environment[3] and travel up to 100 m in groundwater.[4] Several families/genera of waterborne viruses are included on the U.S. Environmental Protection Agency's (EPA) Contaminant Candidate List (both CCL 3 and draft CCL 4) for drinking water, indicating the need for further research into occurrence and treatment.[5] Likewise, the World Health Organization's (WHO) *Guidelines for Drinking Water Quality*[6] cites eight virus categories that are of concern for drinking water, all of which have high persistence and infectivity relative to other pathogens. Although many viruses are only moderately tolerant of conventional water treatment,[6,7] adenoviruses show high resistance to emerging treatment technologies such as UV disinfection.[8] Coagulation can be used to reduce virus loads and minimize the required dose for disinfection. Coagulation is also an effective pre-treatment for virus removal by filtration systems.[9–15]

This review assesses current research of virus reduction by coagulation. Future avenues for research are discussed in light of evidence of the forces influencing virus sorption, as well as recent findings of virus inactivation in coagulation processes. Three coagulation processes are considered: conventional chemical coagulation, enhanced coagulation and electrocoagulation. In conventional chemical coagulation, metal hydrolytes are formed by dissolution of a metal salt

in water. Aluminum and iron salts such as $Al_2(SO_4)_3$ and $FeCl_3$ are commonly used in water treatment,[16] although novel coagulants like polyaluminum chlorides (PACls) have gained particular attention for virus mitigation.[9,10,17–22] Polymeric iron coagulants have also been developed,[23,24] but these coagulants have not been evaluated for virus mitigation.

The EPA's Disinfectants and Disinfection Byproduct Rule (DBPR) promotes enhanced coagulation prior to disinfection of drinking water to prevent the formation of potentially carcinogenic disinfection byproducts.[25] Enhanced coagulation uses high doses of chemical coagulant and/or pH adjustment for effective removal of humic acids, fulvic acids and other dissolved and suspended organic material (collectively called natural organic matter, NOM). For this reason, enhanced coagulation has been evaluated for virus mitigation in waters with high NOM concentrations.[12,26,27]

Electrocoagulation is the *in situ* production of coagulant by electro-oxidation of a sacrificial electrode. Both iron and aluminum sacrificial electrodes have been tested for virus mitigation.[14,28–30] Some researchers consider aluminum electrodes preferable to iron electrodes, because iron is released as soluble ferrous ions and may not be fully oxidized to form insoluble coagulant.[28,29,31] While the coagulant hydrolytes formed by iron electrocoagulation have been characterized,[32,33] less is known about the species formed during aluminum coagulation.

In all variations of coagulation, metal cations are introduced in water to form hydrolyte species. These hydrolytes destabilize colloids by overcoming the repulsive forces between colloidal particles. Colloidal destabilization commonly occurs by 1) neutralizing surface charges or forming bridges between particles to allow incorporation into a developing floc (charge neutralization or inter-particle bridging mechanism) or 2) by sorption of the colloid to a pre-formed floc (sweep flocculation mechanism). The resulting flocs may then be separated by gravity and/or filtration. Colloids are thus physically removed from the water matrix.

Waterborne viruses are typically less than 100 nm in diameter,[4] making them among the smallest colloids removable by coagulation. Physical removal is usually considered the primary mechanism for virus mitigation due to coagulation, although recent research shows that coagulation can also render viruses noninfectious (inactivation mechanism).

This review examines recent studies of virus mitigation by coagulation processes in the context of the latest scientific advances in understanding virus sorption and inactivation. To begin, the forces influencing virus sorption and subsequent physical removal are described, including the role of electrostatic forces, the hydrophobic effect, steric hindrance, hydrodynamics, and cation bridging. Consideration is given to discussion of environmental matrix effects, e.g., the influence of organic matter and divalent cations. Next, the phenomenon of virus inactivation during coagulation processes is addressed, including approaches and challenges to quantifying virus inactivation exclusive of physical removal. Critical analysis of recent discoveries and findings is used to inform recommendations for new research directions for mitigating waterborne viruses by coagulation, including appropriate selection and use of virus surrogates in laboratory and field studies.

2.2. Physical Removal of Virions

Physical removal is generally considered to be the dominant form of virus mitigation in coagulation processes. Therefore, many sources do not distinguish between physical removal and overall virus reduction. A summary of virus coagulation studies is provided in Table 2-1 and Table 2-2. Table 2-1 summarizes results of studies using a single virus for testing, while Table 2-2 summarizes studies testing multiple viruses in tandem to facilitate comparison of results among viruses. As shown in the tables, chemical coagulation has been shown to reduce viruses by 0.5 to 7 $\log_{10}$ (*i.e.,* 90% to 99.99999% reduction*)*, with a typical reduction of approximately 3 $\log_{10}$. In studies of chemical coagulation with post-treatment microfiltration, virus concentrations

Table 2-1. Summary of coagulation studies using a single virus type. Virus reductions are rounded to the nearest 0.5 log_{10}. Unless otherwise noted, reduction values are based on cultural assays, and pH values indicate conditions after coagulant addition. Reduction ranges indicate temporal variation (e.g., in filtration systems).

Coagulation Process	Coagulant	Dose (mg/L Al or Fe)	Bacteriophage	Log_{10} virus reduction	pH	NOM (mg/L DOC)	Source
CC	PACl $AlCl_3$ PACl $AlCl_3$	1	Qβ	4 3 4 1.5	7	0 2.2 (TOC)	22
CC + MF	PACl	1.1	Qβ	6 - 7	6.8	1.1 (TOC)	13
CC + MF	$FeCl_3$	10	MS2	4.5 3.5	6.3 8.3	0	34
CC + MF	PACl	0.5	Qβ	4 - 5	6.8	0.6	11
CC + MF	PACl alum	1.1 1.1	Qβ	7 7 6.5 0.5	6.8 7.8 6.8 7.8	0.9	9
CC + UF	PACl, alum	3	MS2	7	7 †	2.5 (TOC)	15
EnC + MF	PACl $FeCl_3$	4	MS2	7 3 - 4 3 - 4 3 - 4	5.5 † 6.5 † 5 † 6.5 †	4.2	12
ElC	Aluminum electrodes	30	MS2	3	6.2	0	28
ElC + MF	Iron electrodes	10	MS2	5 4.5	6.3 † 7.3 - 8.3 †	0	14
ElC + MF	Iron electrodes	13 11.5	MS2	6.5 1.5 4.5 1	6.4 † 7.5 †	0 4.9 0 4.9	30
ElC + MF	Aluminum electrodes	10	MS2	4	6.4 †	5.2	29

NOM = Natural organic matter, DOC = Dissolved organic carbon, TOC = Total organic carbon,
CC = Chemical coagulation, EnC = Enhanced coagulation, ElC = Electrocoagulation, MF = Microfiltration, UF = Ultrafiltration
DLS = Dynamic light scattering
† Initial pH value (before coagulant addition)

Table 2-2. Summary of comparative coagulation studies using multiple virus types. Virus reduction and inactivation data are rounded to the nearest 0.5 log_{10}. Reported inactivation below 1 log_{10} is shown as "< 1," while negligible inactivation is shown as "<< 1." Darker shading indicates comparatively greater reduction efficiencies for a given experiment. Unless otherwise noted, reduction values are based on cultural assays, and pH values indicate conditions after coagulant addition. Reduction and inactivation ranges indicate temporal variation (*e.g.*, in filtration systems).

Coagulant	Dose (mg Al/L or mg Fe/L)	Virus	Log_{10} virus reduction	Log_{10} virus inactivation/ aggregation	pH	NOM (mg/L DOC)	Source
Chemical Coagulation							
alum	1.1	Bacteriophage MS2	6	1	6.8	1	18
		Bacteriophage Qβ	4	2			
PACl		Bacteriophage MS2	6	2			
		Bacteriophage Qβ	7	5			
$FeCl_3$ + polymer	13.8	Adenovirus type 4	1.5	n.r.	8 †	n.r.	35
		Bacteriophage fr	2				
		Bacteriophage MS2	2				
		Bacteriophage PRD1	1				
		Bacteriophage ΦX174	0.5				
		Feline calicivirus	1.5				
PACl	1.1	Bacteriophage MS2	3	< 1	6.8	0.9	20
		Bacteriophage Qβ	6	4			
PACl	1.1	Bacteriophage f1	1.5	n.r.	6.8	0.9	36
		Bacteriophage f2	2.5				
PACl	1	Bacteriophage MS2	4.5	3.5	4.5 †	0.7	19
		Bacteriophage Qβ	n.r.	3.5			
		Bacteriophage ΦX174	n.r.	<< 1			
PACl	1.9	Bacteriophage MS2	6	3	7 †	0.8	37
	2.2	Bacteriophage Qβ	5.5	2.5		1.3	
alum			2	<< 1			
alum	3.2	Bacteriophage MS2	2 *	1	5.5 - 6.0	n.r.	38
		Norwalk Virus	1.5 *	n.r.			
		Poliovirus1	1.5 *	< 1			
$AlCl_3$	2.7	Coxsackievirus B5	1	n.r.	7 †	2.2	39
		Poliovirus 1	1.5				
PACl		Coxsackievirus B5	3				
		Poliovirus 1	3				

(continued next page)

(Table 2-2 continued)

Chemical Coagulation + Microfiltration							
PACl	1.1	Bacteriophage MS2	5.5	< 1	6.8	0.9	21
		Bacteriophage Qβ	5.5	2.5			
PACl	1.1	Bacteriophage MS2	8	2	6.8	0.76	10
		Bacteriophage Qβ	8	4			
alum	1.1	Bacteriophage MS2	3- 4 *	n.r.	6.8	0.76	40
		Bacteriophage Qβ	1 -2 *				
		Norovirus VLP	> 3 ‡				
PACl	1.1	Bacteriophage MS2	3 - 4 *				
		Bacteriophage Qβ	2 - 3 *				
		Norovirus VLP	> 3 ‡				
Enhanced Coagulation							
$FeCl_3$ + polymer	13.8	Adenovirus type 4	2.5	n.r.	5 - 6	4.6 - 5.6	27
		Feline calicivirus	2.5				
		Bacteriophage fr	2.5			1.8	
		Bacteriophage MS2	2.5				
		Bacteriophage PRD1	2				
		Bacteriophage ΦX174	1.5				
$FeCl_3$ + polymer	13.8	Bacteriophage fr	2	n.r.	5 - 6.5	4.2	26
		Bacteriophage MS2	0.5				
		Bacteriophage PRD1	0.5				
		Bacteriophage ΦX174	1.5				
		Coxsackievirus B6	3				
		Echovirus 12	2				
		Poliovirus Type 1	2.5				

n.r. = not reported for the given data set, NOM = Natural organic matter, DOC = Dissolved organic carbon, VLP = Virus-like particle

* Quantified by quantitative reverse transcription polymerase chain reaction (qRT-PCR)

† Initial pH value (before coagulant addition)

‡ Quantified by enzyme-linked immunosorbent assay (ELISA)

were reduced up to 8 log_{10}, with a typical reduction of 5 log_{10}. Enhanced coagulation has been shown to reduce virus concentrations by up to 4.5 log_{10} [27] and up to 7 log_{10} [12] with post-treatment microfiltration. However, enhanced coagulation has not been studied as thoroughly as conventional chemical coagulation and is used for more challenging water sources. Electrocoagulation with post-treatment microfiltration has shown promising results in mitigating bacteriophage MS2, surpassing the EPA's Surface Water Treatment Rule (SWTR) of 4 log_{10} reduction of viruses.[14,29,30,41]

The physical incorporation of viruses into flocs most likely happens in one of two ways: incorporation in the developing floc (charge neutralization or inter-particle bridging), and/or sorption to surfaces of formed flocs (sweep flocculation). Shirasaki et al.[39] found negligible (< 0.5 $\log_{10}$) reduction of poliovirus on preformed flocs, compared to approximately 3 $\log_{10}$ reduction during floc formation. In another study, Shirasaki et al.[20] found that the physical removal of two bacteriophages occurred during rapid mixing, with little or no additional removal during flocculation and after settling. Kreißel et al.[19] similarly found that significant virus mitigation occurred only during floc formation. In a study of virus removal by electrocoagulation, Tanneru et al.[29] concluded that sweep flocculation was the dominant mechanism of virus removal based on fluorescent microscopy and virus recovery from flocs. This discrepancy may be due to differences in floc formation between electrocoagulation and chemical coagulation. Chemical coagulation is limited by reaction kinetics and forms dense flocs, while electrocoagulation is limited by coagulant ion diffusion and forms sparse flocs.[42] During electrocoagulation, coagulant is continuously released, so treatment cannot be separated into rapid-mix coagulation and flocculation stages. Therefore, it is difficult to determine whether viruses are incorporated into growing flocs or sorbed to the floc surface.

In the absence of coagulant, viruses at high concentrations may also destabilize to form aggregates due to environmental conditions. Aggregate formation is important from both a theoretical and an experimental perspective. Due to larger size and lower surface charge, aggregates are easier to remove than monodispersed virions. In addition to being more susceptible to treatment processes, aggregates lead to artificially low results when quantifying viruses by cultural methods.[43] Unfortunately, aggregation is often a result of laboratory methods and does not necessarily represent natural conditions.

Numerous factors may influence physical removal of virions in flocs, as described in the following sections. These include the electrostatic and van der Waals forces modeled by the Derjaguin, Landau, Verwey and Overbeek (DLVO) theory, as well as non-DLVO factors such as the hydrophobic effect, structural incompatibility between viruses and sorbents (steric hindrance), and interactions with one another (aggregation) and constituents in the water matrix. The impact of these factors depends on the virus itself (e.g., its structure, surface charge, or degree of permeability), the nature of the sorbent (floc characteristics), and the composition of the water matrix. The influence of these phenomena on virus sorption has been studied more extensively for virus transport through porous media.[44–48] Still, many of the lessons learned apply to coagulation as well.

2.2.1.Electrostatic Interactions

Electrostatic forces affect the sorption of virions to surfaces like flocs. Investigators use multiple measures to describe electrostatic forces. Isoelectric point (pI) is the pH at which a particle or surface has a neutral charge in the electrolyte solution. At pH levels above the pI, the surface is negatively charged in solution; below the pI, the surface has a positive charge. Electrophoretic mobility is a measure of particle movement in the presence of an electric field and can be used to infer the electric potential near the particle surface. Electrostatic forces often govern virion sorption due to the long range of electrostatic influence, as well as the low pI of most enteric viruses, indicative of a strong, negative potential near the particle surface at neutral pH. However, electrostatic forces are attenuated at high ionic strength due to screening of the electric field.

2.2.1.1. The Impact of Virion Permeability on Isoelectric Point

Research is inconclusive as to whether virion electrostatic charge is solely defined by the capsid surface, or whether deeper capsid functional groups and/or the interior genome compartment also affect electrostatic interactions between the virion and its environment. Models that account for virion permeability have been advanced by Schaldach et al.[49] as well as Langlet et al.[50], the latter of which was based on Duval and Ohshima's model for "soft" (permeable) colloids.[51] Both models claim that with increasing virion permeability, the more acidic pI of the genome has greater impact on the overall pI.[49,50,52] To test this hypothesis, Langlet et al.[53] evaluated the removal of bacteriophages MS2 and Qβ on hydrophilic membranes. The two bacteriophages are similar in size and measured pI, but Qβ has a larger genome. MS2 was removed to a greater extent, and Langlet et al. concluded that Qβ's genome imparts the virion with a greater negative charge density, which repels the membrane. However, the difference in removal is not necessarily due to the difference in genome size. Qβ has been shown to be more hydrophobic than MS2[54] and would therefore be expected to exhibit less sorption to hydrophilic membranes.

Bacteriophage MS2 has been offered as an example of the effect of the viral genome on pI. The theoretical pI of MS2 based on total charged capsid moieties is approximately 7 – 9,[55,56] while the pI of MS2's RNA genome is approximately 3.[55] The measured pI of MS2 is generally accepted to be between 3 and 4, closer to the RNA pI than the capsid pI.[57] Using another method to calculate the capsid pI, Penrod et al.[44] accurately predicted MS2's measured pI by evaluating only those charged structures exposed on the surface of the capsid. However, Schaldach et al.[49] found better correlation with experimental electrophoretic mobility data when allowing for capsid permeability than using the Penrod method.

However, a study by Dika et al.[52] comparing MS2 bacteriophages and virus-like particles (VLPs) seems to support Penrod et al.'s model for predicting pI. VLPs are assembled by

expression of the viral coat proteins in a bacterial host but lack the viral genome. Instead of having a pI between 7 and 9 as predicted, MS2 VLPs had a measured pI between pH 3 and 4. Dika et al. hypothesize that negatively-charged host material was trapped within the VLPs during propagation. Considering the intricate, optimized packing of the viral genome into the capsid during normal bacteriophage propagation,[58,59] as well as evidence from electron micrographs,[52] VLPs likely do not contain enough host material in their interior to constitute a negative charge density comparable to whole virions. To accept the interpretation of viruses as soft colloids, we should see at least some increase in the pI of VLPs compared to bacteriophages to reflect the influence of the genome. The permeability model may also be more applicable to some virions than others.

2.2.1.2. The Impact of Virion Permeability on Electrostatic Interactions

Several recent investigations have found that accounting for permeability did not yield better predictions of virion sorption or aggregation. Gutiérrez et al.[60] determined that the modeled permeability of rotavirus was low enough that a hard colloid formalism would suffice. Yuan et al.[61] found that the energy barrier to MS2 adsorption was better predicted by the DLVO model for hard (impermeable) colloids than when permeability was considered. In a study by Nguyen et al.,[62] MS2 bacteriophages whose RNA genomes had been degraded at high pH did not significantly differ from intact MS2 bacteriophages in terms of aggregation or adsorption to the water surface at the air-water interface. Nguyen et al. concluded that internal RNA had minimal effect on sorption. Dika et al.[63] responded with a study showing that the virus purification method used by Nguyen et al. (polyethylene glycol precipitation) masks differences between viruses and VLPs.

Researchers have also investigated the impact of the genome on virus-virus sorption phenomena responsible for aggregation. Dika et al.[63] found that MS2 aggregates formed at pH 4

did not re-disperse when the solution was then acidified to pH 2. Other experiments of MS2 aggregation using pH titration confirm this trend.[43,52] By contrast, MS2 VLPs aggregated only near the pI value and dispersed at lower pH. The team hypothesized that the difference in aggregation reversibility was due to the attractive influence of the genome. However, VLPs did not aggregate at any pH at high ionic strength, whereas entire virions did. At high ionic strength, the effective distance of electrostatic forces decreases, so VLPs and entire virions should behave more similarly if permeability impacts surface charge. In this study, the MS2 and MS2 VLPs behaved more similarly at low ionic strength. It is also unclear why the relative absence of RNA in VLPs would explain aggregation in this study, while the presence of residual RNA in VLPs was used to explain the VLP pI measured in Dika et al.'s previous study.[52]

Other tests found similar patterns of irreversible aggregation for somatic bacteriophages PRD1 and ΦX174 and F-specific bacteriophages Qβ and GA.[54,64,65] Bacteriophages PRD1, Qβ, and GA all have measured pI values between 2 and 4 reported in the literature,[57] so aggregation in this pH range is not unusual. From an evolutionary standpoint, enteric viruses and bacteriophages may gain a selective advantage by aggregating to avoid inactivation by proteases in the stomach (pH < 4 [66]), and dispersing in the near-neutral pH of the intestines for the greatest chance of infection. Aggregation has been shown to inhibit virus inactivation by chemical disinfectants.[67]

However, aggregation below pH 4 is unexpected for ΦX174, which has a generally accepted pI of 6.6 from capillary isoelectric focusing, chromatofocusing, and aggregation studies.[57] If the pI of ΦX174 was indeed higher than pH 4, aggregation occurred solely in a pH range where virions should have a positive net charge. Chrysikopoulos and Syngouna[47] and Aronino et al.[64] recently reported lower pI values for ΦX174 (4.4 and 2.6, respectively) based on electrokinetic measurements. However, in an extensive review of virus pIs, Michen and Graule[57]

discounted Aronino et al.'s finding because Aronino et al. did not report purifying their bacteriophages for testing. Chrysikapoulos et al. also did not report purifying virus stocks.[47,68]

2.2.2.Non-electrostatic Sorption Phenomena

When electrostatic interactions are repulsive or neutral, van der Waals and non-DLVO phenomena like the hydrophobic effect, steric hindrance and interactions with constituents in the water matrix may lead to differences in virion sorption. As detailed below, van der Waals and non-DLVO forces tend to modify the effects of electrostatic forces, especially when electrostatic forces are minimized (*e.g.,* by electrostatic screening or near the pI of the particle).

Arising from electronic resonance between surfaces, van der Waals interactions create an attractive force proportional to the polarizability of the virion and the abiotic surface.[16] In practice, van der Waals forces cannot be measured independently of electrostatic and non-DLVO phenomena.[65] In an extensive study of interactions influencing bacteriophage adsorption to surfaces, Armanious et al.[69] found minimal impact of surface polarizability on bacteriophage adsorption. However, the two surfaces compared also differed in hydrophobicity.

The hydrophobic effect arises from hydrogen bonds that preferentially form between water molecules to the exclusion of nonpolar molecules. The hydrophobic effect results in the tendency of nonpolar substances to partition out of the aqueous phase. Armanious et al.[69] found that the hydrophobic effect moderated electrostatic repulsion to allow adsorption of bacteriophages fr, GA, MS2, and Qβ to nonpolar surfaces. Armanious et al. also established a method for quantifying hydrophobicity based on the size and number of nonpolar patches on the capsid surface, and predicted a pattern of decreasing hydrophobicity: Qβ >> fr > GA >> MS2. Armanious et al.'s method was able to explain broad trends in bacteriophage sorption to hydrophobic surfaces, although completely isolating the hydrophobic effect from other

phenomena is not possible. Other researchers[43,54] experimentally determined a relative hydrophobicity of GA > Qβ > MS2.

In two separate studies[54,65], Dika et al. found that surface hydrophobicity could explain differences in the sorption of bacteriophages. Using chemical force microscopy, the hydrophobicity of bacteriophages MS2, Qβ and GA were compared to known hydrophobic and hydrophilic surfaces.[54] Hydrophobicity influenced virus sorption to surfaces even in low ionic strength solution (1 mM $NaNO_3$), where electrostatic forces are expected to dominate.[54] Bacteriophages MS2, PRD1, and ΦX174 were also compared. Despite varying charge densities among the three bacteriophages in low ionic strength electrolyte, they demonstrated similar electrophoretic mobility at high ionic strength (100 mM).[65] Nevertheless, the bacteriophages differed in their affinities for membranes of varying hydrophobicity. Hydrophobicity has also been determined to favorably impact virus sorption to finely powdered activated carbon.[70]

The molecular-level structure of virus capsids and the sorbent surface may also hinder virion adsorption at close range. This steric hindrance occurs when interactions between the adsorbent and adsorbate are limited by the spatial orientation of their molecular structures. Several studies have found evidence of steric hindrance in virus sorption. Penrod et al.[44] found that steric interactions (here considering all non-electrostatic repulsion to be steric in nature) may lead to increased MS2 mobility in porous media when electrostatic forces are screened (*i.e.*, at high ionic strength). Armanious et al.[69] also suggested that the variable topography of bacteriophage fr and MS2 capsids, as determined by x-ray crystallography, may have resulted in poor adsorption to a gold surface in comparison to bacteriophages Qβ and GA. Dika et al.[54] found that bacteriophages preferentially sorbed to stainless steel over glass, despite similar surface hydrophobicity. This trend was more apparent at high ionic strength, which fits with the theory that surface roughness impacts electrostatic interactions when the roughness is on a

scale comparable to the Debye length (a measure of the effective range of electrostatic forces).[54] In all cases, steric hindrance appeared to moderate sorption in conditions of similar electrostatic charge and hydrophobicity, rather than broadly define sorption behavior.

2.2.3.Impact of Water Matrix Composition on Virus Sorption

Suspended and dissolved materials in the water matrix, like NOM and dissolved salts, can dramatically impact virion sorption. Because of the heterogeneous charge distribution and polarity of organic matter in the environment, the effect of NOM on virus sorption involves electrostatic forces, hydrophobicity, and steric interactions. Generally, NOM contains both polar and nonpolar moieties and has a negative charge at neutral and high pH due to deprotonation of carboxyl and phenyl groups.[45,69] In porous media filtration tests, Zhuang and Jin[45] found that MS2 breakthrough was more rapid in the presence of sorbed or dissolved organic material, while ΦX174 breakthrough was relatively unaffected. Zhuang and Jin concluded that NOM both competes for sorption sites on the media and enhances sorption of nonpolar virions by creating hydrophobic sorption sites. Armanious et al.[69] found high sorption of bacteriophages GA and Qβ at pH 6 on a NOM-coated surface, while MS2 and fr sorption was negligible. GA and Qβ sorption decreased significantly from pH 6 to pH 8, likely due to electrostatic repulsion arising from deprotonation of carboxyl groups on the NOM and capsid surfaces. When ionic strength was increased from 10 mM to 100 mM to screen electrostatic forces, Qβ sorption was high even at pH 8, while MS2 sorption was measurable, though low. These results again illustrate that the hydrophobic effect predominates only when electrostatic forces are weak. Yuan et al.[61] found that MS2 deposition on silica was greater than on NOM-coated surfaces, even at ionic strengths high enough to effectively screen electrostatic charges. The team concluded that the results may be due to steric hindrance, by which NOM surface structures prevent binding in contrast to the even surface of silica.

Deposition experiments have shown that cation bridging can significantly increase virion sorption to like-charged surfaces.[60,71,72] In cation bridging, divalent cations (*e.g.*, Ca^{2+} and Mg^{2+}) complex with negatively-charged moieties on both the capsid and the solid surface. The presence of Ca^{2+} and Mg^{2+} ions has been shown to dramatically increase sorption of viruses to repulsive surfaces in comparison to monovalent ions, beyond the expected increase due to screening of electrostatic forces.[60,72] By contrast, rotavirus adsorption to an oppositely-charged (non-repulsive) surface was shown to be independent of Ca^{2+} or Mg^{2+} concentrations.[60] The effect of cation bridging can be significant at Ca^{2+} and Mg^{2+} concentrations typical of drinking water sources.[60] For the bacterium *Pseudomonas aeruginosa*, cation bridging has been shown to significantly enhance sorption to repulsive surfaces at concentrations as low as 10^{-5} M Ca^{2+} or Mg^{2+}.[73] Interactions between MS2 virions have been shown to transition from repulsive to attractive between 10 mM Ca^{2+} and 50 mM Ca^{2+}.[71]

Ca^{2+} ions have been shown to have a greater positive influence on virus sorption to repulsive surfaces than Mg^{2+} ions.[60,72] Ca^{2+} ions are large and have weakly bound spheres of hydration that allow inner-sphere complexation with carboxyl groups on the virus capsid and the solid surface.[60,72] By contrast, Mg^{2+} ions have tightly-bound spheres of hydration that may allow only outer-sphere complexation. The mechanism for the relatively weak sorption observed in the presence of Mg^{2+} may not be bridging, but rather charge neutralization by complexation with negatively-charged moieties on either the virion or the surface.[72] The ability to form bonds with carboxyl groups makes cation bridging particularly important in the sorption of negatively charged viruses to NOM. In an experiment conducted by Pham et al.,[72] Ca^{2+} improved deposition of MS2 on a NOM-coated silica surface to a far greater extent than on a bare silica surface, although the bare silica was more negatively charged than the NOM-coated surface. For comparison, using NOM from the same source but in a monovalent electrolyte,

Yuan et al.[61] found poorer adsorption of MS2 on a NOM-coated surface than a silica surface. Mylon et al.[71] found that a lower concentration of Ca^{2+} was required to destabilize MS2 in the presence of NOM (10 mg/L total organic carbon; TOC).

2.2.4. Implications of Electrostatic and Non-Electrostatic Phenomena for Virus Aggregation

Electrostatic repulsion contributes to virion stability, so aggregation typically occurs at high ionic strength or pH ranges near the virion pI.[43] Non-DLVO forces may also impact virus aggregation. Some investigators have suggested that protein loops extending from the capsid surface may contribute to the high stability of virions by steric hindrance.[62,71] Virus aggregation has been shown to be higher in the presence of divalent cations, although not in the typical range of Ca^{2+} and Mg^{2+} concentrations in drinking water.[60,62,71] Hydrodynamic forces may also influence aggregation. Langlet et al.[43] suggest that the low electrophoretic mobility of virion aggregates may be due to hydrodynamic drag. Aggregates may show greater hydrodynamic drag due to permeability. Because of this drag, aggregates would tend to stay aggregated once formed.[43] From another perspective, the hydrodynamic drag of individual virions due to capsid permeability may counteract the repulsive electrostatic forces of surfaces and neighboring virions, leading to aggregation.

2.2.5. Implications of Electrostatic and Non-electrostatic Phenomena for Coagulation

While porous media studies provide valuable insights, not all lessons can be assumed to apply to virus coagulation. Unlike sorption to solid surfaces, coagulation may occur by sorption to solid flocs and/or complexation of the virion surface by dissolved coagulant (charge neutralization or inter-particle bridging). In addition, metal oxide flocs differ in structure, charge

and polarity from porous media. The challenge lies in determining which parameters are necessary and/or sufficient to describe virion sorption during coagulation/flocculation.

Hydrophobicity is unlikely to have a strong effect on coagulation in many cases, as aluminum and iron hydroxides are polar.[74] However, in the presence of NOM, hydrophobicity may be an important partitioning factor for some viruses. Tanneru et al.[29] found that aluminum flocs became more hydrophobic following sorption of NOM. Rebhun et al.[75] enhanced removal of hydrophobic (log K_{ow} > 4.5) polyaromatic compounds by adding dissolved humic acid. Therefore, NOM may actually enhance sorption of very hydrophobic virions. Due to the rough, fractal structure of aluminum and iron flocs,[76] steric hindrance may also play a role in sorption to flocs.

To the author's knowledge, conclusive evidence of the effect of divalent cations on virus sorption to metal hydroxide flocs (as opposed to electrostatically repulsive and/or nonpolar surfaces) does not exist. In 1958, Chang et al.[77] concluded that Ca^{2+} and Mg^{2+} may have inhibited virus mitigation. However, the comparison was made between tests using synthetic versus raw water sources, so the difference in virus mitigation cannot be conclusively attributed to divalent cations, as opposed to, *e.g.,* NOM. Chaudhuri and Engelbrecht[78] later showed that alum coagulation of bacteriophage T4 was not affected by Ca^{2+} and Mg^{2+} concentrations up to 330 mg/L as $CaCO_3$. However, Chaudhuri and Engelbrecht used a synthetic water free of NOM. The hypothesis of cation bridging between NOM and anionic coagulants/polymers has not been tested for viruses. Inhibition of coagulation by NOM has been documented for bacteriophages MS2[30] and Qβ[22]. However, neither the influence of divalent cations nor the impact of phage hydrophobicity was tested in these studies. Microbalance experiments of virus deposition on aluminum or iron hydroxide surfaces, similar to those conducted on silica and NOM coated

surfaces, could better identify the importance of surface charge, hydrophobicity, and roughness, as well as divalent cations and NOM concentrations.

2.3. Inactivation During Coagulation Processes

In addition to physical removal by sorption and co-precipitation, some studies have investigated bacteriophage inactivation by coagulation processes. Viruses may be inactivated by damage to the virion protein capsid and/or the viral genome. Damage to viral proteins manifests as an inability of the virus to attach to the host cell and/or inject the genome, while genomic damage prevents replication and proliferation of the virus in the host.[79] Whether viruses are physically removed or inactivated is not simply a Talmudic question. Coagulation processes increase sludge production, and sludge must be properly handled. If high levels of virus inactivation can be achieved, sludge treatment and handling will be safer and more cost-effective. Safe sludge handling is critical for decentralized water treatment, especially in developing countries that lack the infrastructure for proper disposal. If people risk contact with the sludge, we must be sure coagulation does not just concentrate pathogens.

Evidence of inactivation has been documented for both chemical coagulation and electrocoagulation, as summarized in Table 2-3. In the case of aluminum coagulants, polynuclear Al_{13} and Al_{30} species are thought to chemically oxidize virions.[19,39] While soluble, monomeric aluminum species are predominantly anionic above pH 6 [16], soluble Al_{13} and Al_{30} species are cationic near neutral pH.[19,39] Since most virions have negative surface charges,[57] the polynuclear cations may interact with and oxidize virions to a greater extent than monomeric anions. PACls produce more polynuclear hydrolytes in solution than simple aluminum salts.[9,39] Correspondingly, the most evidence for virus inactivation has been observed with PACl coagulation.[9,10,17–22] Coagulation with simple aluminum and iron salts (*e.g.*, $Al_2(SO_4)_3$, $AlCl_3$, $FeCl_3$ and $Al(NO_3)_3$) has shown only limited virus inactivation.[17,22,40] Polynuclear iron coagulants have

also been developed,[23,24] but these coagulants have not been evaluated for virus mitigation to the author's knowledge.

Table 2-3. Summary of methodology for studies reporting inactivation by coagulation. Virus inactivation data are rounded to the nearest 0.5 log_{10}. Reported inactivation below 1 log_{10} is shown as "< 1," while negligible inactivation is shown as "<< 1."

Coagulation Process	Coag-ulant	Dose (mg/L Al or Fe)	Bacterio-phage	Log_{10} virus inactivation / aggregation	Inactivation quantification method	Aggregation determination method	Source
CC	PACl	1	Qβ	3.5	plaque assay (with recovery)	phage recovery efficiency	[22]
			T4	2			
			MS2	2.5			
			P1	3			
	alum		Qβ	2			
			T4	< 1			
			MS2	1.5			
			P1	1			
CC	PACl	10	Qβ	2	plaque assay (with recovery)	phage recovery efficiency	[17]
CC	PACl, alum, $AlCl_3$, $AlSO_4$	1	MS2	< 1			
			P1	< 1			
			Qβ	1 - 1.5			
			T4	< 1			
CC	PACl	1.1	MS2	< 1	qRT-PCR (with recovery), plaque assay (with recovery)	DLS	[20]
			Qβ	4			
CC	alum	1.1	MS2	1	qRT-PCR, plaque assay	DLS	[18]
			Qβ	2			
	PACl		MS2	2			
			Qβ	5			
CC	PACl	1.9	MS2	3	qRT-PCR, plaque assay	n.r.	[37]
		2.2	Qβ	2.5			
	alum			<< 1			
CC	PACl	10	MS2	4	qRT-PCR, plaque assay	DLS	[19]
			Qβ	6			
			ΦX174	<< 1			

(continued next page)

(Table 2-3 continued)

EnC	PACl	4	MS2	1 - 2	plaque assay (with recovery)	n.r.	[12]
	$FeCl_3$	8		1 - 2			
CC + MF	PACl	1.1	MS2	<1	qRT-PCR, plaque assay	electron micrography	[21]
			Qβ	2.5			
CC + MF	PACl	1.1	MS2	2	qRT-PCR, plaque assay	n.r.	[10]
			Qβ	4			
ElC	aluminum electrodes	30	MS2	< 1	plaque assay (with recovery)	phage recovery efficiency	[28]
		30, 4 hr flocculation		3.5			
ElC + MF	iron electrodes	10	MS2	1 - 2	plaque assay (with recovery)	phage recovery efficiency	[30]

n.r. = not reported for the given data set
CC = Chemical coagulation, EnC = Enhanced coagulation, ElC = Electrocoagulation, MF = Microfiltration, UF = Ultrafiltration
DLS = Dynamic light scattering, qRT-PCR = quantitative reverse transcription polymerase chain reaction

As in sorption studies, multiple investigators found that inactivation by chemical coagulation occurred concurrently to floc formation, with little to no inactivation when viruses were spiked in a solution with pre-formed flocs.[19,22] Kreißel et al.[19] found that inactivation was greatest when viruses were exposed to soluble PACl at pH 4.5, indicating that inactivation may be related to soluble species rather than insoluble flocs. Other researchers have suggested alternate mechanisms of inactivation, such as deformation of virions by forces at the interphase boundary,[18] and inhibition of infection by irreversible adsorption of coagulant polymers to the capsid surface (*e.g.,* at binding sites).[17]

Electrocoagulation has been shown to disinfect algae and bacteria, although researchers often do not discern between physical removal and inactivation in their results.[80–83] Few studies have investigated virus mitigation by electrocoagulation,[14,28–30] and to date only Tanneru et al.[28,30] have specifically examined virus inactivation by electrocoagulation. Disinfection occurs in

electrocoagulation primarily by the oxidation of chloride to free chlorine.[28,84] For this reason, electrocoagulation has only been shown to inactivate viruses in the presence of chloride ions. Because generation of free chlorine is an oxidative process occurring at the anode,[84] chlorine production is a secondary and competing reaction to the oxidative dissolution of the anode itself. Tanneru et al.[28] noted that bacteriophage inactivation required a prohibitively long contact time due to the low concentrations of free chlorine generated in the study (< 0.1 mg/L). Inclusion in flocs also shields viruses from inactivation by free chlorine.[28]

Tanneru et al.[28] were able to detect damage to both the MS2 genome and proteins after electrocoagulation with extended flocculation times. The team detected conformational changes to proteins and an increase in the concentration of protein oxidation byproducts by attenuated total reflectance Fourier transform infrared spectroscopy (ATR-FTIR). Tanneru et al. also used quantitative reverse transcription polymerase chain reaction (qRT-PCR) amplification to directly investigate damage to the MS2 genome. A 77 bp section of the maturation protein coding region[85] was amplified and compared between treated and initial samples. The short length of the amplicon likely makes this method a conservative indicator of total RNA damage. Tanneru et al. found a rapid decline in copy number in the first hour after electrocoagulation, comparable to the reduction found using a culture-based plaque assay. Tanneru et al. did not find increased genome inactivation with longer contact time, although overall inactivation continued to increase. These results suggest that for electrocoagulation, the mechanism of inactivation may vary over time. Varying mechanisms of inactivation can be at play, even for a given disinfectant. For example, Wigginton et al.[79] found that free chlorine attacked MS2 proteins and genome, and inactivation manifested as an inability to inject the viral genome into the host cell. The method used by Wigginton et al. may offer a less conservative estimate of RNA damage because approximately half of the viral genome was analyzed.

Due to the different hypothesized inactivation mechanisms (*i.e.*, production of free chlorine during electrocoagulation versus polynuclear cations in chemical coagulation), Tanneru et al.'s results cannot be extended to chemical coagulation. Wigginton et al.[79] established that different chemical oxidants (*i.e.*, $^1O_2$, free chlorine, ClO_2) vary in their mechanisms of inactivation. Likewise, the inactivation mechanism likely differs between free chlorine and the large, polynuclear cations suggested to be responsible for inactivation due to chemical coagulation (*e.g.,* Al_{13} and Al_{30}). Use of an approach similar to that of Wigginton et al. or Tanneru et al.[28] would help to clarify the mechanism of inactivation by chemical coagulation. As a preliminary hypothesis, polynuclear aluminum species may predominately attack capsid surface proteins, because access to the internal structure would be limited by size and charge (especially as compared to free chlorine).

The following sections discuss difficulties in assessing virus inactivation in the laboratory. Due to the cost and duration of cultural assays, molecular methods seem to be an attractive option. However, research is required to prove the validity of molecular methods for quantifying inactivation. In addition, a given level of inactivation may be important to treatment efficiency, yet difficult to quantify due to its relative insignificance compared to other treatment fates. Virus aggregation also frustrates attempts to quantify inactivation, and no satisfactory method is available to ensure against aggregation of treated samples.

2.3.1.Quantification of Virus Inactivation

Quantification of virus inactivation presents an experimental challenge. Some authors[17,22,28] have employed a cultural plaque assay to quantify the number of infectious viruses in solution and those sorbed to solids using a recovery protocol. This method may be thought of as a "plaque-forming unit (PFU) balance." After gravitational separation, viruses are both sampled in the supernatant and recovered from the floc. The total virus recovery is

compared to the untreated, control sample to determine inactivation. A PFU balance is distinct from a mass balance in that it is a discrete count of PFUs, not a continuous measure of mass. Like any plaque assay, the PFU balance can discriminate between infectious and inactive viruses but not between a single virus and an aggregate.[86] Comparison of recovered PFUs to the initial concentration allows determination of virus inactivation, within the expected method recovery efficiency.[28] However, the PFU balance approach requires twice the number of plaque assays to analyze the concentrations of viruses in solution and adsorbed to flocs, thereby increasing cost and time inputs.

Other investigators[9,10,18,19,21] have used qPCR (qRT-PCR for RNA viruses) to compare declines in copy number to declines in PFU counts. Compared to plaque assays, qPCR is comparatively rapid, and aggregation does not affect qPCR results. In contrast to plaque assays, qPCR assesses the total number of intact viral genomes in the sample, regardless of infectivity. This allows a comparison between plaque assay and qPCR results to assess total inactivation. However, there are several concerns with comparing molecular and cultural techniques. For one, molecular methods cannot differentiate between physical removal and inactivation due to genome damage. The copy number of even short amplicons can decrease during inactivation, as described by Tanneru et al.[28] When assessing chemical oxidation by soluble PACl, Kreißel et al.[19] also showed a decline in copy number of approximately 1 $\log_{10}$ from the initial concentration. Whether the depressed recovery is an artifact of the method or indicative of genome destruction is unclear. In a coagulation study, this reduction in copy number would be indistinguishable from a reduction due to physical removal, as shown in Figure 2-1. Therefore, qPCR may overstate the importance of physical removal and understate that of inactivation.

Similarly, some fraction of inactivated viruses is likely removed with the flocs and therefore counted as physical removal. Inactivated viruses could even be disproportionately

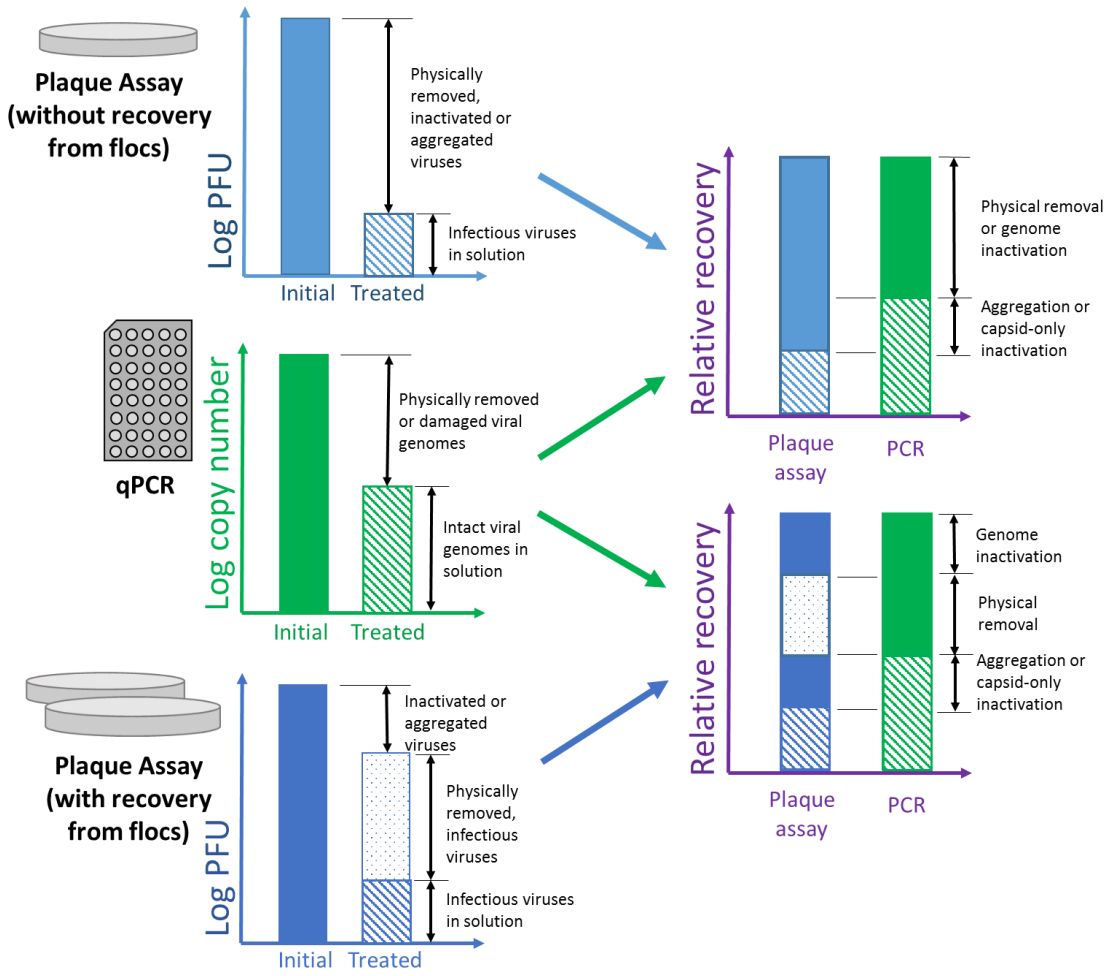

Figure 2-1. The most detailed theoretical categorization of fate possible using three different quantification methods independently and in combination. The relative values shown in stacked columns were chosen only for visual clarity. In practice, resolving many of these quantities may be impossible, because quantities may differ in value and variability by several orders of magnitude.

removed. Destruction of viral proteins can dramatically alter virion structure and genome packing.[87] The effect of morphological changes on sorption cannot be assumed to be negligible. If infectious viruses are more readily removed in flocs, then qPCR analysis of treated water would provide an appropriate means of quantifying total viruses (infectious + inactive). If inactive viruses are readily removed in the floc phase, qPCR analysis would again systematically underreport inactivation.

In one study, Shirasaki et al.[20] analyzed both the liquid phase and dissolved floc of treated water by qPCR and plaque assay -- essentially performing both a PFU balance and a copy number balance. Despite significant reductions in amplicons in the liquid phase, Shirasaki et al. recovered approximately all MS2 and Qβ amplicons from the floc (confidence intervals including 100% efficiency). The high recovery indicates that MS2 and Qβ inactivation by genome destruction was below detection in this study. This lack of genome inactivation may reflect the inactivation mechanism of PACl. However, Qβ inactivation was evident in both the floc and liquid phases, indicating the removal of inactivated viruses in flocs. For both bacteriophages, greater discrepancy between molecular and cultural quantification was observed in the liquid phase than in the floc phase. The greater discrepancy in the liquid phase could possibly be due to aggregation, especially considering that the liquid phase was only centrifuged (2000 *x g*, 10 min), not dissolved and agitated for resuspension like the floc phase. Regardless, Shirasaki et al.'s results suggest that genome inactivation may not significantly impact qPCR results for some bacteriophages and treatment processes. However, using qPCR without recovery from flocs may under-represent inactivation due to sorption of inactivated viruses in the floc, as in the case of Qβ. Shirasaki et al. do not report using this same approach in subsequent papers. Application-specific research is required to establish a firm methodological basis before using qPCR and plaque assays without recovery from flocs.

Figure 2-1 summarizes the extent of information that could theoretically be learned using the quantification methods discussed above. The combination of plaque assay with recovery from flocs provides the most detailed account of virus fate; however, one or more of these fates are likely to be undetectable in practice. A plaque assay with recovery also provides more relevant information (*i.e.,* the concentration of infectious viruses in the sludge) than qPCR and plaque assay without recovery. If some fates could be considered inconsequential for a

particular application (*esp.*, inactivation due to genome damage), the combination of qPCR and plaque assay without recovery would be comparable to plaque assay with recovery.

2.3.2.Detecting Low Levels of Inactivation

Working with high levels of virus reduction, such that logarithmic representations are customary, also presents an interesting conundrum. Whether quantified by molecular or cultural methods, inactivation is determined by subtracting a concentration of recovered PFUs or amplicons from an initial concentration that may be several orders of magnitude higher. Since the error of each quantity is relative to the concentration, inactivation can only be determined to a statistical degree of certainty when inactivation is a primary mechanism of reduction, as illustrated in Figure 2-2.

In addition, inactivation is usually treated as independent from physical removal, rather than additive. If inactivation works as a polishing step, small numbers of inactivated viruses could have a great impact. For example, if an additional 0.09% of the initial virus concentration is inactivated beyond the 99.9% that can be removed in flocs, that minimal reduction means the difference between satisfying the EPA's SWTR requirements or not.[41] The limited information available suggests inactivation might have this polishing effect. As discussed in Section 2.3.1, Shirasaki et al.[20] found greater inactivation of MS2 and Qβ in the liquid phase than the floc phase, which indicates that inactivation may contribute to virus reduction beyond the capacity of physical removal alone. In other words, inactivated viruses would not necessarily have been physically removed were they not inactivated. The 'polishing' effect of inactivation would significantly reduce the concentration of viruses remaining in the treated water after physical

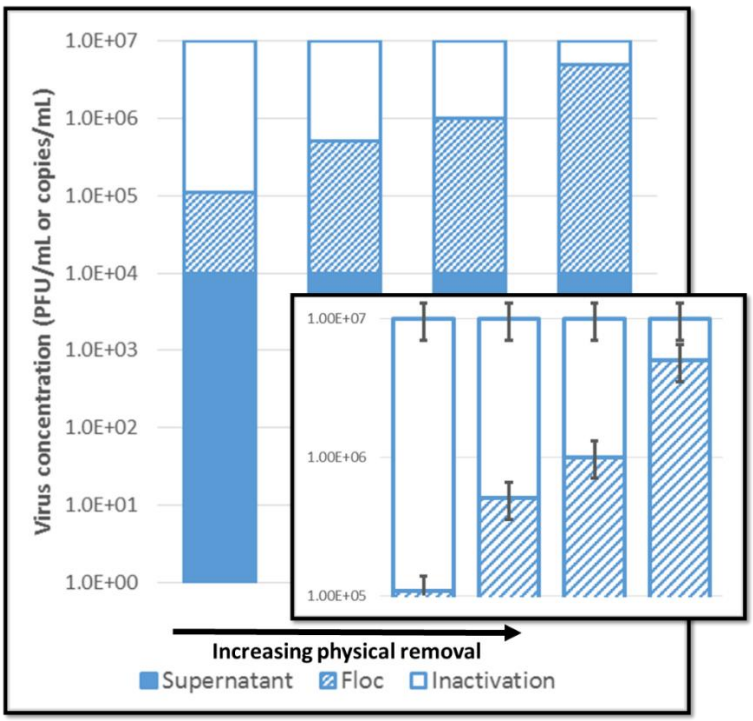

Figure 2-2. Confidence in quantifying decreasing amounts of inactivation. In this theoretical case, recovery of bacteriophages from the supernatant remains constant for all bars (10^4 PFU/mL), while the number of bacteriophages recovered from the floc increases from 10^5 to 5 x 10^6 PFU/mL. The standard error of the mean for all measurements is set as 30% (error bars, inset). The quantity recovered from the supernatant has no significant impact on inactivation. However, as inactivation decreases to near 0.5 $\log_{10}$ reduction, the confidence intervals begin to overlap, and inactivation cannot be distinguished from the analytical uncertainty.

removal. However, this small virus reduction would be lost on the scale of the original, spiked concentration. Therefore, the amount of inactivation, although important for disinfection, would be difficult to discern experimentally. If the inactivation cannot be accurately assessed, conditions for inactivation cannot be optimized.

2.3.3.Determination of Virus Aggregation

In all methods, aggregation remains quantitatively indistinguishable from at least some inactivation, as shown in Figure 2-1. Aggregation leads to artificially low plaque counts, because each plaque originates from many viruses instead of one. Based on aggregate size, Langlet et al.[86] found that aggregation could be responsible for more than 4 $\log_{10}$ reduction in PFUs (from

an initial concentration of approximately 10^{11} PFU/mL). However, an additional control can provide some 'insurance' against aggregation for the plaque assay with recovery method. The method recovery efficiency can be tested under conditions of minimal inactivation (*e.g.,* adsorbing viruses to pre-formed flocs or quenching oxidants with sodium thiosulfate). The recovery efficiency shows not only that viruses can be recovered from the flocs, but also that the viruses in the treated water are no more aggregated than in the initial virus solution. Some investigators[21,52] have also relied on electron micrographs to qualitatively show the presence or absence of aggregates.

Dynamic Light Scattering (DLS) is a method for determining both electrokinetic response of colloids and the size distribution of particles in solution. Many studies[18–20,65,86] have used DLS analysis to determine conditions in which virions aggregate. However, DLS analysis requires very high virus concentrations (greater than 10^9 PFU/mL)[43] -- higher than even the typical spiking concentrations used for testing (usually 10^7 - 10^8 PFU/mL). Therefore, researchers cannot directly assess aggregation in the same samples to be tested by plaque assay and/or qPCR. Instead, researchers must try to show whether or not aggregation occurs in conditions similar to those tested.

A significant quantity of virus stock solution is necessary to achieve the required concentrations for DLS. These stock solutions may have higher ionic strengths and differ greatly in composition from natural waters. Electrolyte composition can significantly affect electrokinetic responses like aggregation.[57] Aggregation has been shown to be greater in phosphate-buffered saline (PBS), commonly used for virus stocks, than in deionized water or bicarbonate solution.[61] Preferably, virus stocks should be purified and spiked into the same water matrix used for coagulation tests. However, the method of virus purification may also significantly affect virion properties. As previously mentioned, Dika et al.[63] compared three

methods of MS2 purification: polyethylene glycol (PEG) precipitation, successive dialyses in deionized water and 1 mM $NaNO_3$, and ultracentrifugation in a CsCl gradient. PEG precipitation resulted in a larger hydrodynamic radius of unaggregated viruses, with aggregation observed at pH 6. Dialysis resulted in aggregation at pH 4, while viruses separated in a CsCl gradient did not aggregate at any pH. Dika et al. note that each method has drawbacks: PEG appears to adhere to the capsid surface, dialysis retains viral and non-viral particles based only on membrane exclusion, and cesium ions may permanently deform protein structures. The experiment does not clarify which purification best approximates virus behavior in the environment, however. In addition, Dika et al. did not use a solvent wash after PEG precipitation to promote monodispersion, as used by many investigators.[26,27,88–90] A solvent like chloroform or Vertrel™ may be able to strip adhered PEG from the capsid surface. If not, dialysis may best reproduce virus behavior in the environment, because foreign compounds are not introduced. To date, the best course of action is to control against aggregation by testing at pH values and ionic strengths where virions are likely to be stable. Aggregation may then be measured under similar conditions using DLS or qualitatively assessed by electron microscopy.

2.4. Inactivation via Ferrous Iron Oxidation

Coagulation processes involving zero-valent or ferrous iron have the added complexity of redox reactions. Unlike aluminum, iron has multiple stable valence states. The products formed by mixed-valent iron precipitation are varied, from primarily ferrous minerals like green rust and magnetite to ferric minerals like ferrihydrite, lepidocrocite, and goethite.[32,33,91–93] The particular precipitation products formed depend to some degree on the ions in solution, but the oxidative conditions ultimately determine the valence state of iron.[33,91,93] The oxidation of iron via dissolved oxygen has the further potential to catalyze the oxidation of other metals and organic compounds.[94–97] Ferrous oxidation has recently been investigated for disinfection

applications as well.[98,99] Accordingly, one potential mechanism of virus mitigation via ferrous chloride coagulation/iron electrocoagulation is inactivation due to ferrous iron oxidation.

Kim et al.[98,100] demonstrated virus inactivation by iron oxidation, both due to Fenton's reagent as well as ferrous/zero-valent iron alone. The team found that disinfection was greatest at low pH (pH 5.5 to 6), which was likely due to increased contact time with ferrous ions, and/or greater production of radical oxygen species. Kim et al. found greater MS2 reductions using zero-valent iron nanoparticles than ferrous ions. In particular, the nanoparticles were less dependent on dissolved oxygen. The team hypothesized that viruses may have been inactivated by surface interactions in the absence of oxygen to create hydrogen peroxide, leading to Fenton-like reactions.[98]

Using enzyme-linked immunosorbent assay (ELISA) to detect a decrease in antigenicity and quantitative reverse transcriptase polymerase chain reaction (qRT-PCR) to detect chromosomal damage, Kim et al.[98] determined that capsid damage (lower antigenicity) was a mechanism of MS2 disinfection for ferrous ions, while qRT-PCR did not reveal genomic damage. Zero-valent nanoparticles were found to inactivate viruses by both capsid and genome damage. Though the study used ELISA and qRT-PCR in addition to cultural methods to confirm virus inactivation, the contribution of virus aggregation to log reduction in PFUs cannot be entirely ruled out, as the MS2 phages were not eluted after treatment. In addition, though widely accepted as a surrogate virus for filtration treatment units, MS2 may be more susceptible to some forms of disinfection than other possible bacteriophage surrogates for human viruses of interest.[101]

2.4.1. Generation of Intermediate Oxidants by Ferrous Iron Oxidation

The mechanisms of virus inactivation by iron oxidation are poorly understood. However, lessons can be taken from the wealth of research on iron oxidation of chemical species. Iron-

based oxidation has a long history in the Fenton process. The Fenton process uses ferrous iron and hydrogen peroxide at acidic pH (pH ≈ 3) to generate oxidants.[102] The evolution of reactive oxygen species (ROS) using iron via the Fenton process has been well documented.[103–105] Even without the addition of hydrogen peroxide, oxidation of zero-valent iron by dissolved oxygen has been shown to generate Fenton's reagent (Fe^{II} and H_2O_2), as well as ROS associated with the Fenton reaction, such as hydroxyl- (•OH) and superoxide ($\bullet O_2^-$) radicals.[96,98] The apparent similarity of the Fenton reaction and autooxidation of ferrous iron in the absence of hydrogen peroxide is beneficial, because far more research has been devoted to the former. However, lessons taken from the Fenton reaction must be applied with caution to the oxidation of iron by dissolved oxygen, due to the availability of hydrogen peroxide in the Fenton reaction.

The Fenton reaction is generally considered ineffective near neutral pH.[96] Nevertheless, researchers[96–98,106] have demonstrated the oxidative effects of zero-valent and ferrous iron near neutral pH. Near neutral pH, oxidant generation arises predominately from the oxidation of ferrous iron by dissolved oxygen, rather than oxidation of zero-valent iron to ferrous iron.[95] Oxidation at circumneutral pH is commonly attributed to the formation of ferryl ions ($Fe^{IV}O^{2+}$),[106,107] though the subject continues to be a matter of debate.[97]

Ferryl iron is an unstable intermediate of ferrous oxidation,[94] with an oxidation potential of approximately 1.4 V for the Fe^{3+}/Fe^{4+} couple.[108] As early as the 1930s, ferryl iron was hypothesized to degrade hydrogen peroxide in the Fenton process.[107] Because ferryl species are ephemeral, direct detection of Fe(IV) presents practical challenges. The gold standard of high-valent detection, Mössbauer spectroscopy, requires rapid freeze-quenching of samples prior to analysis in liquid nitrogen or helium.[109,110] Pestovsky et al.[109] confirmed by Mössbauer spectroscopy that the oxidation of ferrous ions by ozone produced $[(H_2O)_5Fe^{IV}{=}O]^{2+}$ in acidic solutions, and that the primary intermediate oxidant at pH 1 was •OH. Because samples must be

frozen within milliseconds in order to quantify iron (IV) and (V), tests are typically conducted at very low temperatures not representative of standard conditions.[110] Mössbauer spectroscopy is also prohibitively expensive for labs not specializing in iron speciation.

Attempts have also been made to identify oxidant species generated via the Fenton reaction or iron autoxidation using specific organic probes. Both the ability of the probe to quench oxidation and the oxidation byproducts formed can help to identify the presence of known oxidants. However, the identity of novel oxidants (*e.g.*, ferryl species) can only be inferred by these processes. Superoxide dismutase, an $\bullet O_2^-$ scavenger, has been found to impede the slow phase of the Fenton reaction, in which oxidants are only produced by regenerating iron (II) from iron (III). However, superoxide dismutase does not impede the initial, rapid reaction caused by the initial oxidation of ferrous ions.[100] Therefore, superoxide is not a relevant oxidant to ferrous oxidation at neutral pH.

At low pH, •OH is the primary oxidant produced, but •OH is not a significant intermediate of iron oxidation above pH 5.[95,96,98] Using a spin quencher with electron spin resonance (ESR) spectroscopy, Reinke et al.[106] found that •OH degradation products were formed in the Fenton process at pH 7.4, but not in the autooxidation of ferrous iron (in the absence of hydrogen peroxide). Oxidation of zero-valent iron shows variable quenching with selective •OH probe compounds at high and low pH,[95–97,111] providing further evidence of a switch to an oxidant other than •OH.

Bataineh et al.[103] proposed a model by which ferryl iron becomes the primary intermediate in the Fenton process near neutral pH (pH 6 – 7). This model was based on a pH-dependent change in dimethylsulfoxide (DMSO) oxidation byproducts, whereby oxidation due to •OH at low pH was supplanted by a shorter-lived, less reactive oxidant at high pH. However, the half-life of ferryl species is generally considered to be much longer (on the order of seconds)

compared to that of •OH (on the order of nanoseconds).[112,113] Pang et al.[97] came to the opposite conclusion that ferryl iron is *not* an intermediate oxidant in the Fenton reaction at neutral pH based on the failure of zero-valent iron species to produce appropriate byproducts in the presence of a methyl phenyl sulfoxide probe.

One possible reason for the wide disagreement between studies is that small experimental perturbations can impact iron oxidation products. Even the type of intermediate oxidant produced can be influenced by the composition of the water matrix. For example, Bataineh et al.[103] found that •OH was produced via the Fenton process in phosphate buffer from pH 6.1 to 8, but not in amine buffers over the same pH range. Hug and Leupin[111] found that arsenic oxidation via the Fenton process increased with the bicarbonate concentration. In the presence of organic matter, organic radicals can be formed instead of •OH.[114] In addition, merely changing the rate of ferrous addition to the system can substantially alter the yield of oxidation byproducts.[103]

2.4.2. Sequential Iron Electrocoagulation – Electrooxidation

Iron electrocoagulation (EC) is one potential technology in which ferrous-based disinfection might play a role. In iron EC, a sacrificial, zero-valent iron electrode is oxidized by passing current through the cell. Iron is released into solution as ferrous cations, which then further oxidize in the presence of dissolved oxygen.[32,94,115] The iron precipitates as solids such as green rust and magnetite in anoxic conditions or lepidocrocite in oxygenated conditions.[32,91] EC has primarily been considered for physical removal of contaminants, including viruses. However, oxidation of arsenite via EC has been reported.[94] Inactivation of bacteriophage MS2 via iron EC has also been proposed, though the mechanisms and application were not explored.[30]

Electrooxidation (EO) uses non-sacrificial electrodes to oxidize contaminants by two potential mechanisms: generation of oxidants in solution (indirect oxidation) and electron

exchange at the electrode surface (direct oxidation). Electro-disinfection by EO has been demonstrated extensively for bacteria,[116–123] but less attention has been paid to virus mitigation via EO.[124–126] Viruses may be more recalcitrant to electro-disinfection; bacteriophage MS2 and recombinant adenovirus demonstrated poorer removal than *E. coli* and *Enterococcus* in a toilet-water electro-disinfection system featuring a semiconductor anode.[126] Therefore, virus mitigation by EO represents a critical gap in the electro-disinfection literature.

Boron-doped diamond (BDD) electrodes are commonly used in EO research as they are highly resistant to chemical and thermal degradation.[127,128] BDD also has a broad solvent window, meaning that the electrode reacts with solvents only at high positive and negative electrode potentials. Particularly, BDD has a high oxygen (O_2) overpotential. For electroanalytical methods, the high O_2 overpotential aids in reversible cyclic voltammetry. For water treatment, the high O_2 overpotential means that oxygen generation competes less with anodic oxidation of contaminants.

Electro-disinfection via BDD EO typically occurs due to the formation of ROS from dissolved oxygen, or free chlorine and chlorine dioxide from chloride.[118,129,130] In the absence of chloride, •OH is the primary oxidant species.[131] Many researchers[117,118,129,132] have found that chloride improves BDD electro-disinfection, indicating that chlorine generation yields greater disinfection than ROS alone. The presence of chloride has also been found to increase ROS generated by BDD EO.[118] Since ROS are short-lived, oxidation takes place predominately at the electrode surface.[120,131] Therefore, pathogens must be transported to the electrode surface for effective disinfection. Transport may occur via either electrophoresis or convection/diffusion. Electrophoresis is the movement of charged species in an applied electric field. While charged contaminants are subject to both electrophoresis and convection, uncharged contaminants must be transported from the bulk solution to the electrode surface by diffusion only.[133,134]

EO and EC have high potential to be complementary technologies. Both technologies trade a demand for electrical power with compactness and portability. In addition, the presence of residual iron due to EC may enhance oxidation via EO. Ferrous-catalyzed ozonation has been found to be more effective than ozonation alone in oxidizing organic pollutants and COD.[135–137] Researchers have found that ferric iron has similar, though possibly lesser, catalytic effects for ozonation of organic pollutants.[136,138] Though disinfection studies using iron-enhanced oxidation are scarce, Sjogren and Sierka[139] found that TiO_2 photocatalysis achieved an additional 2 $\log_{10}$ reduction of MS2 when augmented with 2 µM ferrous sulfate. Using an oxidation method (*e.g.,* ozonation) could also regulate iron oxidation to maximize disinfection and minimize soluble iron residuals. In addition, EC is an effective technology for removal of NOM and turbidity.[31,32,140–142] Therefore, EC could serve as a pretreatment step for EO by removing NOM and turbidity, thereby reducing the oxidant demand. Acidifying water to pH 4 – 5 prior to EC can also improve NOM removal efficiency by promoting charge neutralization.[143,144]

2.5. Use of Virus Surrogates in Coagulation Studies

Understanding the basis of virion sorption and inactivation is necessary not only for predicting and explaining virus reduction by coagulation technologies, but also for choosing appropriate bacteriophage surrogates for evaluating unit processes. Bacteriophage surrogates are most often used in lab and pilot studies for safety considerations, and because bacteriophage assays require significantly less time and resources than mammalian virus assays. In addition, human viruses are often difficult to propagate in large enough concentrations to show required reductions, e.g., the 4 $\log_{10}$ reduction required by the SWTR.[41]

Very few studies have directly compared the effect of coagulation on both bacteriophage surrogates and the human viruses of interest, as shown in Table 2-2. Among those studies, there is no common consensus on the relative performance of bacteriophage

surrogates and human viruses. For example, Mayer et al.[26] found MS2 to be a conservative surrogate for poliovirus 1, while Shin and Sobsey[38] found MS2 reduction to be greater than that of poliovirus 1. However, too many parameters differ between these studies to draw firm conclusions. Numerous factors, including the type and dose of coagulant, ionic strength, pH, and composition of the water matrix, play a significant role in the absolute and relative reduction of different viruses.

Clear trends in removal and inactivation between bacteriophages are also difficult to discern, as shown in Table 2-2. MS2 and Qβ have been compared in the greatest number of coagulation studies. MS2 and Qβ are both commonly used as surrogates in water treatment studies as well. Both bacteriophages infect the F-pilus of *E. coli*, i.e., they are F-specific.[145] MS2 and Qβ are of similar size (20 - 30 nm),[43] with similar pI values (2 - 4) reported in the literature.[57] Both bacteriophages have single-stranded RNA genomes, although Qβ's genome (4217 nt) is about 18% longer than that of MS2 (3569 nt).[145] Out of 8 direct comparisons of reduction of MS2 and Qβ by coagulation (see Table 2-2), MS2 was reduced to a greater extent in 4 studies, with a negligible overall difference in reduction. However, the mechanism of mitigation was likely different for each bacteriophage. Qβ was inactivated to a greater extent than MS2 in a majority (5 of 7) of direct comparisons, with an average of 1.5 $\log_{10}$ greater inactivation. In two tests using alum as the coagulant, treatment efficiency of MS2 was greater in both, while tests with PACl showed greater average reduction of Qβ. Thus, the suitability of MS2 or Qβ as a surrogate may depend both on the mechanism of reduction and the coagulant used. The variability of these well-studied bacteriophages illustrates the great need for additional head-to-head comparison studies.

Even tests performed using nearly identical conditions can differ significantly. Some tests comparing MS2 and Qβ used the same coagulant type and dose (1.1 mg/L PACl) with

varying results,[10,20–22,40] as shown in Table 2-2. Similarly, Mayer et al.[26] and Abbaszadegan et al.[27] used the same methods and source water (though the source water composition varied over time). Mayer et al. found relative virus reductions following the order of: fr > ΦX174 > MS2 ≥ PRD1. Abbaszadegan et al. found greater reduction for all four bacteriophages with the same coagulant dose, and bacteriophage reduction followed the order of: fr ≥ MS2 > PRD1 > ΦX174. The only clear difference between the conditions of the two studies was that Mayer et al.'s source water for bacteriophage tests had a higher NOM concentration, as shown in Table 2-2. In both tests, the four bacteriophages were considered to be either conservative or representative surrogates for the human viruses of interest. However, in a third test by Abbaszadegan et al.,[35] bacteriophages fr and MS2 were reduced to a greater extent than the target viruses, while PRD1 and ΦX174 were conservative surrogates.

When inactivation plays a significant role in virus reduction, the biology of the virus -- its morphology and infectious pathway -- must be considered in addition to its physical properties. Sigstam et al.[146] explain that the easily-oxidized amino acids cysteine and methionine are potential indicators of virus capsid degradation, although protein conformation determines the exposure of those amino acids to disinfectants. Sigstam et al. therefore used a complex model to explain cleavage at a particular methionine using the thermodynamics of oxidation in relation to the bonds between capsid proteins, and the "solvent accessible surface area" of that site. The team found that when genome inactivation was the primary disinfection mechanism, inactivation of F-specific bacteriophages fr, GA and MS2 was similar. However, when capsid destruction was the primary disinfection mechanism, subtle variations in the protein coat of the four bacteriophages led to differing inactivation.

As with pI, even closely related virus strains can differ in susceptibility to inactivation. For example, Engelbrecht et al.[147] measured significantly different free chlorine inactivation

rates between serotypes of coxsackievirus (A9 and B5), echovirus (1 and 5), and poliovirus (1 and 2). Virus strains may differ in inactivation depending on the disinfectant as well. In a study by Cromeans et al.,[148] echoviruses 1 and 11 had similar free chlorine inactivation rates, but the rate of echovirus 11 inactivation by monochloramine was two orders of magnitude slower than that of echovirus 1. Cromeans et al. also found significant differences in inactivation between serotypes of both human adenovirus (2 and 40, 41) and echovirus (1 and 11), although trends were similar between free chlorine and chloramine. Sigstam et al.[146] suggest that closely-related viruses may be appropriate surrogates when the primary inactivation mechanism is genome destruction, but not necessarily for capsid-based inactivation. For chemical coagulation, the charge and large size of polynuclear cations may restrict oxidation to only the capsid surface. In this case, conservative surrogates must be chosen by direct comparison with the viruses of interest. For the generation of free chlorine by electrocoagulation, the inactivation mechanism is likely less specific, because both the viral proteins and genome are oxidized by free chlorine.[28,79]

Regarding bacteriophage surrogates, Kreißel et al.[19] advance the hypothesis that F-specific bacteriophages may be uniquely susceptible to inactivation. F-specific bacteriophages have only one copy of the maturation protein responsible for binding to and infecting the F-pilus structure. The MS2 maturation protein (A protein) is known to be exposed near one of the five-fold vertices, possibly beneath a pore.[149] Qβ maturation protein (A2 protein) is similarly located near the five-fold vertex, although conformation may be slightly less rigid than in MS2.[149] This orientation may be similar in other F-specific bacteriophages. Kreißel et al. argue that the single maturation protein might be easily blocked or damaged, and F-specific bacteriophages would therefore show greater inactivation than somatic coliphages, which have multiple binding sites.

Most studies of inactivation by coagulation have used F-specific bacteriophages, as shown in Table 2-3. Therefore, the use of these surrogates may overstate virus inactivation.

Kreißel et al. recommend using the somatic coliphage ΦX174 as a more conservative surrogate for coagulation studies. In their study, ΦX174 was insensitive to inactivation by PACl. The pI values for ΦX174 reported in the literature are higher than the pH 4.5 used in the Kreißel et al. study. If polyaluminum cations were responsible for virus inactivation, the coagulant should show little or no attraction to positively charged ΦX174 virions. However, Kreißel et al. measured a negative electrophoretic mobility for ΦX174 by DLS. From a practical perspective, ΦX174 forms large, ill-defined plaques if allowed to incubate overnight,[19,150] so shorter incubation times are recommended.

If F-specific bacteriophages are more structurally fragile than somatic bacteriophages, they should also be more susceptible to indiscriminate disinfectants. However, experimental results are inconclusive. ΦX174 may be more sensitive than MS2 to chemical disinfection by •OH.[56] In a study of iodine inactivation,[151] MS2 was slightly more sensitive than ΦX174, although neither was nearly as resistant to disinfection as bacteriophage GA, another F-specific bacteriophage. GA also has a relatively high resistance to temperature and pH.[152] In contrast, Sigstam et al.[146] found GA to be comparable or more susceptible than MS2 and fr to a range of disinfectants, including free chlorine. Regardless, GA's low susceptibility to some disinfectants and high persistence in the environment casts some doubt on the hypothesis that F-specific bacteriophages are structurally more sensitive to inactivation. In the case of free chlorine oxidation, Wigginton et al.[79] noted that extensive damage to the MS2 A protein did not cause an inability to bind to host pili. Rather, damage to the capsid protein was likely responsible for inactivation. Therefore, the A protein may be robust to chemical oxidation. More importantly,

the case of bacteriophage GA illustrates that a surrogate may be conservative in one application and overly susceptible in another.

In addition, a conservative surrogate for coagulation must be robust to both physical removal and disinfection. ΦX174 is less hydrophobic than MS2[47,65] and may therefore be a more conservative surrogate for physical removal in the presence of NOM. ΦX174 and MS2 reduction in raw waters due to $FeCl_3$ coagulation was compared in three studies,[26,27,35] but the results conflicted as to which bacteriophage was reduced to a greater extent. GA has been shown to persist to a far greater degree than MS2 and Qβ in a pilot coagulation/ultrafiltration treatment plant.[153] Jofre et al.[154] found that in three water treatment plants, somatic coliphages were found in slightly more samples after prechlorination-flocculation-sedimentation and post-chlorination than F-specific coliphages, but phages of *Bacteroides fragilis* were yet more resistant. Suffice it to say that not enough is known about common bacteriophage surrogates, let alone the countless other possible bacteriophages available for research.

Resistance to inactivation or physical removal does not automatically make for an excellent surrogate -- the surrogate must be tested alongside the actual virus of interest. A good surrogate should be conservative compared to the human virus, but more importantly it must be representative. A 'worst-case scenario' is only valuable insofar as it is remotely possible. By using a surrogate that is especially insensitive, researchers may over-design treatment systems at great cost. Insensitive surrogates may also lead researchers to miss a potential treatment strategy that could be optimized for insensitive targets. This is particularly true in the case of inactivation due to coagulation. As illustrated in Section 2.3.2, inactivation of less than 1 $\log_{10}$ may be statistically indiscernible when physical removal is dominant. Therefore, the best surrogate is one tailored to the application. If possible, research should employ more than one surrogate, with different electrostatic charge, hydrophobicity and/or resistance to inactivation,

as appropriate. Of course, additional research is required to assess these properties for the many possible bacteriophage surrogates.

2.6. Conclusions

At this stage in coagulation research, viruses can no longer be assumed to be inert nanoparticles. Both the complexity of viruses as bioparticles and the phenomenon of virus inactivation must be embraced. In particular, the role of permeability in virus sorption and aggregation remains unclear. Virion permeability has been estimated by interpreting empirical electrophoretic mobility data.[55] However, to the author's knowledge, no empirical measures of virion permeability exist, and a clear link between permeability and virion composition and morphology has not been advanced. Furthermore, the direct influence of inner virion structures on surface charge or sorption has not been conclusively demonstrated.

Non-DLVO forces must also be considered to explain and predict virus sorption behavior. Research shows that hydrophobicity is an important contributor to sorption, especially for nonpolar virions. Other forces, such as steric interactions and hydrodynamics, are likely to play a significant role when electrostatic forces are repulsive or minimal (*e.g.*, at high ionic strength or near the virus or floc pI). In addition, the composition of the water matrix is also likely to play a strong role for many viruses. NOM may compete for sorption sites on flocs when repulsive electrostatic charges govern NOM-virion interactions, or NOM may act as a sorbent to enhance flocculation of hydrophobic virions. Ca^{2+} and Mg^{2+} enhance sorption of viruses to similarly-charged species like NOM, either by cation bridging or surface complexation. Most importantly, current research demonstrates that sorption varies by both virion and environmental conditions.

The potential for inactivation in coagulation processes is both a source of frustration and a promising avenue for water treatment research. Inactivation muddles unit treatment

performance testing with artificially high reduction rates. However, future coagulation systems could be optimized for inactivation. Coagulation systems using zero-valent or ferrous iron have the potential to disinfect via iron oxidation, with potential applications in processes like electrocoagulation and electrooxidation. The evolution of oxidants in the iron oxidation process has shown initial positive results in the inactivation of bacteriophage MS2, though follow-up studies using an elution method are required to ensure that bacteriophage removal is truly due to inactivation rather than sorption. In addition, the process has not yet been tested on other bacteriophages or human viruses.

Applied research should include at least two bacteriophage surrogates with varying susceptibility to physical removal and inactivation. To inform surrogate selection, and to enable design of improved treatment systems, the mechanism of inactivation by chemical coagulation must be determined. If viruses are inactivated by capsid protein damage, determining a surrogate by physical similarities may be inappropriate. This highlights the need for basic research into coagulation that directly compares human viruses of interest and bacteriophages. More comparisons between bacteriophages are also needed. With more systematic comparisons of multiple bacteriophages, researchers could begin to hypothesize about the variability in bacteriophage performance between experiments.

Plaque assays with recovery from flocs remains the gold standard for quantifying inactivation. More research is required to confirm the validity of using a combination of qRT-PCR and plaque assay without recovery from flocs. The combination of qRT-PCR and plaque assays may prove to be both acceptable and cost-saving for some viruses, but only if future research can show that the method does not underreport inactivation. Furthermore, continued research is needed to determine how inactivation impacts total virus reduction by coagulation. If inactivation of viruses acts as a polishing step for coagulation, seemingly insignificant

inactivation would be critical for meeting treatment goals. Further studies comparing the recovery of viruses from flocs by both plaque assay and qRT-PCR could help delineate the relationship between coagulation and inactivation. In addition, inactivation must be separated from aggregation, but quantitative assessment of virus aggregation in treated samples is currently not possible.

Ideally, continued research into the physicochemical properties of viruses will allow us to predict sorption and inactivation behavior. This type of modeling would help to better identify bacteriophage surrogates as well. Currently, surrogates are often selected based on qualities like size and pI. Unfortunately, the complexity of virus sorption and inactivation eludes such simple measures. Therefore, it is essential to begin to draw connections between virus morphology and physical chemistry. Important strides in this direction have been referenced in this review, such as Langlet et al.'s model of virus electrokinetics,[50] Sigstam et al.'s model of virus capsid susceptibility to inactivation[146] and Armanious et al.'s method for assessing hydrophobicity from virion surface structure.[69] However, these models are still under investigation and cannot yet confidently predict behavior of viruses. Through comparisons of morphologically similar bacteriophages, we can learn more about how minor changes in structure impact sorption and inactivation properties. In the future, we may be able to predict virus behavior and identify new bacteriophage surrogates based on subtle aspects like protein structures or genome size and conformation. The benefits of this work would extend far beyond use in coagulation -- from filtration systems, to inactivation by nanoparticles, to modeling virus fate and persistence in the environment.

2.7. References

1. Blacklow NR, Greenberg HB. Viral gastroenteritis. *N Engl J Med*. 1991;325(4):252-264.

2. Fong T-T, Lipp EK. Enteric viruses of humans and animals in aquatic environments: Health

risks, detection, and potential water quality assessment tools. *Microbiol Mol Biol Rev*. 2005;69(2):357-371. doi:10.1128/MMBR.69.2.357

3. Kocwa-Haluch R. Waterborne Enteroviruses as a Hazard for Human Health. *Polish J Environ Stud*. 2001;10(6):485-487.

4. Abbaszadegan M, Lechevallier M, Gerba CP. Occurrence of Viruses in US Groundwaters. *J Am Water Works Assoc*. 2003;95(9):107-120.

5. United States Environmental Protection Agency. Contaminant Candidate List (CCL) and Regulatory Determination. http://www.epa.gov/ccl. Published 2015. Accessed January 1, 2016.

6. World Health Organization, ed. *WHO Guidelines for Drinking-Water Quality.* 4th ed. Geneva: World Health Organization; 2011. doi:10.1016/S1462-0758(00)00006-6

7. Centers for Disease Control and Prevention. Effect of chlorination on inactivating selected pathogens. http://www.cdc.gov/safewater/effectiveness-on-pathogens.html. Published 2012. Accessed January 1, 2015.

8. Gerba CP, Gramos DM, Nwachuku N. Comparative inactivation of enteroviruses and adenovirus 2 by UV light. *Appl Environ Microbiol*. 2002;68(10):5167. doi:10.1128/AEM.68.10.5167

9. Shirasaki N, Matsushita T, Matsui Y, Urasaki T, Kimura M, Ohno K. Virus removal by an in-line coagulation-ceramic microfiltration process with high-basicity polyaluminum coagulation pretreatment. *Water Sci Technol Water Supply*. 2014;14(3):429-437. doi:10.2166/ws.2013.218

10. Shirasaki N, Matsushita T, Matsui Y, Kobuke M, Ohno K. Feasibility of in-line coagulation as a pretreatment for ceramic microfiltration to remove viruses. *J Water Supply Res Technol*. 2010;59(8):501-511.

11. Shirasaki N, Matsushita T, Matsui Y, Ohno K. Effects of reversible and irreversible membrane fouling on virus removal by a coagulation–microfiltration system. *J Water Supply Res Technol*. 2008;57(7):501. doi:10.2166/aqua.2008.048

12. Meyn T, Leiknes T. MS2 removal from high NOM content surface water by coagulation - ceramic microfiltration, for potable water production. *AlChE*. 2012;58(7):2270-2281. doi:10.1002/aic.12731

13. Matsushita T, Matsui Y, Shirasaki N, Kato Y. Effect of membrane pore size, coagulation time, and coagulant dose on virus removal by a coagulation-ceramic microfiltration hybrid system. *Desalination*. 2005;178:21-26. doi:10.1016/j.desal.2004.11.026

14. Zhu B, Clifford DA, Chellam S. Comparison of electrocoagulation and chemical coagulation pretreatment for enhanced virus removal using microfiltration membranes. *Water Res*. 2005;39(13):3098-3108. doi:10.1016/j.watres.2005.05.020

15. Fiksdal L, Leiknes T. The effect of coagulation with MF/UF membrane filtration for the

removal of virus in drinking water. *J Memb Sci*. 2006;279(1-2):364-371. doi:10.1016/j.memsci.2005.12.023

16. Crittenden JC, Trussell RR, Hand DW, Howe KJ, Tchobanoglous G. *MWH's Water Treatment: Principles and Design*. 3rd ed. Hoboken, New Jersey: John Wiley & Sons, Inc.; 2012.

17. Matsushita T, Matsui Y, Inoue T. Irreversible and reversible adhesion between virus particles and hydrolyzing-precipitating aluminium: a function of coagulation. *Water Sci Technol*. 2004;50(12):201-206. http://www.ncbi.nlm.nih.gov/pubmed/15686022.

18. Matsushita T, Shirasaki N, Matsui Y, Ohno K. Virus inactivation during coagulation with aluminum coagulants. *Chemosphere*. 2011;85(4):571-576. doi:10.1016/j.chemosphere.2011.06.083

19. Kreißel K, Bösl M, Hügler M, Lipp P, Franzreb M, Hambsch B. Inactivation of F-specific bacteriophages during flocculation with polyaluminum chloride - A mechanistic study. *Water Res*. 2014;51:144-151. doi:10.1016/j.watres.2013.12.026

20. Shirasaki N, Matsushita T, Matsui Y, Urasaki T, Ohno K. Comparison of behaviors of two surrogates for pathogenic waterborne viruses, bacteriophages Qbeta and MS2, during the aluminum coagulation process. *Water Res*. 2009;43(3):605-612. doi:10.1016/j.watres.2008.11.002

21. Shirasaki N, Matsushita T, Matsui Y, Kobuke M, Ohno K. Comparison of removal performance of two surrogates for pathogenic waterborne viruses, bacteriophage Qβ and MS2, in a coagulation–ceramic microfiltration system. *J Memb Sci*. 2009;326(2):564-571. doi:10.1016/j.memsci.2008.10.037

22. Matsui Y, Matsushita T, Sakuma S, et al. Virus inactivation in aluminum and polyaluminum coagulation. *Environ Sci Technol*. 2003;37(22):5175-5180. http://www.ncbi.nlm.nih.gov/pubmed/14655704.

23. Zouboulis AI, Moussas PA, Vasilakou F. Polyferric sulphate: Preparation, characterisation and application in coagulation experiments. *J Hazard Mater*. 2008;155(3):459-468. doi:10.1016/j.jhazmat.2007.11.108

24. Lei G, Ma J, Guan X, Song A, Cui Y. Effect of basicity on coagulation performance of polyferric chloride applied in eutrophicated raw water. *Desalination*. 2009;247(1-3):518-529. doi:10.1016/j.desal.2008.06.026

25. United States Environmental Protection Agency. *Stage 1 Disinfectants and Disinfection Byproducts Rule*.; 2001. doi:EPA 816-F-01-014

26. Mayer BK, Ryu H, Abbaszadegan M. Treatability of U.S. Environmental Protection Agency contaminant candidate list viruses: Removal of coxsackievirus and echovirus using enhanced coagulation. *Environ Sci Technol*. 2008;42(18):6890-6896. doi:10.1021/es801481s

27. Abbaszadegan M, Mayer BK, Ryu H, Nwachuku N. Efficacy of removal of CCL viruses

under enhanced coagulation conditions. *Environ Sci Technol*. 2007;41(3):971-977. doi:10.1021/es061517z

28. Tanneru CT, Jothikumar N, Hill VR, Chellam S. Relative insignificance of virus inactivation during aluminum electrocoagulation of saline waters. *Environ Sci Technol*. 2014;48(24):14590-14598. doi:10.1021/es504381f

29. Tanneru CT, Chellam S. Sweep flocculation and adsorption of viruses on aluminum flocs during electrochemical treatment prior to surface water microfiltration. *Environ Sci Technol*. 2013;47:4612-4618.

30. Tanneru CT, Chellam S. Mechanisms of virus control during iron electrocoagulation--microfiltration of surface water. *Water Res*. 2012;46(7):2111-2120. doi:10.1016/j.watres.2012.01.032

31. Ghernaout D, Ghernaout B, Boucherit A, Naceur MW, Khelifa A, Kellil A. Study on mechanism of electrocoagulation with iron electrodes in idealised conditions and electrocoagulation of humic acids solution in batch using aluminium electrodes. *Desalin Water Treat*. 2009;8:91-99.

32. Dubrawski KL, Mohseni M. In-situ identification of iron electrocoagulation speciation and application for natural organic matter (NOM) removal. *Water Res*. 2013;47(14):5371-5380. doi:10.1016/j.watres.2013.06.021

33. Moreno C. HA, Cocke DL., Gomes JA, et al. Electrochemical Generation of Green Rust using Electrocoagulation. *ECS Trans*. 2007;3(18):67-78.

34. Zhu B, Clifford DA, Chellam S. Virus removal by iron coagulation-microfiltration. *Water Res*. 2005;39(20):5153-5161. doi:10.1016/j.watres.2005.09.035

35. Abbaszadegan M, Monteiro P, Nwachuku N, Alum A, Ryu H. Removal of adenovirus, calicivirus, and bacteriophages by conventional drinking water treatment. *J Environ Sci Heal Part A*. 2008;43(2):171-177. doi:10.1080/10934520701781541

36. Shirasaki N, Matsushita T, Matsui Y, Urasaki T, Ohno K. Difference in behaviors of F-specific DNA and RNA bacteriophages during coagulation-rapid sand filtration and coagulation-microfiltration processes. *Water Sci Technol Water Supply*. 2012;12(5):666-673. doi:10.2156/WS.2012.041

37. Shirasaki N, Matsushita T, Matsui Y, Oshiba A, Marubayashi T, Sato S. Improved virus removal by high-basicity polyaluminum coagulants compared to commercially available aluminum-based coagulants. *Water Res*. 2014;48:375-386. doi:10.1016/j.watres.2013.09.052

38. Shin G-A, Sobsey MD. Removal of norovirus from water by coagulation, flocculation and sedimentation processes. *Water Sci Technol Water Supply*. 2015;15(1):158-163. doi:10.2166/ws.2014.100

39. Shirasaki N, Matsushita T, Matsui Y, Marubayashi T. Effect of aluminum hydrolyte species on human enterovirus removal from water during the coagulation process. *Chem Eng J*.

2016;284(2016):786-793. doi:10.1016/j.cej.2015.09.045

40. Shirasaki N, Matsushita T, Matsui Y, Urasaki T, Oshiba A, Ohno K. Evaluation of norovirus removal performance in a coagulation-ceramic microfiltration process by using recombinant norovirus virus-like particles. *Water Sci Technol*. 2010;61(8):2027-2034. doi:10.2166/wst.2010.125

41. United States Environmental Protection Agency. Microbial and Disinfection Byproduct Rules Simultaneous Compliance Guidance Manual. *EPA 815-R-99-015*. 1999;(August).

42. Harif T, Khai M, Adin A. Electrocoagulation versus chemical coagulation: Coagulation/flocculation mechanisms and resulting floc characteristics. *Water Res*. 2012;46(10):3177-3188. doi:10.1016/j.watres.2012.03.034

43. Langlet J, Gaboriaud F, Duval JFL, Gantzer C. Aggregation and surface properties of F-specific RNA phages: Implication for membrane filtration processes. *Water Res*. 2008;42(10-11):2769-2777. doi:10.1016/j.watres.2008.02.007

44. Penrod SL, Olson TM, Grant SB. Deposition Kinetics of Two Viruses in Packed Beds of Quartz Granular Media. *Langmuir*. 1996;12(23):5576-5587. doi:10.1021/la950884d

45. Zhuang J, Jin Y. Virus retention and transport as influenced by different forms of soil organic matter. *J Environ Qual*. 2003;32(3):816-823. doi:10.2134/jeq2003.8160

46. Bales RC, Li S, Maguire KM, Yahya MT, Gerba CP. MS-2 and Poliovirus Transport in Porous Media: Hydrophobic Effects and Chemical Perturbations. *Water Resour Res*. 1993;29(4):957-963.

47. Chrysikopoulos C V., Syngouna VI. Attachment of bacteriophages MS2 and ΦX174 onto kaolinite and montmorillonite: Extended-DLVO interactions. *Colloids Surfaces B Biointerfaces*. 2012;92(2012):74-83. doi:10.1016/j.colsurfb.2011.11.028

48. Dowd SE, Pillai SD, Wang S, Corapcioglu Y. Delineating the Specific Influence of Virus Isoelectric Point and Size on Virus Adsorption and Transport through Sandy Soils. *Appl Environ Microbiol*. 1998;64(2):405-410.

49. Schaldach CM, Bourcier WL, Shaw HF, Viani BE, Wilson WD. The influence of ionic strength on the interaction of viruses with charged surfaces under environmental conditions. *J Colloid Interface Sci*. 2006;294(1):1-10. doi:10.1016/j.jcis.2005.06.082

50. Langlet J, Gaboriaud F, Gantzer C, Duval JFL. Impact of chemical and structural anisotropy on the electrophoretic mobility of spherical soft multilayer particles: the case of bacteriophage MS2. *Biophys J*. 2008;94(8):3293-3312. doi:10.1529/biophysj.107.115477

51. Duval JFL, Ohshima H. Electrophoresis of soft particles. *Langmuir*. 2006;22(8):3533-3546. doi:10.1021/la0528293

52. Dika C, Duval JFL, Ly-Chatain HM, Merlin C, Gantzer C. Impact of internal RNA on aggregation and electrokinetics of viruses: Comparison between MS2 phage and corresponding virus-like particles. *Appl Environ Microbiol*. 2011;77(14):4939-4948.

doi:10.1128/AEM.00407-11

53. Langlet J, Ogorzaly L, Schrotter JC, et al. Efficiency of MS2 phage and Qβ phage removal by membrane filtration in water treatment: Applicability of real-time RT-PCR method. *J Memb Sci*. 2009;326(1):111-116. doi:10.1016/j.memsci.2008.09.044

54. Dika C, Ly-Chatain MH, Francius G, Duval JFL, Gantzer C. Non-DLVO adhesion of F-specific RNA bacteriophages to abiotic surfaces: Importance of surface roughness, hydrophobic and electrostatic interactions. *Colloids Surfaces A Physicochem Eng Asp*. 2013;435:178-187. doi:10.1016/j.colsurfa.2013.02.045

55. Duval JFL, Gaboriaud F. Progress in electrohydrodynamics of soft microbial particle interphases. *Curr Opin Colloid Interface Sci*. 2010;15(3):184-195. doi:10.1016/j.cocis.2009.12.002

56. Mayer BK, Yang Y, Gerrity DW, Abbaszadegan M. The impact of capsid proteins on virus removal and inactivation during water treatment processes. *Microbiol Insights*. 2015;8(Suppl 2):15-28. doi:10.4137/Mbi.s31441.TYPE

57. Michen B, Graule T. Isoelectric points of viruses. *J Appl Microbiol*. 2010;109(2):388-397. doi:10.1111/j.1365-2672.2010.04663.x

58. Borodavka A, Tuma R, Stockley PG. Evidence that viral RNAs have evolved for efficient, two-stage packaging. *Proc Natl Acad Sci*. 2012;109(39):15769-15774. doi:10.1073/pnas.1204357109

59. Stockley PG, Twarock R, Bakker SE, et al. Packaging signals in single-stranded RNA viruses: Nature's alternative to a purely electrostatic assembly mechanism. *J Biol Phys*. 2013;39(2):277-287. doi:10.1007/s10867-013-9313-0

60. Gutiérrez L, Mylon SE, Nash B, Nguyen TH. Deposition and aggregation kinetics of rotavirus in divalent cation solutions. *Environ Sci Technol*. 2010;44(12):4552-4557. doi:10.1021/es100120k

61. Yuan B, Pham M, Nguyen TH. Deposition kinetics of bacteriophage MS2 on a silica surface coated with natural organic matter in a radial stagnation point flow cell. *Environ Sci Technol*. 2008;42(20):7628-7633. doi:10.1021/es801003s

62. Nguyen TH, Easter N, Gutiérrez L, et al. The RNA core weakly influences the interactions of the bacteriophage MS2 at key environmental interfaces. *Soft Matter*. 2011;7(21):10449-10456. doi:10.1039/c1sm06092a

63. Dika C, Gantzer C, Perrin A, Duval JFL. Impact of the virus purification protocol on aggregation and electrokinetics of MS2 phages and corresponding virus-like particles. *Phys Chem Chem Phys*. 2013;15(15):5691-5700. doi:10.1039/c3cp44128h

64. Aronino R, Dlugy C, Arkhangelsky E, et al. Removal of viruses from surface water and secondary effluents by sand filtration. *Water Res*. 2009;43(1):87-96. doi:10.1016/j.watres.2008.10.036

65. Dika C, Duval JFL, Francius G, Perrin A, Gantzer C. Isoelectric point is an inadequate descriptor of MS2, Phi X 174 and PRD1 phages adhesion on abiotic surfaces. *J Colloid Interface Sci*. 2015;446(1):327-334. doi:10.1016/j.jcis.2014.08.055

66. Patrick T. Intraluminal pH of the human gastrointestinal tract. *Dan Med Bull*. 1999;46(3):183-196. doi:10.1037/0022-3514.90.4.644

67. Mattle MJ, Crouzy B, Brennecke M, Wigginton KR, Perona P, Kohn T. Impact of virus aggregation on inactivation by peracetic acid and implications for other disinfectants. *Environ Sci Technol*. 2011;45(18):7710-7717. doi:10.1021/es201633s

68. Syngouna VI, Chrysikopoulos C V. Transport of biocolloids in water saturated columns packed with sand: Effect of grain size and pore water velocity. *J Contam Hydrol*. 2012;129-130(3-4):11-24. doi:10.1016/j.jconhyd.2012.01.010

69. Armanious A, Aeppli M, Jacak R, et al. Viruses at Solid-Water Interfaces: A Systematic Assessment of Interactions Driving Adsorption. *Environ Sci Technol*. 2015;50(2):732-743. doi:10.1021/acs.est.5b04644

70. Matsushita T, Suzuki H, Shirasaki N, Matsui Y, Ohno K. Adsorptive virus removal with super-powdered activated carbon. *Sep Purif Technol*. 2013;107:79-84. doi:10.1016/j.seppur.2013.01.017

71. Mylon SE, Rinciog CI, Schmidt N, Gutiérrez L, Wong GCL, Nguyen TH. Influence of salts and natural organic matter on the stability of bacteriophage MS2. *Langmuir*. 2010;26(2):1035-1042. doi:10.1021/la902290t

72. Pham M, Mintz EA, Nguyen TH. Deposition kinetics of bacteriophage MS2 to natural organic matter: Role of divalent cations. *J Colloid Interface Sci*. 2009;338(1):1-9. doi:10.1016/j.jcis.2009.06.025

73. De Kerchove AJ, Elimelech M. Calcium and magnesium cations enhance the adhesion of motile and nonmotile Pseudomonas aeruginosa on alginate films. *Langmuir*. 2008;24(7):3392-3399. doi:10.1021/la7036229

74. Banwart SA. Surface Processes in Water Technology. In: Bidoglio G, Stumm W, eds. *Chemistry in Aquatic Systems: Local and Global Perspectives*. 1st ed. Springer Netherlands; 1994:337-374. doi:10.1007/978-94-017-1024-4

75. Rebhun M, Meir S, Laor Y. Using dissolved humic acid to remove hydrophobic contaminants from water by complexation-flocculation process. *Environ Sci Technol*. 1998;32(7):981-986. doi:10.1021/es9707163

76. Xiao F, Yi P, Pan XR, Zhang BJ, Lee C. Comparative study of the effects of experimental variables on growth rates of aluminum and iron hydroxide flocs during coagulation and their structural characteristics. *Desalination*. 2010;250(3):902-907. doi:10.1016/j.desal.2008.12.050

77. Chang S, Stevenson R, Bryant A, Woodward R, Kabler P. Removal of Coxsackie and Bacterial Viruses in Water by Flocculation II. *Am J Public Heal Nations Heal*.

1958;48(2):159-169.

78. Chaudhuri M, Engelbrecht RS. Removal of Viruses From Water By Chemical Coagulation and Flocculation. *J Am Water Works Assoc*. 1970;62(9):563-567.

79. Wigginton KR, Pecson BM, Sigstam T, Bosshard F, Kohn T. Virus Inactivation Mechanisms: Impact of Disinfectants on Virus Function and Structural Integrity. *Environ Sci Technol*. 2012;46:12069-12078. doi:10.1021/es3029473

80. Ghernaout D, Badis A, Kellil A, Ghernaout B. Application of electrocoagulation in Escherichia coli culture and two surface waters. *Desalination*. 2008;219(1-3):118-125. doi:10.1016/j.desal.2007.05.010

81. Ndjomgoue-Yossa AC, Nanseu-Njiki CP, Kengne IM, Ngameni E. Effect of electrode material and supporting electrolyte on the treatment of water containing Escherichia coli by electrocoagulation. *Int J Environ Sci Technol*. 2015;12(6):2103-2110. doi:10.1007/s13762-014-0609-9

82. Vakil KA, Sharma MK, Bhatia A, Kazmi AA, Sarkar S. Characterization of greywater in an Indian middle-class household and investigation of physicochemical treatment using electrocoagulation. *Sep Purif Technol*. 2014;130:160-166. doi:10.1016/j.seppur.2014.04.018

83. Symonds EM, Cook MM, McQuaig SM, et al. Reduction of nutrients, microbes, and personal care products in domestic wastewater by a benchtop electrocoagulation unit. *Sci Rep*. 2015;5:9380. doi:10.1038/srep09380

84. Gao S, Du M, Tian J, et al. Effects of chloride ions on electro-coagulation-flotation process with aluminum electrodes for algae removal. *J Hazard Mater*. 2010;182(1-3):827-834. doi:10.1016/j.jhazmat.2010.06.114

85. O'Connell KO, Bucher JR, Anderson PE, et al. Real-time fluorgenic reverse transcription-PCR assays for detection of bacteriophage MS2. *Appl Environ Microbiol*. 2006;72(1):478-483. doi:10.1128/AEM.72.1.478-483.2006

86. Langlet J, Gaboriaud F, Gantzer C. Effects of pH on plaque forming unit counts and aggregation of MS2 bacteriophage. *J Appl Microbiol*. 2007;103(5):1632-1638. doi:10.1111/j.1365-2672.2007.03396.x

87. Kuzmanovic DA, Elashvili I, Wick C, O'Connell C, Krueger S. The MS2 Coat Protein Shell is Likely Assembled Under Tension: A Novel Role for the MS2 Bacteriophage A Protein as Revealed by Small-angle Neutron Scattering. *J Mol Biol*. 2006;355(5):1095-1111. doi:10.1016/j.jmb.2005.11.040

88. Ryu H, Mayer BK, Abbaszadegan M. Applicability of quantitative PCR for determination of removal efficacy of enteric viruses and Cryptosporidium by water treatment processes. *J Water Health*. 2009;7(1). doi:10.2166/wh.2009.008

89. Bae J, Schwab KJ. Evaluation of murine norovirus, feline calicivirus, poliovirus, and MS2 as surrogates for human norovirus in a model of viral persistence in surface water and

groundwater. *Appl Environ Microbiol*. 2008;74(2):477-484. doi:10.1128/AEM.02095-06

90. Thurston-Enriquez JA, Haas CN, Jacangelo J, Riley KR, Gerba CP. Inactivation of Feline Calicivirus and Adenovirus Type 40 by UV Radiation. *Appl Environ Microbiol*. 2003;69(1):577-582. doi:10.1128/AEM.69.1.577

91. Dubrawski KL, Van Genuchten CM, Delaire C, Amrose SE, Gadgil AJ, Mohseni M. Production and transformation of mixed-valent nanoparticles generated by Fe(0) electrocoagulation. *Environ Sci Technol*. 2015;49(4):2171-2179. doi:10.1021/es505059d

92. van Genuchten CM, Peña J, Amrose SE, Gadgil AJ. Structure of Fe(III) precipitates generated by the electrolytic dissolution of Fe(0) in the presence of groundwater ions. *Geochim Cosmochim Acta*. 2014;127(2014):285-304. doi:10.1016/j.gca.2013.11.044

93. Drissi SH, Refait P, Abdelmoula M, Génin JMR. The preparation and thermodynamic properties of Fe(II)Fe(III) hydroxide-carbonate (green rust 1); Pourbaix diagram of iron in carbonate-containing aqueous media. *Corros Sci*. 1995;37(12):2025-2041. doi:10.1016/0010-938X(95)00096-3

94. Li L, van Genuchten CM, Addy SEA, Yao J, Gao N, Gadgil AJ. Modeling As(III) oxidation and removal with iron electrocoagulation in groundwater. *Environ Sci Technol*. 2012;46(21):12038-12045. doi:10.1021/es302456b

95. Keenan CR, Sedlak DL. Factors Affecting the Yield of Oxidants from the Reaction of Nanoparticulate Zero-Valent Iron and Oxygen Factors Affecting the Yield of Oxidants from the Reaction of Nanoparticulate Zero-Valent Iron and Oxygen. *Env Sci Technol*. 2008;42(4):1262-1267. doi:10.1021/es801387s

96. Katsoyiannis IA, Ruettimann T, Hug SJ. pH dependence of Fenton reagent generation and As(III) oxidation and removal by corrosion of zero valent iron in aerated water. *Env Sci Technol*. 2008;42(19):7424-7430.

97. Pang SY, Jiang J, Ma J. Oxidation of sulfoxides and arsenic(III) in corrosion of nanoscale zero valent iron by oxygen: Evidence against ferryl ions (Fe(IV)) as active intermediates in fenton reaction. *Environ Sci Technol*. 2011;45(1):307-312. doi:10.1021/es102401d

98. Kim JY, Lee C, Love DC, Sedlak DL, Yoon J, Nelson KL. Inactivation of MS2 coliphage by ferrous ion and zero-valent iron nanoparticles. *Environ Sci Technol*. 2011;45(16):6978-6984. doi:10.1021/es201345y

99. Delaire C, Van Genuchten CM, Nelson KL, Amrose SE, Gadgil AJ. Escherichia coli attenuation by Fe electrocoagulation in synthetic Bengal groundwater: effect of pH and natural organic matter. *Environ Sci Technol*. 2015;49(16):9945-9953. doi:10.1021/acs.est.5b01696

100. Kim JY, Lee C, Sedlak DL, Yoon J, Nelson KL. Inactivation of MS2 coliphage by Fenton's reagent. *Water Res*. 2010;44(8):2647-2653. doi:10.1016/j.watres.2010.01.025

101. Heffron J, Mayer BK. Virus mitigation by coagulation: recent discoveries and future directions. *Environ Sci Water Res Technol*. 2016;2(3):443-459. doi:10.1039/C6EW00060F

102. Pawar V, Gawande S. An overview of the Fenton Process for Industrial Wastewater. *J Mech Civ Eng*. 2015:127-136.

103. Bataineh H, Pestovsky O, Bakac A. pH-induced mechanistic changeover from hydroxyl radicals to iron(iv) in the Fenton reaction. *Chem Sci*. 2012;3(5):1594-1599. doi:10.1039/c2sc20099f

104. Neyens E, Baeyens J. A review of classic Fenton's peroxidation as an advanced oxidation technique. *J Hazard Mater*. 2003;98(1-3):33-50. doi:10.1016/S0304-3894(02)00282-0

105. Pignatello J, Oliveros E, MacKay A. Advanced oxidation processes for organic contaminant destruction based on the Fenton reaction and related chemistry. *Crit Rev Environ Sci Technol*. 2006;36:1-84. doi:10.1080/10643380500326564

106. Reinke LA, Rau JM, Mccay PB. Characteristics of an Oxidant formed during Iron(II) Autoxidation. *Free Radic Biol Med*. 1994;16(4):485-492.

107. Rush JD, Maskos Z, Koppenol WH. Distinction between hydroxyl radical and ferryl species. *Methods Enzymol*. 1990;186(C):148-156. doi:10.1016/0076-6879(90)86104-4

108. Bossmann SH, Oliveros E, Göb S, et al. New evidence against hydroxyl radicals as reactive intermediates in the thermal and photochemically enhanced fenton reactions. *J Phys Chem A*. 1998;102(28):5542-5550. doi:10.1021/jp980129j

109. Pestovsky O, Stoian S, Bominaar EL, et al. Aqueous FeIV=O: Spectroscopic identification and oxo-group exchange. *Angew Chemie - Int Ed*. 2005;44(42):6871-6874. doi:10.1002/anie.200502686

110. Sharma VK, Zboril R. Ferryl and Ferrate Species: Mössbauer Spectroscopy Investigation. *Croat Chem Acta*. 2015;88(4):363-368. doi:10.5562/cca2686

111. Hug SJ, Leupin OX. Iron-catalyzed oxidation of arsenic (III) by oxygen and by hydrogen peroxide: pH-dependent formation of oxidants in the Fenton reaction RN - Environ. Sci. Technol., vol. 37, pp. 2734-2742. 2003;37(12):2734-2742.

112. He J, Yang X, Men B, Wang D. Interfacial mechanisms of heterogeneous Fenton reactions catalyzed by iron-based materials: A review. *J Environ Sci (China)*. 2016;39:97-109. doi:10.1016/j.jes.2015.12.003

113. Oleg Pestovsky, Bakac A. Identification and Characterization of Aqueous Ferryl(IV) Ion. In: *Ferrates*. ; 2008:167-176.

114. Goldstein S, Meyerstein D, Czapski G. The Fenton reagents. *Free Radic Biol Med*. 1993;15:435-445. doi:10.1201/9781351072922

115. Lakshmanan D, Clifford DA. Ferrous and Ferric Ion Generation During Iron Electrocoagulation. *Env Sci Technol*. 2009;43(10):3853-3859.

116. Hussain SN, de las Heras N, Asghar HMA, Brown NW, Roberts EPL. Disinfection of water by adsorption combined with electrochemical treatment. *Water Res*. 2014;54:170-178.

doi:10.1016/j.watres.2014.01.043

117. Lacasa E, Tsolaki E, Sbokou Z, Rodrigo MA, Mantzavinos D, Diamadopoulos E. Electrochemical disinfection of simulated ballast water on conductive diamond electrodes. *Chem Eng J*. 2013;223:516-523. doi:10.1016/j.cej.2013.03.003

118. Rajab M, Heim C, Letzel T, Drewes JE, Helmreich B. Electrochemical disinfection using boron-doped diamond electrode - The synergetic effects of in situ ozone and free chlorine generation. *Chemosphere*. 2015;121:47-53. doi:10.1016/j.chemosphere.2014.10.075

119. Ahmadi A, Wu T. Inactivation of E. coli using a novel TiO2 nanotube electrode. *Environ Sci Water Res Technol*. 2017;3:534-545. doi:10.1039/C6EW00319B

120. Bruguera-Casamada C, Sirés I, Brillas E, Araujo RM. Effect of electrogenerated hydroxyl radicals, active chlorine and organic matter on the electrochemical inactivation of Pseudomonas aeruginosa using BDD and dimensionally stable anodes. *Sep Purif Technol*. 2017;178:224-231. doi:10.1016/j.seppur.2017.01.042

121. Cotillas S, Llanos J, Cañizares P, Mateo S, Rodrigo MA. Optimization of an integrated electrodisinfection/electrocoagulation process with Al bipolar electrodes for urban wastewater reclamation. *Water Res*. 2013;47(5):1741-1750. doi:10.1016/j.watres.2012.12.029

122. Bruguera-Casamada C, Sires I, Prieto MJ, Brillas E, Araujo RM. The ability of electrochemical oxidation with a BDD anode to inactivate Gram-negative and Gram-positive bacteria in low conductivity sulfate medium. *Chemosphere*. 2016;163:516-524. doi:10.1016/j.chemosphere.2016.08.042

123. Cossali G, Routledge EJ, Ratcliffe MS, Blakes H, Karayiannis TG. Inactivation of E . coli , Legionella and Pseudomonas in Tap Water Using Electrochemical Disinfection. *J Environ Eng*. 2016;142(12):04016063. doi:10.1061/(ASCE)EE.1943-7870.0001134.

124. Fang Q, Shang C, Chen G. MS2 Inactivation by Chloride-Assisted Electrochemical Disinfection. *J Environ Eng*. 2006;132(1):13-22. doi:10.1061/(ASCE)0733-9372(2006)132:1(13)

125. Drees KP, Abbaszadegan M, Maier RM. Comparative electrochemical inactivation of bacteria and bacteriophage. *Water Res*. 2003;37:2291-2300. doi:10.1016/S0043-1354(03)00009-5

126. Huang X, Qu Y, Cid CA, et al. Electrochemical disinfection of toilet wastewater using wastewater electrolysis cell. *Water Res*. 2016;92:164-172. doi:10.1016/j.watres.2016.01.040

127. Radjenovic J, Sedlak DL. Challenges and Opportunities for Electrochemical Processes as Next-Generation Technologies for the Treatment of Contaminated Water. *Environ Sci Technol*. 2015;49(19):11292-11302. doi:10.1021/acs.est.5b02414

128. Macpherson J V. A practical guide to using boron doped diamond in electrochemical

research. *Phys Chem Chem Phys*. 2015;17(5):2935-2949. doi:10.1039/c4cp04022h

129. Polcaro AM, Vacca A, Mascia M, Palmas S, Rodiguez Ruiz J. Electrochemical treatment of waters with BDD anodes: Kinetics of the reactions involving chlorides. *J Appl Electrochem*. 2009;39(11):2083-2092. doi:10.1007/s10800-009-9870-x

130. Palmas S, Polcaro AM, Vacca A, Mascia M, Ferrara F. Influence of the operating conditions on the electrochemical disinfection process of natural waters at BDD electrodes. *J Appl Electrochem*. 2007;37(11):1357-1365. doi:10.1007/s10800-007-9368-3

131. Jeong J, Kim JY, Yoon J. The role of reactive oxygen species in the electrochemical inactivation of microorganisms. *Environ Sci Technol*. 2006;40(19):6117-6122. doi:10.1021/es0604313

132. Mascia M, Vacca A, Palmas S. Electrochemical treatment as a pre-oxidative step for algae removal using Chlorella vulgaris as a model organism and BDD anodes. *Chem Eng J*. 2013;219:512-519. doi:10.1016/j.cej.2012.12.097

133. Bard AJ, Faulkner LR. *Electrochemical Methods - Fundamentals and Applications*. 2nd ed. New York: John Wiley & Sons, Inc.; 2001.

134. Bagotsky VS. *Fundamentals of Electrochemistry*. 2nd ed. Hoboken, New Jersey: John Wiley & Sons, Inc; 2006.

135. Arslan-Alaton I. Treatability of a simulated disperse dye-bath by ferrous iron coagulation, ozonation, and ferrous iron-catalyzed ozonation. *J Hazard Mater*. 2001;85(3):229-241. doi:10.1016/S0304-3894(01)00232-1

136. Beltrán FJ, Rivas FJ, Montero-De-Espinosa R. Iron type catalysts for the ozonation of oxalic acid in water. *Water Res*. 2005;39(15):3553-3564. doi:10.1016/j.watres.2005.06.018

137. Legube B, Karpel Vel Leitner N. Catalytic ozonation: a promising advanced oxidation technology for water treatment. *Catal Today*. 1999;53(1):61-72. doi:10.1016/S0920-5861(99)00103-0

138. Sreethawong T, Chavadej S. Color removal of distillery wastewater by ozonation in the absence and presence of immobilized iron oxide catalyst. *J Hazard Mater*. 2008;155(3):486-493. doi:10.1016/j.jhazmat.2007.11.091

139. Sjogren JC, Sierka RA. Inactivation of phage MS2 by iron-aided titanium dioxide photocatalysis. *Appl Environ Microbiol*. 1994;60(1):344-347.

140. Vepsäläinen M, Pulliainen M, Sillanpää M. Effect of electrochemical cell structure on natural organic matter (NOM) removal from surface water through electrocoagulation (EC). *Sep Purif Technol*. 2012;99(2012):20-27. doi:10.1016/j.seppur.2012.08.011

141. Ben-Sasson M, Zidon Y, Calvo R, Adin A. Enhanced removal of natural organic matter by hybrid process of electrocoagulation and dead-end microfiltration. *Chem Eng J*. 2013;232:338-345. doi:10.1016/j.cej.2013.07.101

142. Adapureddy SM, Goel S. Optimizing Electrocoagulation of Drinking Water for Turbidity Removal in a Batch Reactor. In: *International Conference on Environmental Science and Technology IPCBEE*. Vol 30. ; 2012:97-102.

143. Koparal AS, Yildiz Y, Keskinler B, Demircioglu N. Effect of initial pH on the removal of humic substances from wastewater by electrocoagulation. *Sep Purif Technol*. 2008;59(2):175-182. doi:10.1016/j.seppur.2007.06.004

144. Vepsäläinen M, Ghiasvand M, Selin J, et al. Investigations of the effects of temperature and initial sample pH on natural organic matter (NOM) removal with electrocoagulation using response surface method (RSM). *Sep Purif Technol*. 2009;69(3):255-261. doi:10.1016/j.seppur.2009.08.001

145. Acheson NH. *Fundamentals of Molecular Virology*. 1st ed. Hoboken, New Jersey: John Wiley & Sons, Inc.; 2007.

146. Sigstam T, Gannon G, Cascella M, Pecson BM, Wigginton KR, Kohn T. Subtle differences in virus composition affect disinfection kinetics and mechanisms. *Appl Environ Microbiol*. 2013;79(11):3455-3467. doi:10.1128/AEM.00663-13

147. Engelbrecht RS, Weber MJ, Salter BL, Schmidt CA. Comparative inactivation of viruses by chlorine. *Appl Environ Microbiol*. 1980;40(2):249-256.

148. Cromeans TL, Kahler AM, Hill VR. Inactivation of adenoviruses, enteroviruses, and murine norovirus in water by free chlorine and monochloramine. *Appl Environ Microbiol*. 2010;76(4):1028-1033. doi:10.1128/AEM.01342-09

149. Toropova K, Stockley PG, Ranson NA. Visualising a viral RNA genome poised for release from its receptor complex. *J Mol Biol*. 2011;408(3):408-419. doi:10.1016/j.jmb.2011.02.040

150. Beck NK, Callahan K, Nappier SP, Kim H, Sobsey MD, Meschke JS. Development of a spot-titer culture assay for quantifying bacteria and viral indicators. *J Rapid Methods Autom Microbiol*. 2009;17(4):455-464. doi:10.1111/j.1745-4581.2009.00182.x

151. Brion GM, O'Banion NB, Marchin GL. Comparison of bacteriophages for use in iodine inactivation: Batch and continuous flow studies. *J Water Health*. 2004;2(4):261-266.

152. Yang Y, Griffiths MW. Comparative persistence of subgroups of F-specific RNA phages in river water. *Appl Environ Microbiol*. 2013;79(15):4564-4567. doi:10.1128/AEM.00612-13

153. Boudaud N, Machinal C, David F, et al. Removal of MS2, Qβ and GA bacteriophages during drinking water treatment at pilot scale. *Water Res*. 2012;46(8):2651-2664. doi:10.1016/j.watres.2012.02.020

154. Jofre J, Ollé E, Ribas F, Vidal A, Lucena F. Potential usefulness of bacteriophages that infect Bacteroides fragilis as model organisms for monitoring virus removal in drinking water treatment plants . These include : Potential Usefulness of Bacteriophages That Infect Bacteroides fragilis as Model O. *Appl Environ Microbiol*. 1995;61(9):3227-3231.

3. OBJECTIVE 1: BACTERIOPHAGE INACTIVATION AS A FUNCTION OF FERROUS IRON OXIDATION

Abstract

Iron-based disinfection has promise as a low-cost, low-byproduct means of virus mitigation. This research determined that virus inactivation due to ferrous iron was impacted both by the extent of iron oxidation (from ferrous to ferric iron) and the rate of iron oxidation. Log inactivation of bacteriophages increased linearly with ferrous iron concentration at low doses (< 3 mg/L Fe), but higher doses limited disinfection, likely due to floc formation. Stumm and Lee's model of ferrous iron oxidation was adapted to explain the impacts of iron oxidation on bacteriophage inactivation. Bacteriophage inactivation increased with the inverse of pH and dissolved oxygen concentration, suggesting that slower iron oxidation rates allow better contact between viruses and reactive ferrous iron. Ferrous iron showed potential as a means of disinfection, though engineering controls (*e.g.*, pH adjustment) are necessary to regulate iron oxidation and precipitation.

3.1. Introduction

Waterborne viruses are a pervasive source of gastric and respiratory illnesses, both acute and chronic.[1,2] The World Health Organization's (WHO) *Guidelines for Drinking Water Quality*[3] identifies eight enteric viruses of concern for drinking water, all of which have high infectivity and persistence in the environment relative to other pathogens. Though enteric viruses in general are classified as "moderately tolerant" to chlorine disinfection by the U.S. Centers for Disease Control and Prevention,[4] adenoviruses are particularly resistant to UV disinfection.[5] With diameters generally less than 100 nm,[6] enteric viruses are also less susceptible to particle separation than other pathogens.[7]

Water treatment technologies featuring various iron species have attracted attention in virus mitigation research. Such technologies include iron oxide-augmented sand filtration,[8,9] iron-embedded membranes,[10] iron granules in columns or batch reactors,[11] iron nanoparticles,[12] and electrocoagulation with iron electrodes.[13] Iron-based disinfectants contribute less to disinfection byproducts (DBPs) than conventional disinfectants. Ferrate (Fe^{VI}) salts are currently receiving attention as a green oxidant because ferrates do not contribute to chlorinated or brominated DBPs.[14] Compared to ferrate salts, ferrous salts and zero-valent iron are inexpensive and readily available. Ferric salts are often added in water treatment as a coagulant; ferric hydroxide flocs formed from oxidizing zero-valent iron or ferrous salts could serve the same function. Therefore, iron-based oxidation could be achieved in traditional water treatment facilities with a single chemical (*e.g.*, a ferrous salt) for a combined disinfection and coagulation treatment process.

Several researchers[8,11–13,15] have reported irreversible virus reduction – *i.e.*, viruses that cannot be recovered by elution – as well as damage to viral genomes and capsid proteins using iron-based technologies.[12] These reports suggest that inactivation is a significant mechanism of virus mitigation in addition to charge neutralization and physical adsorption to iron surfaces.[8,11–13,15] Using an enzyme-linked immunosorbent assay (ELISA) to detect a decrease in antigenicity and quantitative reverse transcriptase polymerase chain reaction (qRT-PCR) to detect genomic damage, Kim et al.[12] determined that capsid damage (lower antigenicity) was a mechanism of MS2 inactivation via ferrous iron, while genomic damage was not detected.

In the presence of dissolved oxygen, ferrous iron is oxidized to ferric iron via ferryl iron (Fe^{IV}), an unstable intermediate.[16] Ferryl iron is a strong oxidant with an oxidation potential of 1.4 V for the Fe^{4+}/Fe^{3+} couple,[17] slightly lower than that of hypochlorite ($OCl^–/Cl^–$, 1.48 V).[18] Other species may be oxidized during the reduction of ferryl to ferric iron, due to either direct

oxidation by ferryl iron or the production of reactive oxygen species (ROS).[16,17] The evolution of ROS using iron via the Fenton process has been well documented.[19–21] Even without the addition of hydrogen peroxide, oxidation of zero-valent iron by dissolved oxygen has been shown to generate Fenton's reagent (ferrous iron and H_2O_2), as well as ROS associated with the Fenton reaction, such as hydroxyl ($^{\bullet}OH$) and superoxide ($^{\bullet}O_2^-$) radicals.[12,22,23] The Fenton reaction is generally considered ineffective near neutral pH.[22] Nevertheless, researchers[12,22,24] have demonstrated the oxidative effects of zero-valent and ferrous iron near neutral pH, commonly attributed to the formation of ferryl ions ($Fe^{IV}O^{2+}$).[24,25]

Despite initial confirmation that iron-based disinfection of viruses does occur, the process is poorly understood. Near neutral pH, oxidant generation arises predominately from the oxidation of ferrous iron by dissolved oxygen.[26] Accordingly, the oxidation of ferrous iron seems to be essential to bacteriophage degradation.[12] Disinfection of MS2 bacteriophage due to ferrous/zero-valent iron is greatest at low pH (pH 5.5 to 6),[12,27] though generation of ROSs by iron oxidation have not been observed in this range.[24,26] Therefore, rapid iron oxidation may lead to shorter exposure and therefore poorer contact between the virus and reactive ferrous iron, and therefore less efficient disinfection.

The goal of this research was to better delineate how the extent and rate of ferrous iron oxidation impacts bacteriophage inactivation. Bacteriophages are frequently used as surrogates for human viruses in water treatment process research.[28–32] Irreversible reduction in bacteriophage concentrations was measured to determine the degree to which the ferrous iron dose, retention time, chemical quenching, and oxidation rate impacted virus inactivation. The iron oxidation rate was altered by varying pH and dissolved oxygen. The impact of dose, pH, and dissolved oxygen on bacteriophage inactivation was used to evaluate an inactivation model based on iron oxidation kinetics. In addition to advancing a model relating ferrous oxidation and

inactivation, the results of this study corroborate previous research by using a virus elution method to verify that bacteriophage reduction is due to inactivation rather than physical removal via coagulation/filtration.

3.2. Materials and Methods

3.2.1. Preparation of Test Waters

Sodium bicarbonate (2.97 mM) was added to PureLab ultrapure water (ELGA LabWater, UK) to provide alkalinity (150 mg/L as $CaCO_3$) and prevent pH from fluctuating with the addition of varying doses of ferrous chloride. The pH was adjusted using 0.5 N HCl or NaOH as required. In tests of the effect of pH on bacteriophage inactivation, the test water was adjusted to achieve pH values between 6 and 8.5; all other tests were performed at pH 7.0. To test the effect of dissolved oxygen on bacteriophage inactivation, dissolved oxygen was adjusted by degassing the solution with argon to achieve concentrations of 0.25 to 6.5 mg/L O_2. Dissolved oxygen, pH, and conductivity were measured using a Symphony multiparameter meter (VWR, Batavia, IL).

3.2.2. Virus Propagation and Quantification

Two bacteriophages were used as surrogates for human viruses: MS2 (ATCC 15597-B1) and P22 (ATCC 19585-B1). MS2 is an F-specific coliphage with a single-stranded RNA genome (Baltimore group IV), while P22 is a tailed enterobacteria phage with a double-stranded DNA genome (Baltimore group I).[31] *Escherichia coli* C-3000 (ATCC 15597) and *Salmonella enterica* subsp. *enterica* serovar Typhimurium strain LT2 (ATCC 19585) were used as the host bacteria for MS2 and P22, respectively. Bacteriophages were propagated using the double-agar layer (DAL) method and purified by two cycles of polyethylene glycol (PEG) precipitation followed by a Vertrel XF (DuPont, Wilmington, DE) purification, as described by Mayer et al.[33] Bacteriophages were quantified using the spot titer plaque assay method as described by Beck et al.[34] Samples

containing bacteriophages were diluted in tenfold series, and ten 10-µL drops of each dilution were plated. Only those sets of plaque counts which did not include zero within the 95% confidence interval were considered.

Virus inactivation was determined based on infectious virus recovery by elution in beef broth.[35,36] Homogenized solutions were sampled from reactors and vortexed 10 s with an equal volume of 6% beef broth (pH 9.5) immediately prior to dilution and plating. Recoverable viruses represented the total infectious viruses present in solution, and the reduction in viruses between untreated (control) samples and treated samples (ferrous chloride) represented inactivated viruses. Confirmation of recovery by elution is provided in Appendix A.1.

3.2.3.Batch Reactor Tests

Iron-based inactivation was performed in 200-mL polypropylene batch reactors. Bacteriophages were spiked at concentrations of approximately 10^7 PFU/mL. Ferrous chloride ($FeCl_2 \bullet 4H_2O$) or ferric chloride ($FeCl_3 \bullet 6H_2O$) was diluted in ultrapure water to a concentration of 9 mM, and then added to individual reactors to achieve target concentrations ranging from 0.25 mg/L Fe to 9.7 mg/L Fe. Reactors were stirred using magnetic stir bars (16 mm length, 8 mm diameter) at 600 rpm for 30 s after addition of the iron salt to simulate rapid mixing, and then at a slower stir rate of 60 rpm for the remainder of the retention time (flocculation). Retention time ranged from 30 s to 120 min for kinetic tests and up to 48 h for tests achieving 99% iron oxidation. For tests demonstrating bacteriophage inactivation during iron oxidation (*i.e.*, before total oxidation), an excess of sodium thiosulfate (25 g/L) was added to samples taken after partial iron oxidation to prevent further oxidation during sample dilution and plating.

Total and ferrous iron concentrations were measured using Hach FerroVer Total Iron and Ferrous Iron Reagent (Hach, Loveland, CO). Absorbance was measured at 510 nm using a

Genesys 20 spectrophotometer (Thermo Fisher Scientific, Waltham, MA). Ferrous iron concentrations were measured at the same time the samples were plated for virus quantification. Total iron concentrations were measured after all samples had been plated for virus quantification.

3.2.4. Ferrous Oxidation Modeling

To evaluate the correlation between bacteriophage inactivation to ferrous oxidation, a hypothetical model was developed against which to test the assumptions that the extent and rate of iron oxidation impact virus mitigation. According to fundamental work by Stumm and Lee,[37] the rate of ferrous iron oxidation is directly proportional to the ferrous iron concentration, dissolved oxygen concentration, and the square of the hydroxide concentration:

$$-\frac{d[Fe(II)]}{dt} = k[Fe(II)][O_2][OH^-]^2 \quad (3\text{-}1)$$

To test the hypothesis that virus mitigation is improved by both a higher dose of ferrous iron (C_0) and a slower rate of ferrous oxidation, the following possible correlations were evaluated:

$$\ln\left(\frac{N}{N_0}\right) \propto C_0\left[\frac{d[Fe(II)]}{dt}\right]^{-1} \propto \frac{-C_0}{k[O_2][OH^-]^2} \quad (3\text{-}2)$$

where N is the concentration of bacteriophages after treatment (PFU/mL), N_0 is the initial concentration of bacteriophages, and C_0 is the initial ferrous dose. Therefore, log inactivation would be expected to be directly proportional to the initial ferrous iron dose and inversely proportional to the concentration of dissolved oxygen ($[O_2]$) and the square of the hydroxide concentration ($[OH^-]^2$) if this hypothesis holds true.

However, actual ferrous oxidation rates were found to deviate from this hypothesized model. Apparent 4th-order rate constant (k') values for ferrous oxidation were determined by adding ferrous chloride (2.5 mg/L Fe) to 400 mL batch reactors and measuring ferrous

concentrations for 60 min. Ferrous oxidation was fit to an exponential curve at each pH tested (5.99 to 8.06). As shown in Figure 3-1, the apparent rate constant values (*k'*) calculated from ferrous oxidation kinetics over this pH range were inversely proportional to the hydroxide concentration. In terms of the Stumm and Lee model, the *k'* value decreased as a function of the hydroxide concentration. Since $k' \sim k[OH^-]^{-1}$, Equation 3-2 can be rewritten as:

$$\ln\left(\frac{N}{N_0}\right) \propto \frac{-C_0}{k'[O_2][OH^-]} \tag{3-3}$$

(A) Ferrous oxidation **(B) apparent k values (*k'*)**

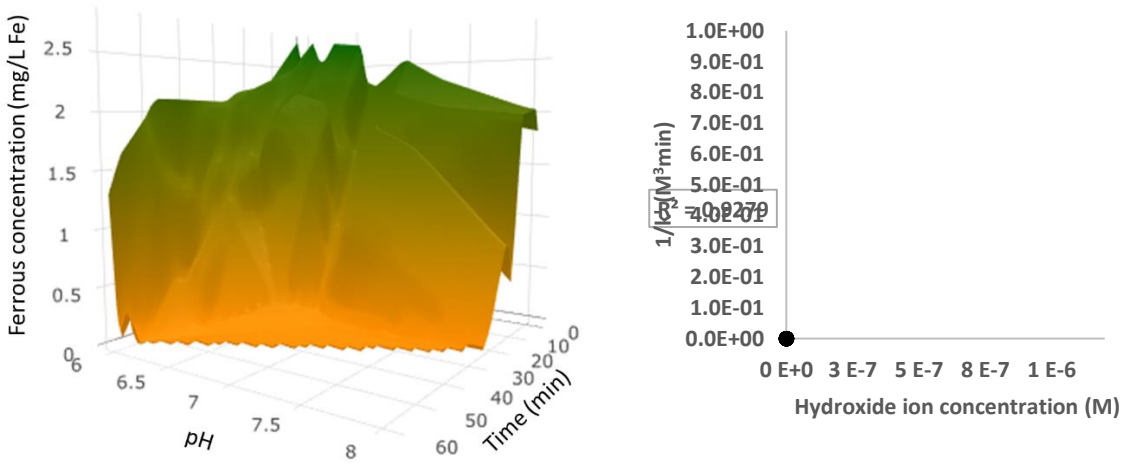

Figure 3-1. Ferrous oxidation kinetics as a function of pH. Part (A) shows ferrous oxidation over time as a function of pH, while part (B) shows the corresponding relationship of the inverse apparent rate constant value (k') to hydroxide concentration. Decrease in ferrous iron concentration was measured in 3 mM $NaHCO_3$ solution at pH 5.99 to 8.02. Over this pH range, k' was not constant, as predicted by the Stumm and Lee ferrous oxidation model, but was rather inversely proportional to the hydroxide concentration. The surface shown in part (A) was interpolated from >100 data points.

The actual rate of ferrous oxidation over this pH range was therefore proportional to the inverse of the hydroxide concentration, rather than the square of the inverse. This deviation from Stumm and Lee's model is likely due to speciation of ferrous iron and carbonate. In sodium bicarbonate solutions greater than 2 mM, slower-oxidizing iron carbonate species (*esp.*, $Fe(CO_3)_2^{2+}$) increasingly dominate iron oxidation kinetics between pH 6 and 8.[38]

3.2.5.Rate of Floc Formation

Floc formation over time was measured by dynamic light scattering using a ZetaSizer Nano-ZS (Malvern Panalytical, Worcestershire, UK). Ferrous chloride was added to 200-mL reactors in doses ranging from 0.26 to 12.2 mg/L Fe, as in inactivation tests. After vigorous agitation for 10 s, 4-mL aliquots were transferred to cuvettes for particle size measurement. Floc formation was measured within the cuvettes in order to collect continuous data during floc formation and avoid breaking up flocs while transferring samples. Particle size was measured multiple times (7 – 10) over approximately one hour. Cuvettes were gently inverted between particle size readings to simulate gentle mixing.

3.2.6.Data Analysis

Bacteriophage inactivation was correlated to parameters of percent iron oxidation, ferrous iron dose, pH and dissolved oxygen concentration by linear regression. Linear regressions and data transformations were performed in the R statistical language using the stats package.[39] A link for the R script is provided in Appendix A.3. Models were evaluated for residual distribution, normality, and leverage points (Cook's distance) using the plot.lm() function, and significance of variables was evaluated by analysis of variance with the anova() function.[39] Linear regression models for mean floc size as a function of time and ferrous iron dose were developed using the same methods.

3.3. Results and Discussion

3.3.1. Extent of Iron Oxidation

The effect of iron oxidation was initially tested by evaluating bacteriophage inactivation over time at a dose of 1 mg/L Fe. Bacteriophage inactivation increased over time and significantly correlated to the extent of iron oxidation (p_{MS2} = 6.95x10^{-10}, p_{P22} = 3.60x10^{-9}), as shown in Figure 3-2A and summarized in Appendix A.4. However, inactivation was not linearly related to the cumulative ferrous exposure (*i.e.*, the ferrous concentration integrated over time, analogous to Ct), as predicted by Chick-Watson disinfection kinetics:

$$\ln\left(\frac{N}{N_0}\right) = -\Lambda_{CW} \int_0^t C\ dt \tag{3-4}$$

Ferrous iron is an indirect oxidizer, in that it must itself be oxidized to a high-valent state (*e.g.*, by dissolved oxygen) before in turn generating an intermediate oxidant, regardless of whether that oxidant is an ROS or high-valent iron species.[16,19] Therefore, ferrous iron would likely not behave as common, "primary" oxidizers (*e.g.*, free chlorine, chloramines, ozone, etc.), in that the ambient ferrous concentration has no effect on virus inactivation. Only the ferrous iron that becomes oxidized has an ability to inactivate viruses; thus the log-linear correlation between inactivation and ferrous oxidation rather than a log-linear correlation with the cumulative impact of ferrous exposure.

Based solely on this test of the kinetics of inactivation (Figure 3-2A), the correlation between inactivation and extent of iron oxidation could indicate that both phenomena are related to time. For this reason, bacteriophage inactivation was also tested over a constant retention time (30 min) using doses of sodium thiosulfate from 0.5 to 4 mg/L to retard iron

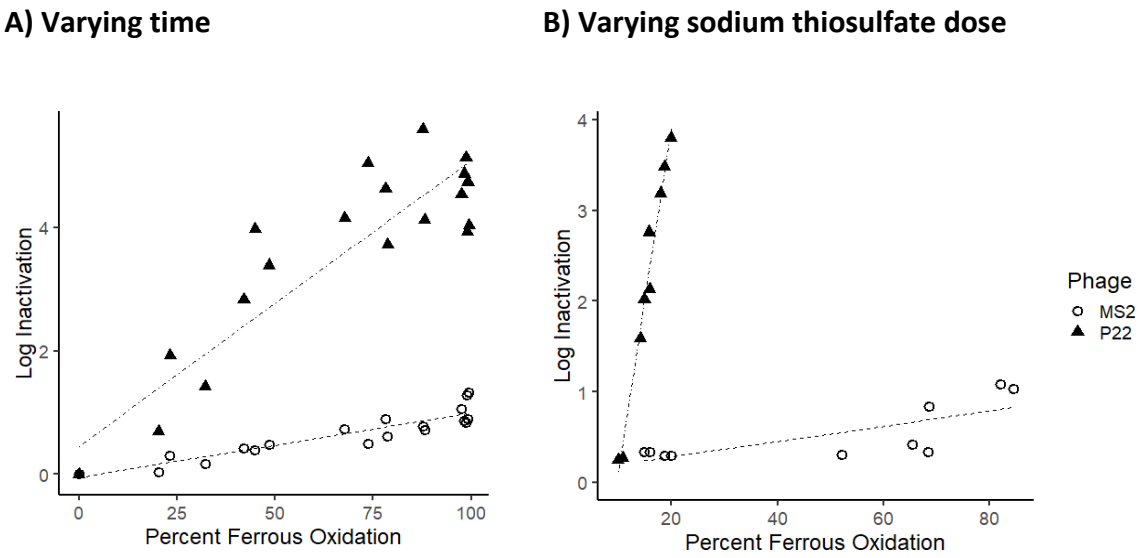

Figure 3-2. Increasing bacteriophage inactivation with ferrous iron oxidation. Iron oxidation was controlled by varying A) time (0.5 to 120 min), and B) sodium thiosulfate dose (0.5 to 4 mg/L). Iron was added as ferrous chloride (1 mg/L Fe). Over a constant retention time of 30 min, bacteriophage inactivation correlated with iron oxidation. Each point represents a single experiment.

oxidation to varying degrees. Iron was again added as ferrous chloride (1 mg/L Fe). Bacteriophage inactivation still significantly correlated to iron oxidation using constant retention time, as shown in Figure 3-2B. A summary of all model parameters is given in Appendix A.4. Log inactivation of the bacteriophages increased with iron oxidation. Since sodium thiosulfate is a reducing agent, this test did not rule out inactivation by secondary reactions other than ferrous oxidation. However, test results showed that inactivation correlated to the extent of ferrous oxidation independent of contact time. In both the variable and constant time tests, P22 inactivation occurred more rapidly and to a far greater extent than MS2, as shown in Figure 3-2. As a tailed bacteriophage, P22's physical structure for attachment and penetration to host bacteria is exposed to the environment,[40] which may make P22 more susceptible to chemical disinfection.

3.3.2.Modeling Inactivation as a Function of Ferrous Iron Oxidation

Though cumulative ferrous exposure did not have a linear impact on inactivation, the rate of ferrous oxidation ostensibly played a critical role. The intermediate oxidants (whether ROS or ferryl species) are short-lived, with half-lives ranging from nanoseconds to seconds.[41,42] In addition, the reduction of ferryl iron to ferric iron can oxidize an equivalent of ferrous iron.[16,19] In this way, ferrous iron may itself compete with viruses for oxidants. Therefore, close proximity between ferrous iron and the virus may be necessary to ensure that virus inactivation can compete with ferrous autoxidation. Both MS2 and P22 are negatively charged near neutral pH,[10,43] and would therefore attract positively-charged ferrous species. A slower rate of oxidation would allow more time for electrostatic accumulation of ferrous ions near the virus surface.

3.3.3.Ferrous Iron Dose

To test the hypothesized effect of C_0 in Equation 3-3, inactivation tests were conducted at varying doses of ferrous chloride. Whereas the tests described in Section 3.3.1 evaluated the kinetics of bacteriophage inactivation during the oxidation process, these tests were conducted to achieve near-total iron oxidation. The duration of the tests was based on the time required to reach 99% oxidation under the slowest oxidizing conditions (4 h). In this way, retention time was held constant in each set of experiments.

Below approximately 3 mg/L Fe, ferrous concentration had a linear positive relationship with log inactivation, as shown in Figure 3-3. The direct linear correlation was significant for both MS2 (p = 6.5x10^{-7}) and P22 (p = 0.000213), as shown in Appendix A.4. This positive linear relationship supports the hypothesized relationship of ferrous concentration in Equation 3-3. However, log inactivation did not continue to increase linearly with ferrous doses higher than 3 mg/L Fe. At this dose, floc formation was visibly more evident than at lower doses, as shown in

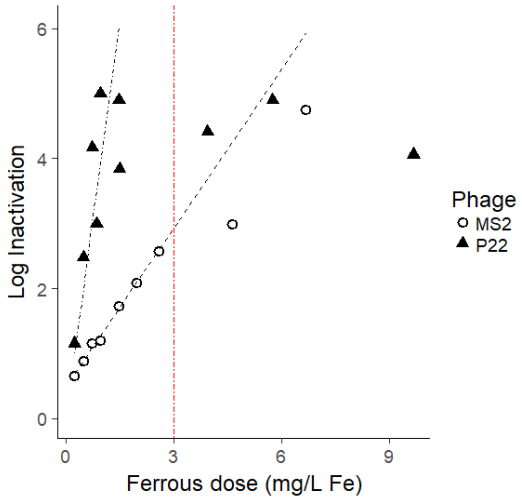

Figure 3-3. The effect of ferrous iron dose on bacteriophage inactivation. Below approximately 3 mg/L Fe (indicated by the vertical red line), both phages showed an approximately linear relationship between ferrous iron concentration and log inactivation, as illustrated by the regression trendlines. Log inactivation did not linearly increase with higher ferrous doses, likely due to rapid floc formation inhibiting contact with the ferrous iron disinfectant. Each point represents a single experiment.

Appendix A.5. When evaluated by dynamic light scattering, both the ultimate particle size and the rate of floc formation, as indicated by the slope coefficient (β) of the time variable, increased with ferrous doses from 0.25 to 2 mg/L Fe (Figure 3-4 and summarized in Appendix A.4). However, floc formation was more rapid and independent of ferrous concentration at doses above 3 mg/L Fe.

Previous research[35,44] has reported that virus inclusion in flocs can inhibit chlorine disinfection. The more rapid flocculation at higher ferrous concentration likely prevents contact between the enmeshed phages and oxidizing iron. The shielding of bacteriophages within flocs thus inhibits the greater disinfection expected at higher doses. Furthermore, ferrous iron bound in particles is not available to oxidize viruses. Keenan and Sedlak[26,45] confirmed that precipitation of iron species inhibits oxidant generation. Therefore, particle formation poses another engineering hurdle for design of ferrous iron disinfection systems, as disinfection and

floc formation happen simultaneously. However, decreasing pH could help to maintain appropriate disinfection conditions by reducing the rate of particle formation.

3.3.4.Rate of Iron Oxidation

The rate of oxidation was evaluated by varying the factors in Equation 3-3, *i.e.*, hydroxide ions (pH), and dissolved oxygen. As in Section 3.3.3, experiments were conducted until 99% oxidation was achieved under the most limiting conditions. This time varied based on the conditions of each set of experiments: 4 h for dissolved oxygen tests and 48 h for pH tests.

3.3.4.1. Effect of pH on Virus Inactivation

Given the correlation between virus inactivation and iron oxidation, the role of pH in virus inactivation is somewhat counterintuitive. At higher pH, iron oxidation is increasingly rapid, yet bacteriophage inactivation is greater at low pH, as shown in Figure 3-5. Nevertheless, the inverse relationship between hydroxide concentration and log inactivation is anticipated by Equation 3-3. Models for both MS2 and P22 showed a very strong correlation (p values $\approx 10^{-6}$ to 10^{-7}) between log inactivation and the simple inverse that explained over 90% of the variation in the data (adjusted $R^2 > 0.90$). Previous work by Kim et al.[12] also showed greater log MS2 removal at low pH with ferrous iron. However, since this study focused on kinetics rather than carrying iron oxidation out to an endpoint, slower iron oxidation rates at low pH would lead to lower effective doses of oxidized iron. Therefore, the relationship between the hydroxide concentration and log inactivation was less dramatic than the inverse curve shown in Figure 3-5. To test the hypothesized model in this study, consistent doses were needed.

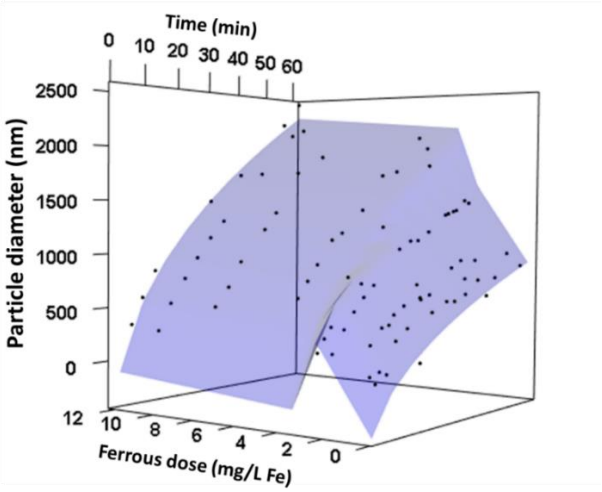

Figure 3-4. Floc formation over time for varying ferrous doses. Points represent single particle diameter readings. The blue surface represents the combined models based on the data points for low (<3 mg/L Fe) and high (> 3 mg/L Fe) ferrous doses.

At higher pH, particles formed far more rapidly than at low pH, as shown in Appendix A.6. Oxidation of iron encourages precipitation of ferrous iron as mixed-valent precipitates such as magnetite.[46] In an equilibrium model of iron speciation using MINEQL+, solid magnetite ($Fe^{II}Fe^{III}_2O_4$) completely replaced ferrous ions (Fe^{2+}) as the dominant species as the stoichiometric ratio of Fe^{III} to Fe^{II} increased from 0 to 2 (Appendix A.6). The thermodynamic favorability of solid magnetite over ferrous ions suggests that the oxidation of ferrous iron has a negative feedback effect on further oxidation by precipitating mixed-valent particles. Thus, faster rates of ferrous oxidation also lead to more rapid particle formation, and thereby poorer oxidant generation/availability, as discussed in Section 3.3.3.

However, the effect of pH cannot be attributed specifically to the rate of ferrous oxidation alone. As mentioned in Section 3.3.2, speciation of iron in carbonate solutions undergoes rate-defining changes in the pH range of 6 to 8. Several researchers[22,26,47] have also hypothesized that the intermediate oxidizer evolved during iron oxidation shifts from hydroxyl radicals at low pH to a putative ferryl oxidant near neutral pH. However, hydroxyl radical

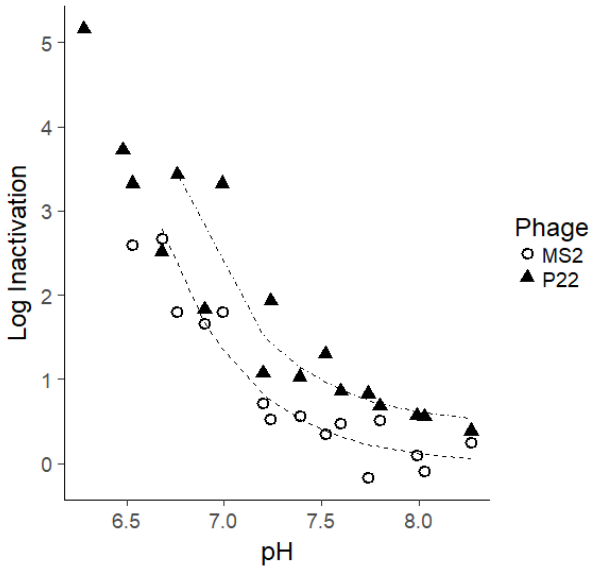

Figure 3-5. Effect of pH on bacteriophage reduction by ferrous iron (0.5 mg/L Fe). Both phages showed an approximately inverse relationship between hydroxide ion concentration (reflected here by plotting pH on the x-axis) and inactivation, as illustrated by the regression trendlines. Each point represents a single experiment.

generation due to iron oxidation is most relevant at pH 5 and below, whereas hydroxyl radical formation is minimal near neutral pH.[22,23,26] In addition, the Fenton reaction has been shown to oxidize organic substrates to form organic radicals.[48] If ferrous iron is sorbed to the capsid surface, the formation of organic radicals may suggest an entirely different mechanism of inactivation.

3.3.4.2. Effect of Dissolved Oxygen on Virus Inactivation

To confirm that a slower oxidation rate increases bacteriophage inactivation, ferrous iron disinfection was performed under a range of dissolved oxygen conditions. As shown in Figure 3-6, greater inactivation was observed at lower dissolved oxygen concentrations below approximately 3 mg/L, whereas inactivation was insensitive to oxygen concentration above 3 mg/L. Earlier work by Kim et al.[12], found overall greater MS2 inactivation by ferrous iron in air saturated water versus deaerated water (dissolved oxygen concentration below detection).

However, Kim et al. found no difference between air saturated and deaerated water at ferrous doses 0.1 mM and lower, the range investigated in this study. In addition, the previous research focused on reaction kinetics over the span of 1 h rather than allowing near-total iron oxidation as in this study. Since ferrous oxidation becomes exponentially slower approaching 0 mg/L dissolved oxygen, stopping the reaction at 1 h would result in a great difference in the extent of iron oxidation between the aerated and deaerated samples.

The regression models of the dissolved oxygen tests revealed very significant correlations between log inactivation and the inverse of the dissolved oxygen concentration for both MS2 ($p = 9.65\text{x}10^{-4}$) and P22 ($p = 6.0\text{x}10^{-4}$), as shown in Appendix A.4. This confirms the effect of dissolved oxygen on inactivation to a high degree of confidence. However, the dissolved oxygen models for MS2 and P22 described less of the variation in the data compared to models for other parameters in this study. The greater unexplained variation was likely due to difficulty in maintaining constant dissolved oxygen concentrations throughout the 4-hour test duration. The argon sparging process also caused a change in pH, requiring pH correction of individual reactors at very low (< 1 mg/L) dissolved oxygen concentrations. Since small changes in pH can affect inactivation (see Figure 3-5), pH most likely contributed to variation as well. By adding final pH and dissolved oxygen concentrations to the regression models, the explanatory power of the models improved slightly ($R^2_{adj} = 0.788$ for MS2 and 0.520 for P22). Regardless, the inverse dissolved oxygen concentration remained significant in the adjusted models for both bacteriophages.

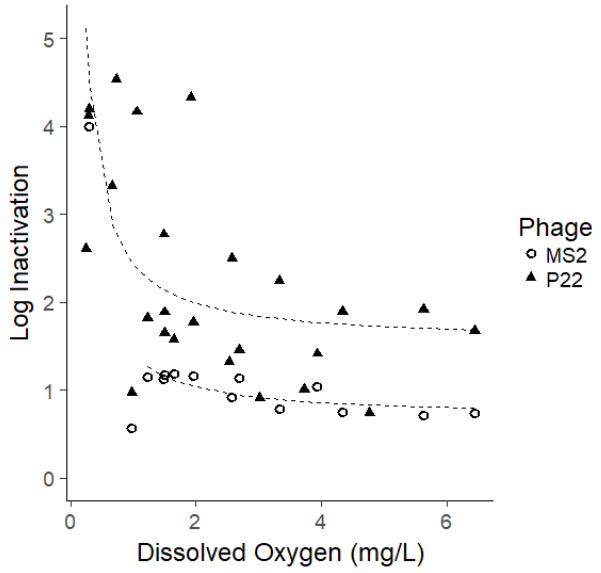

Figure 3-6. Effect of dissolved oxygen on bacteriophage reduction by iron oxidation (0.5 mg/L Fe). Both phages showed an approximately inverse relationship between dissolved oxygen concentration and inactivation, as illustrated by the regression trendlines. Each point represents a single experiment.

3.4. Conclusions

This research demonstrated that bacteriophage inactivation at circumneutral pH relies not only on the extent, but also the rate, of iron oxidation. Decreases in pH and dissolved oxygen both led to greater inactivation, therefore supporting the hypothesis that slower oxidation promotes inactivation. Though inactivation was not correlated to cumulative exposure to ferrous iron, available reactive ferrous iron was necessary for virus inactivation. Based on the hypothesized short-lived oxidants generated by iron oxidation, close contact, or even sorption of ferrous iron, to virus capsids may be necessary for inactivation. In addition, particle formation in faster ferrous oxidation conditions likely inhibited inactivation by shielding viruses and/or inhibiting oxidant generation.

If all ferrous iron is eventually oxidized, the slower oxidation rate achieves greater inactivation. However, for a working treatment process, whether or not all ferrous iron is

oxidized is an important question. Iron oxidation may be too rapid to offer a practical means of disinfection in waters above neutral pH or saturated with dissolved oxygen, while iron oxidation may be impractically slow in groundwater or mildly acidic waters (< pH 6). Pairing iron oxidation with pH control, as in enhanced coagulation, may allow greater disinfection by retarding ferrous oxidation. The pH could then be increased for the flocculation stage to encourage particle formation.

3.5. References

1. Blacklow NR, Greenberg HB. Viral gastroenteritis. *N Engl J Med*. 1991;325(4):252-264.

2. Fong T-T, Lipp EK. Enteric viruses of humans and animals in aquatic environments: Health risks, detection, and potential water quality assessment tools. *Microbiol Mol Biol Rev*. 2005;69(2):357-371. doi:10.1128/MMBR.69.2.357

3. World Health Organization, ed. *WHO Guidelines for Drinking-Water Quality.* 4th ed. Geneva: World Health Organization; 2011. doi:10.1016/S1462-0758(00)00006-6

4. Centers for Disease Control and Prevention. Effect of chlorination on inactivating selected pathogens. http://www.cdc.gov/safewater/effectiveness-on-pathogens.html. Published 2012. Accessed January 1, 2015.

5. Gerba CP, Gramos DM, Nwachuku N. Comparative inactivation of enteroviruses and adenovirus 2 by UV light. *Appl Environ Microbiol*. 2002;68(10):5167. doi:10.1128/AEM.68.10.5167

6. Abbaszadegan M, Lechevallier M, Gerba CP. Occurrence of Viruses in US Groundwaters. *J Am Water Works Assoc*. 2003;95(9):107-120.

7. Tanneru CT, Chellam S. Sweep flocculation and adsorption of viruses on aluminum flocs during electrochemical treatment prior to surface water microfiltration. *Environ Sci Technol*. 2013;47:4612-4618.

8. Ryan JN, Harvey RW, Metge D, Elimelech M, Navigato T, Pieper AP. Field and laboratory investigations of inactivation of viruses (PRD1 and MS2) attached to iron oxide-coated quartz sand. *Environ Sci Technol*. 2002;36(11):2403-2413. doi:10.1021/es011285y

9. Bradley I, Straub A, Maraccini P, Markazi S, Nguyen TH. Iron oxide amended biosand filters for virus removal. *Water Res*. 2011;45(15):4501-4510. doi:10.1016/j.watres.2011.05.045

10. Fidalgo De Cortalezzi MM, Gallardo M V., Yrazu F, et al. Virus removal by iron oxide ceramic membranes. *J Environ Chem Eng*. 2014;2(3):1831-1840.

doi:10.1016/j.jece.2014.08.006

11. You Y, Han J, Chiu PC, Jin Y. Removal and inactivation of waterborne viruses using zerovalent iron. *Environ Sci Technol*. 2005;39(23):9263-9269. doi:10.1021/es050829j

12. Kim JY, Lee C, Love DC, Sedlak DL, Yoon J, Nelson KL. Inactivation of MS2 coliphage by ferrous ion and zero-valent iron nanoparticles. *Environ Sci Technol*. 2011;45(16):6978-6984. doi:10.1021/es201345y

13. Tanneru CT, Chellam S. Mechanisms of virus control during iron electrocoagulation--microfiltration of surface water. *Water Res*. 2012;46(7):2111-2120. doi:10.1016/j.watres.2012.01.032

14. Sharma VK. Oxidation of inorganic contaminants by ferrates (VI, V, and IV)-kinetics and mechanisms: A review. *J Environ Manage*. 2011;92:1051-1073. doi:10.1016/j.jenvman.2010.11.026

15. Kohn T. Adsorption and inactivation of bacteriophage fr on iron oxide coated sand. 2009.

16. Li L, van Genuchten CM, Addy SEA, Yao J, Gao N, Gadgil AJ. Modeling As(III) oxidation and removal with iron electrocoagulation in groundwater. *Environ Sci Technol*. 2012;46(21):12038-12045. doi:10.1021/es302456b

17. Bossmann SH, Oliveros E, Göb S, et al. New evidence against hydroxyl radicals as reactive intermediates in the thermal and photochemically enhanced fenton reactions. *J Phys Chem A*. 1998;102(28):5542-5550. doi:10.1021/jp980129j

18. Sharma G, Choi J, Shon HK, Phuntsho S. Solar-powered electrocoagulation system for water and wastewater treatment. *Desalin Water Treat*. 2011;32(1-3):381-388. doi:10.5004/dwt.2011.2756

19. Bataineh H, Pestovsky O, Bakac A. pH-induced mechanistic changeover from hydroxyl radicals to iron(iv) in the Fenton reaction. *Chem Sci*. 2012;3(5):1594-1599. doi:10.1039/c2sc20099f

20. Neyens E, Baeyens J. A review of classic Fenton's peroxidation as an advanced oxidation technique. *J Hazard Mater*. 2003;98(1-3):33-50. doi:10.1016/S0304-3894(02)00282-0

21. Pignatello J, Oliveros E, MacKay A. Advanced oxidation processes for organic contaminant destruction based on the Fenton reaction and related chemistry. *Crit Rev Environ Sci Technol*. 2006;36:1-84. doi:10.1080/10643380500326564

22. Katsoyiannis IA, Ruettimann T, Hug SJ. pH dependence of Fenton reagent generation and As(III) oxidation and removal by corrosion of zero valent iron in aerated water. *Env Sci Technol*. 2008;42(19):7424-7430.

23. Harada T, Yatagai T, Kawase Y. Hydroxyl radical generation linked with iron dissolution and dissolved oxygen consumption in zero-valent iron wastewater treatment process. *Chem Eng J*. 2016;303:611-620. doi:10.1016/j.cej.2016.06.047

24. Reinke LA, Rau JM, Mccay PB. Characteristics of an Oxidant formed during Iron(II) Autoxidation. *Free Radic Biol Med*. 1994;16(4):485-492.

25. Rush JD, Maskos Z, Koppenol WH. Distinction between hydroxyl radical and ferryl species. *Methods Enzymol*. 1990;186(C):148-156. doi:10.1016/0076-6879(90)86104-4

26. Keenan CR, Sedlak DL. Factors Affecting the Yield of Oxidants from the Reaction of Nanoparticulate Zero-Valent Iron and Oxygen Factors Affecting the Yield of Oxidants from the Reaction of Nanoparticulate Zero-Valent Iron and Oxygen. *Env Sci Technol*. 2008;42(4):1262-1267. doi:10.1021/es801387s

27. Kim JY, Lee C, Sedlak DL, Yoon J, Nelson KL. Inactivation of MS2 coliphage by Fenton's reagent. *Water Res*. 2010;44(8):2647-2653. doi:10.1016/j.watres.2010.01.025

28. Boudaud N, Machinal C, David F, et al. Removal of MS2, Qβ and GA bacteriophages during drinking water treatment at pilot scale. *Water Res*. 2012;46(8):2651-2664. doi:10.1016/j.watres.2012.02.020

29. Ferrer O, Casas R, Galvañ C, et al. Challenge tests with virus surrogates: an accurate membrane integrity evaluation system? *Desalin Water Treat*. 2013;51(1):4947-4957. doi:10.1080/19443994.2013.795339

30. Amarasiri M, Kitajima M, Nguyen TH, Okabe S, Sano D. Bacteriophage removal efficiency as a validation and operational monitoring tool for virus reduction in wastewater reclamation: Review. *Water Res*. 2017;121:258-269. doi:10.1016/j.watres.2017.05.035

31. Grabow WOK. Bacteriophages: Update on application as models for viruses in water. *Water SA*. 2001;27(2):251-268. doi:10.4314/wsa.v27i2.4999

32. Heffron J, Mayer BK. Virus mitigation by coagulation: recent discoveries and future directions. *Environ Sci Water Res Technol*. 2016;2(3):443-459. doi:10.1039/C6EW00060F

33. Mayer BK, Ryu H, Abbaszadegan M. Treatability of U.S. Environmental Protection Agency contaminant candidate list viruses: Removal of coxsackievirus and echovirus using enhanced coagulation. *Environ Sci Technol*. 2008;42(18):6890-6896. doi:10.1021/es801481s

34. Beck NK, Callahan K, Nappier SP, Kim H, Sobsey MD, Meschke JS. Development of a spot-titer culture assay for quantifying bacteria and viral indicators. *J Rapid Methods Autom Microbiol*. 2009;17(4):455-464. doi:10.1111/j.1745-4581.2009.00182.x

35. Tanneru CT, Jothikumar N, Hill VR, Chellam S. Relative insignificance of virus inactivation during aluminum electrocoagulation of saline waters. *Environ Sci Technol*. 2014;48(24):14590-14598. doi:10.1021/es504381f

36. Zhu B, Clifford DA, Chellam S. Virus removal by iron coagulation-microfiltration. *Water Res*. 2005;39(20):5153-5161. doi:10.1016/j.watres.2005.09.035

37. Stumm W, Lee FG. Oxygenation of ferrous iron. *Ind Eng Chem*. 1961;53(2):143-146. doi:10.1021/ie50614a030

38. King DW. Role of carbonate speciation on the oxidation rate of Fe(II) in aquatic systems. *Environ Sci Technol*. 1998;32(19):2997-3003. doi:10.1021/es980206o

39. R Core Team. R: A language and environment for statistical computing. 2014.

40. Prevelige PE. Bacteriophage P22. In: Calendar R, ed. *The Bacteriophages*. ; 1988:457-468.

41. He J, Yang X, Men B, Wang D. Interfacial mechanisms of heterogeneous Fenton reactions catalyzed by iron-based materials: A review. *J Environ Sci (China)*. 2016;39:97-109. doi:10.1016/j.jes.2015.12.003

42. Oleg Pestovsky, Bakac A. Identification and Characterization of Aqueous Ferryl(IV) Ion. In: *Ferrates*. ; 2008:167-176.

43. Mayer BK, Yang Y, Gerrity DW, Abbaszadegan M. The impact of capsid proteins on virus removal and inactivation during water treatment processes. *Rev*. 2016.

44. Ohgaki S, Mongkonsiri P. Effects of Floc-Virus Association on Chlorine Disinfection Efficiency. In: Hahn HH, Klute R, eds. *Chemical Water and Wastewater Treatment*. Heidelberg: Springer Verlag; 1990:75-84.

45. Keenan CR, Sedlak DL. Ligand-enhanced reactive oxidant generation by nanoparticulate zero-valent iron and oxygen. *Env Sci Technol*. 2008;42(18):6936-6941.

46. Dubrawski KL, Van Genuchten CM, Delaire C, Amrose SE, Gadgil AJ, Mohseni M. Production and transformation of mixed-valent nanoparticles generated by Fe(0) electrocoagulation. *Environ Sci Technol*. 2015;49(4):2171-2179. doi:10.1021/es505059d

47. Hug SJ, Leupin OX. Iron-catalyzed oxidation of arsenic (III) by oxygen and by hydrogen peroxide: pH-dependent formation of oxidants in the Fenton reaction RN - Environ. Sci. Technol., vol. 37, pp. 2734-2742. 2003;37(12):2734-2742.

48. Goldstein S, Meyerstein D, Czapski G. The Fenton reagents. *Free Radic Biol Med*. 1993;15:435-445. doi:10.1201/9781351072922

4. OBJECTIVE 2: DETERMINE THE MECHANISMS OF VIRUS MITIGATION AND SUITABILITY OF BACTERIOPHAGES AS SURROGATES IN DRINKING WATER TREATMENT BY IRON ELECTROCOAGULATION

Abstract

Emerging water treatment technologies using ferrous and zero-valent iron show promising virus mitigation by both inactivation and adsorption. In this study, iron electrocoagulation was investigated for virus mitigation in drinking water via bench-scale batch experiments. Relative contributions of physical removal and inactivation were investigated for three mammalian viruses (adenovirus, echovirus, and feline calicivirus) and four bacteriophage surrogates (fr, MS2, P22, and ΦX174). Though no one bacteriophage exactly represented mitigation of the mammalian viruses in all water matrices, bacteriophage ΦX174 was the only surrogate that showed overall removal comparable to that of the mammalian viruses. Bacteriophages fr, MS2, and P22 were all more susceptible to inactivation than the three mammalian viruses, raising concerns about the suitability of these common surrogates as indicators of virus mitigation. To determine why some bacteriophages were particularly susceptible to inactivation, mechanisms of bacteriophage mitigation due to electrocoagulation were investigated. Physical removal was primarily due to inclusion in flocs, while inactivation was primarily due to ferrous iron oxidation. Greater electrostatic attraction, virus aggregation, and capsid durability were proposed as reasons for virus susceptibility to ferrous-based inactivation. Results suggest that overall treatment claims based on bacteriophage mitigation for any iron-based technology should be critically considered due to higher susceptibility of bacteriophages to inactivation via ferrous oxidation.

4.1. Introduction

From 1993 to 2012, viruses were responsible for at least 24 US drinking water outbreaks reported to the Centers for Disease Control and Prevention (CDC), or 9% of all reported drinking water outbreaks in the US.[1] Viruses may be responsible for many more outbreaks that are unreported or of unknown etiology.[2] Most waterborne viruses follow a fecal-oral route of infection, meaning sewage-impaired waters are a primary cause of infection.[2] Worldwide, 1.8 billion people rely on sewage-contaminated drinking water.[3] Viruses are persistent in the environment and resistant to many water treatment disinfection processes.[4] In addition, virus' small size makes them difficult to remove by particle separation.[5]

Among the viruses identified in the US Environmental Protection Agency's Contaminant Candidate List (CCL4) are caliciviruses (including norovirus), adenoviruses, and enteroviruses (including echovirus).[6] Norovirus is the leading cause of infectious diarrhea worldwide, causing as many as half of all gastroenteritis outbreaks.[7,8] Norovirus is characterized by high contagiousness, effective transmission, and rapid evolution.[8] Due to difficulty in culturing human norovirus, surrogates such as feline calicivirus or murine norovirus are often used in laboratory tests.[9,10] Adenoviruses can cause gastroenteritis in humans, as well as conjunctivitis and respiratory disease.[11] Adenoviruses are persistent in the environment and resistant to adverse conditions, as well as ultraviolet (UV) irradiation.[7] Echoviruses are common pathogens in human-impacted water systems. Echoviruses cause a range of diseases in humans, including gastroenteritis, meningitis, fever, and respiratory disease.[11] With diameters typically less than 30 nm, echoviruses are also among the smallest viruses.[7] Therefore, norovirus, adenovirus, and echovirus provide a representative suite of viruses for evaluating treatment process efficacy, due to relevance (e.g., CCL4), resistance to inactivation, and resistance to physical separation.

Electrocoagulation (EC) is a promising technology for small-scale water treatment systems due to its portability and potential for automation. EC is the *in situ* production of coagulant by passing electrical current through a zero-valent sacrificial electrode, typically consisting of iron or aluminum. Portability and potential for automation make EC a good candidate for small-scale water treatment in rural or emergency applications. Small-scale treatment systems are an important market, as more than half of the public water systems in the US serve fewer than 500 people.[12] Recently, EC has been considered for mitigating viruses in drinking water.[5,13–15] EC has shown promising results in treating bacteriophage MS2, surpassing the Surface Water Treatment Rule of 4-log virus reduction and outperforming conventional chemical coagulation for MS2 mitigation in some water matrices.[5,16]

In iron EC, iron is released in solution as ferrous ions (Fe^{2+}).[17,18] Oxidation of ferrous iron during EC can also inactivate *E. coli*,[19] and steel electrodes have demonstrated higher effectiveness than aluminum or graphite electrodes for mitigating *E. coli*.[20] Ferrous iron oxidation also inactivates bacteriophages.[21,22] However, the relative contributions of ferrous iron inactivation and physical removal have not been determined for virus inactivation during iron EC.

Bacteriophages are used as surrogates for human viruses in water treatment process research.[15,23,24] Compared to human viruses, bacteriophage surrogates have simpler quantification and propagation protocols, propagate rapidly, and are safer to handle. To the author's knowledge, bacteriophage MS2 has been the only virus investigated for EC or ferrous iron inactivation.[5,13,14,21,25] MS2 is small (approximately 25 nm diameter) and negatively charged at neutral pH.[26] Therefore, MS2 is a representative surrogate for physical treatment processes, because its small, charged capsid is difficult to destabilize by charge neutralization or remove by size exclusion. However, the suitability of any surrogate must be investigated for each novel

application. In the case of EC, MS2's negative charge and small size may make the bacteriophage more susceptible to transport to the anode surface and/or electrostatic attraction to a ferrous disinfectant in comparison to human viruses.

The goal of this research was to determine the fate of viruses during EC, as well as the suitability of bacteriophage surrogates to indicate enteric virus mitigation in drinking water due to EC. Fate of viruses was distinguished as physical removal or inactivation by comparing physical removal of flocs by microfiltration and elution of the bulk solution for recovery of infectious viruses. The effect of pH and other water parameters on virus mitigation was also investigated to assess the suitability of bacteriophage surrogates in a range of water matrices. To determine the mechanisms of bacteriophage mitigation, log reduction of bacteriophages due to EC was compared to chemical coagulation with ferrous and ferric chloride, sorption on floc surfaces, and electrooxidation with insoluble titanium electrodes.

4.2. Materials and Methods

4.2.1. Electrocoagulation

EC tests were conducted in a 500 mL glass beaker with two plate electrodes (60 cm^2 submerged area, 1 cm inter-electrode distance) consisting of iron (mild steel), as described by Maher et al.[27] Constant current (100 mA) was supplied by a Sorensen XEL 60-1.5 variable DC power supply (AMETEK, San Diego, CA) over a retention time of 5 min. This current and retention time were selected to achieve measurable log reduction of viruses in a range of water matrices. Current polarity was alternated at regular intervals (30 s) to maintain even electrode wear and prevent passivation.[27] The reactor was stirred with a magnetic stir bar at a rate of 60 rpm. The electrodes and polarity-alternating controller were kindly provided by A.O. Smith Corporation. Electrodes were polished with 400 Si-C sandpaper, washed with ultrapure water

and sterilized with UV light 30 minutes on each side in a biological safety cabinet before each test. All tests were performed in triplicate and compared to a control reactor not receiving treatment.

All tests were performed in synthetic water matrices by adding constituents to PureLab ultrapure water (ELGA LabWater, UK). Sodium nitrate (3.3 mM) was chosen as a monovalent background electrolyte, because multivalent ions can form complexes with protein moieties and thus impact surface charge.[28,29] Nitrate was chosen over chloride to avoid inactivation due to free chlorine, because chloride ions can be oxidized to form free chlorine during EC.[25] Sodium bicarbonate was also added to achieve alkalinity typical of soft to moderately alkaline water (50 mg/L as $CaCO_3$) and prevent dramatic pH fluctuations not representative of natural water matrices.[30]

In independent tests, pH, chloride, turbidity and natural organic matter were adjusted to assess their impact on virus mitigation. Chloride was added as NaCl, while 15 mg/L total organic carbon and 50 NTU turbidity were added as Suwannee River natural organic matter (NOM) and A2 test dust, respectively. The water constituents and concentrations for all test waters are provided in Table 4-1.

Total and ferrous iron generation due to EC was measured using Hach FerroVer Total Iron and Ferrous Iron Reagent (Hach, Loveland, CO), respectively. After EC, electrodes were rinsed with a small volume (< 5 mL) of ultrapure water to remove adsorbed flocs. Generation of free chlorine was measured using Hach DPD Free Chlorine Reagent. After the addition of reagent, sample absorbance was measured using a Genesys 20 spectrophotometer (Thermo Fisher Scientific, Waltham, MA) at 510 nm (total and ferrous iron) and 530 nm (free chlorine).

Table 4-1. Constituents added to ultrapure water to formulate synthetic waters.

	$NaNO_3$ (mg/L)	$NaHCO_3$ (mg/L)	NaCl (mg/L)	Suwanee River Natural Organic Matter (mg/L TOC)	A2 Test Dust (NTU)	pH
Baseline	283	84				7
Chemical coagulation	151	252				7
pH 6	283	84				6
pH 8	283	84				8
Chloride		84	190			7
NOM	283	84		15		7
Turbidity	283	84			50	7

4.2.2.Effect of Water Constituents on Virus Mitigation

To determine the effect of water quality on virus mitigation, the background electrolyte solution was altered as shown in . EC performance under these varying conditions was compared to EC in the $NaNO_3$/$NaHCO_3$ electrolyte. The pH of the test water was adjusted using 0.5 N HNO_3 or NaOH. A Symphony benchtop multiparameter meter (VWR, Batavia, IL) was used to measure pH. Chloride (115 mg/L Cl^-) was added by replacing the background electrolyte ($NaNO_3$) with NaCl. To assess the impact of natural organic matter (NOM), total organic carbon was increased by adding Suwannee River NOM (IHSS, St. Paul, MN). For turbidity tests, A2 test dust (Powder Technology Inc., Arden Hills, MN) was added to achieve approximately 50 NTU. NOM and turbidity conditions were chosen to represent challenging surface waters for drinking water treatment.

Table 4-2. Properties of bacteriophage surrogates and mammalian viruses, adapted from Mayer et al [26]. except where otherwise cited. Asterisks (*) indicate theoretical rather than measured isoelectric points.

Virus	ATCC No.	Baltimore Classification	Diameter (nm)	Isoelectric point
		Bacteriophage		
fr	15767-B1	IV ((+)ssRNA)	19 - 23	8.9 - 9.0 *, 3.5 [31]
MS2	15597-B1	IV ((+)ssRNA)	24 - 27	3.1 - 3.9 [28]
P22	19585-B1	I (dsDNA)	52 - 60 [32]	3.4 [33]
ΦX174	13706-B1	II (ssDNA)	23 - 27	6.0 - 7.0 [28]
		Mammalian Virus		
Adenovirus 4 (ADV)	VR-1572	I (dsDNA)	70 -100	5.2 *
Echovirus 12 (ECV)	VR-1563	IV ((+)ssRNA)	24 - 30	6.2 *
Feline calicivirus (FCV)	VR-782	IV ((+)ssRNA)	27 – 41[34]	4.6 *

4.2.3.Virus Propagation

Four bacteriophages were used as model viruses: MS2, fr, P22, and ΦX174. The properties of these bacteriophages are summarized in Table 4-2. In addition, three mammalian viruses were tested in varying water matrices: adenovirus 4 (ADV), echovirus 12 (ECV), and feline calicivirus (FCV; a surrogate for human norovirus), also summarized in Table 4-2. Bacteriophages were stored at 4° C, while viruses were stored at -20 °C. Cryopreservant was not used to prevent adding oxidant demand associated with the virus stock solutions. Bacteriophages were spiked at concentrations of approximately 10^7 PFU/mL, while mammalian viruses were spiked at approximately 10^4 $TCID_{50}$/mL due to limitations in virus propagation.

Bacteriophages were propagated using the double-agar layer (DAL) method in tryptic soy agar (BD, Franklin Lakes, NJ).[35] Mammalian viruses were propagated in cell cultures (see Appendix C.1) in sterile, 175 cm^2 culture flasks until cell monolayers were reduced to approximately 10 - 20% confluence, then subjected to three freeze-thaw cycles (-20° C/22° C).

All viruses were purified by two cycles of polyethylene glycol (PEG) precipitation followed by a Vertrel XF (DuPont, Wilmington, DE) purification, as described by Mayer et al.[36]

4.2.4.Virus Sampling and Quantification

Virus samples were taken immediately after EC. Two samples were taken from each reactor, including the control (untreated) reactor. First, a filtered sample was collected using sterile, 20-mL syringes and 0.45 µm PTFE syringe filters. Some form of physical separation is required in any coagulation process; microfiltration was chosen for this study to thoroughly separate flocs without a long flocculation step. The filter was primed with 15 mL of sample before reserving 4 mL of filtrate. The reactor was then homogenized by rapid stirring (600 rpm for 15 s), and a 20-mL sample was taken for virus elution to determine the total concentration of viable viruses in the bulk solution. To dissolve flocs and increase electrostatic repulsion between coagulant and viruses, elution was performed by adding an equal volume of 6% beef broth to homogenized samples and vortexing for approximately 10 s. Samples containing bacteriophages were diluted in tenfold series, and ten 10-µL drops of each dilution were plated using the spot titer plaque assay method, as described by Beck et al.[37] Mammalian viruses were quantified using the Reed & Muench $TCID_{50}$ method.[38] Virus recovery was confirmed in numerous tests, *e.g.*, at pH 8 (Figure 4-1) and in waters containing turbidity and NOM (Figure 4-2). Confirmation of bacteriophage recovery by elution was demonstrated using chemical coagulation with ferric chloride (Figure 4-3).

Virus mitigation was distinguished as inactivation or physical removal based on recovery of infectious viruses from the filtered and eluted samples. The log reduction in infectious viruses between the filtered control and filtered treated samples represented total mitigation (Eqn. 4-1). The log reduction in infectious viruses between the eluted control and eluted treated

samples represented inactivation, *i.e.*, viruses that could not be recovered from the bulk solution (including flocs, Eqn. 4-2). Mitigation due to physical removal was therefore the difference between total mitigation and inactivation, *i.e.*, the fraction of total mitigation that was recoverable from the bulk solution by elution (Eqn. 4-3).

$$Total\ Mitigation = Filtrate_{Control} - Filtrate_{Treated} \quad (4\text{-}1)$$

$$Inactivation = Eluate_{Control} - Eluate_{Treated} \quad (4\text{-}2)$$

$$Coagulation = Total\ Mitigation - Inactivation \quad (4\text{-}3)$$

4.2.5.Mechanisms of Virus Mitigation

To establish mechanisms of virus mitigation, log reduction due to EC was compared to similar physical/chemical processes (chemical coagulation and electrochemical oxidation). These tests were only performed with bacteriophages due to limited inactivation of mammalian viruses by EC.

4.2.5.1. Chemical Coagulation

Chemical coagulation using ferrous chloride ($FeCl_2$) and ferric chloride ($FeCl_3$) was compared to EC to help determine the susceptibility of bacteriophages to inactivation/physical removal ($FeCl_2$) versus physical adsorption alone ($FeCl_3$). Doses of 2.3 mg Fe/L were used to approximate doses achieved by EC batch tests. Test waters were prepared to maintain similar conductivity to EC tests, while also providing more sodium bicarbonate alkalinity (150 mg/L as $CaCO_3$) to prevent pH fluctuation upon addition of coagulant salts, as shown in Table 4-1.

4.2.5.2. Pre-formed Flocs

Viruses were added to pre-formed flocs created by EC to test for the importance of sorption to the surfaces of flocs. EC reactors were operated as for regular EC tests, except that

viruses were only added to the solution after the reaction had completed. Viruses were retained for the same amount of time (5 min) under slow mixing (60 rpm) prior to sampling.

4.2.5.3. Titanium Electrodes

To determine the potential for non-ferrous oxidant generation and oxidation at the electrode surface, iron electrodes were replaced with non-sacrificial, Grade 2 titanium plate electrodes (Performance Titanium, San Diego, CA) of the same dimensions (60 cm^2 submerged area, 1 cm inter-electrode distance). Titanium is oxidized in air to form a passive, inert electrode surface.[39] Titanium electrooxidation reactors were operated with the same parameters as the iron EC reactor (100 mA, 5 min, 30 s polarity reversal interval), as described in Section 4.2.1.

4.2.6.Zeta Potential Measurement

The zeta potential of bacteriophage fr and A2 test dust were confirmed by dynamic light scattering using a Zetasizer Nano-ZS (Malvern Panalytical, Malvern, UK), software version 7.11. Bacteriophage fr was chosen for zeta potential analysis due to wide discrepancy in isoelectric point values reported in the literature, as shown in Table 4-2. The buffer demand-free (BDF) solution used for fr propagation was replaced with “Baseline” electrolyte (Table 4-1) by dialysis. The fr bacteriophage stock was transferred to Slide-A-Lyzer 20 kDa MWCO dialysis cassettes (Thermo Scientific, Waltham, MA) and stirred at 4^{o} C for 3 days with daily replacement of electrolyte solution. A2 test dust was diluted to 0.6 g/L in ultrapure water. The “Baseline” electrolyte was adjusted to near target pH (pH 1.0 – 9.3) with 0.5 M NaOH or HNO_3. Samples were added to pH-adjusted electrolyte in a 1:4 dilution. Final pH was read simultaneously with zeta potential readings.

4.2.7. Data Analysis

All statistical analyses were performed in the R statistical language using the stats package.[40] Mean log reduction by physical removal and inactivation was compared between test conditions using independent, 2-tailed Student's t-tests with a Bonferroni correction for multiple comparisons. The effect of pH on bacteriophage inactivation was evaluated by linear regression. (The mammalian viruses did not show a uniform trend of inactivation, so inactivation at pH 6, 7, and 8 was compared by t-tests.) Models were evaluated for residual distribution, normality, and leverage points using the plot.lm() function, and significance of variables was evaluated by analysis of variance with the anova() function.[40] A link for all R scripts is provided in Appendix C.2.

4.3. Results and Discussion

4.3.1. Effect of Water Constituents on Virus Mitigation

4.3.1.1. Effect of pH

Both mammalian viruses and bacteriophages were inactivated and physically removed to some degree over the pH range tested (pH 6 – 8), as shown in Figure 4-1. However, whereas inactivation was the dominant fate for bacteriophages fr, MS2, and P22, mitigation of bacteriophage ΦX174 and mammalian viruses showed the greatest mitigation due to physical removal.

Inactivation was most pronounced at low pH. All four bacteriophages (including ΦX174) demonstrated a significant exponential relationship between log inactivation and pH (correlation to pH and pH^2), as summarized in Appendix C.3. Similarly, inactivation was greatest at low pH (pH 6) for all mammalian viruses except FCV, which was not effectively inactivated at any pH ($p > 0.21$). Inactivation was significantly greater at pH 6 than pH 7 for ADV ($p = 0.0027$)

and ECV (p = 0.00025), though only approximately 0.7 log inactivation was achieved at pH 6 for either virus. These results support Chapter 3 and previous findings[21] that MS2 and P22 inactivation in ferrous iron-based treatment processes is greater at lower pH. However, this phenomenon has only been demonstrated previously with bacteriophages. These results show that bacteriophages commonly used in water treatment testing were inactivated to a far greater degree than the mammalian viruses in this study.

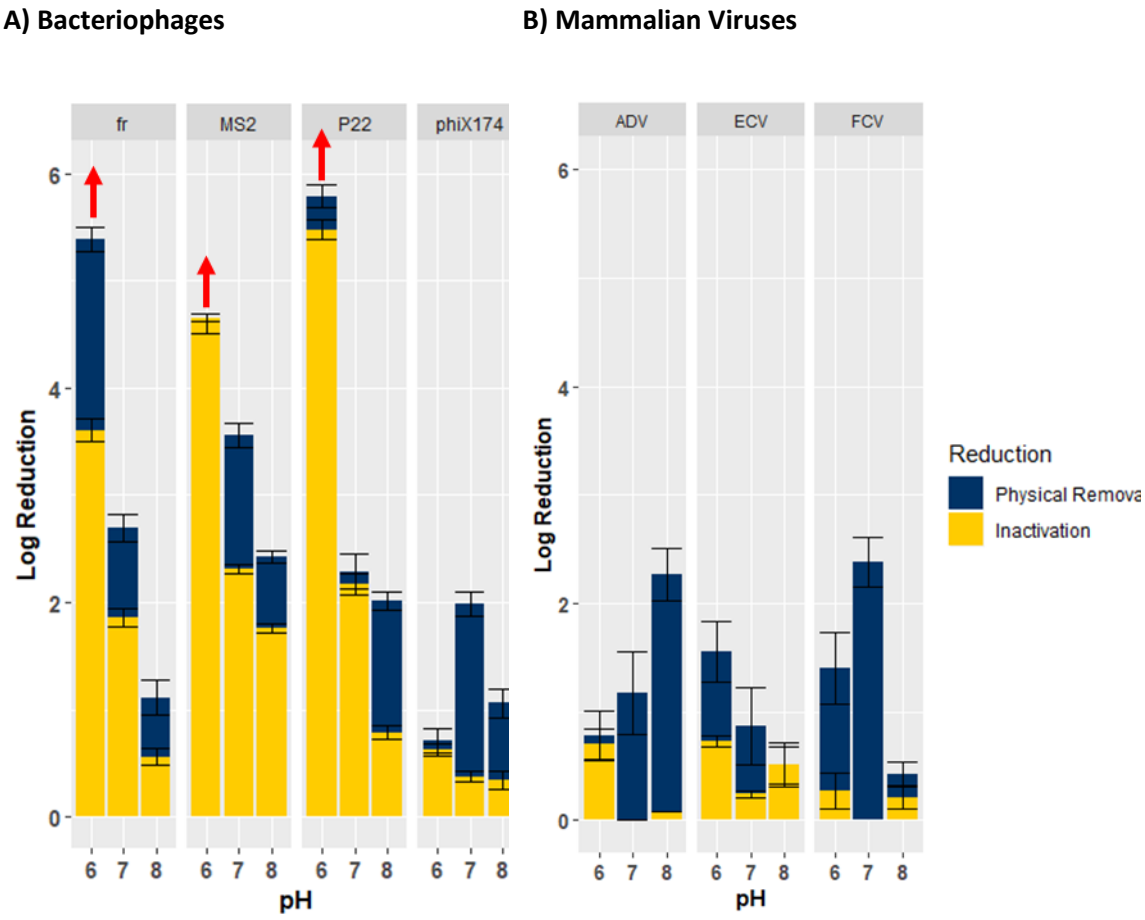

Figure 4-1. Effect of pH on inactivation and physical removal of A) bacteriophages and B) mammalian viruses due to electrocoagulation. Upward arrows indicate log reduction beyond the countable limit, so values shown are the limit of quantification. Error bars represent standard error of the mean of triplicate tests.

Bacteriophage ΦX174 was far more resistant to inactivation than the other bacteriophages, with only 0.6 log inactivation at pH 6. Total ΦX174 mitigation was greatest at pH 7. Since the isoelectric point (pI) of ΦX174 is near neutral.[28] ΦX174 would be more likely to destabilize and aggregate due to van der Waals interactions at pH 7, which likely contributed togreater physical removal at pH 7. In addition, aggregation can reduce the efficacy of disinfection.[41] The impact of pH on physical removal was difficult to interpret for bacteriophages fr, MS2, and P22, because differences in physical removal may have been an artifact of the decrease in total mitigation at higher pH.

As with inactivation, physical removal of the mammalian viruses was more similar to that of ΦX174 than the other bacteriophage surrogates. Total mitigation varied slightly with pH for the mammalian viruses, though no unifying trend was apparent. ECV showed a weak trend of greater physical removal at low pH. The theoretical pI of ECV is approximately 6.2,[26] which could explain greater physical removal by at pH 6. Only FCV showed a significant difference in physical removal between pH levels, with poorer removal at pH 8 than pH 7 (p = 0.000250). Conversely, ADV showed a weak trend of greater physical removal with increasing pH. However, the low mitigation of the mammalian viruses relative to the variance makes it difficult to make meaningful inferences between means. For the purpose of identifying a representative virus surrogate, the very fact that mammalian virus removal was consistently low (< 2.5 log) is more important. Only bacteriophage ΦX174 mitigation remained below the bar of 2.5 log total mitigation over the pH range tested.

4.3.1.2. Effect of Natural Organic Matter

The presence of NOM was generally inhibitory to both inactivation and physical removal, as shown in Figure 4-2. Suwannee River NOM consists primarily of fulvic acid (65% by

weight) with a lesser fraction of humic acid (10%).[42] The pKa of fulvic acids found in Suwannee River NOM is in the range of 2 to 4, indicating a negative charge at neutral pH.[43] Therefore, NOM may inhibit physical removal and disinfection by sorbing the iron required for virus destabilization and disinfection. Once complexed with NOM, ferrous iron is resistant to oxidation by dissolved oxygen or free chlorine.[44] Tanneru and Chellam[13] similarly found poor mitigation of MS2 using iron EC in natural river water and synthetic waters containing humic acid. Bacteriophage ΦX174 mitigation was nearly completely inhibited (< 0.25 log reduction), indicating that ΦX174 continued to be an appropriate surrogate for the mammalian viruses in high-NOM water matrices.

4.3.1.1. Effect of Turbidity

Turbidity also inhibited inactivation, though the impact of turbidity on physical removal was mixed, as shown in Figure 4-2. Bacteriophages fr, MS2, and P22 all demonstrated poorer inactivation in turbid water, while ΦX174 showed minimal inactivation even without added turbidity. A2 test dust consists primarily of silica (69 – 77%) and alumina (8 – 14%), as well as various metal oxides.[45] The presence of metal oxides in A2 test dust may scavenge oxidants and therefore inhibit viral inactivation.

Turbidity also inhibited physical removal of fr, MS2, and ΦX174. A2 dust was demonstrated by dynamic light scattering to have a strong negative zeta potential around neutral pH, as shown in Appendix C.4. Therefore, the test dust likely had a coagulant demand that inhibited virus removal at low coagulant doses. Zhu et al.[14] found that silica increased MS2 reduction by ferric chloride coagulation–microfiltration; however, silica created a coagulant demand that impaired treatment at low coagulant doses (< 5 mg/L) similar to those used in this experiment.

A) Bacteriophages **B) Mammalian Viruses**

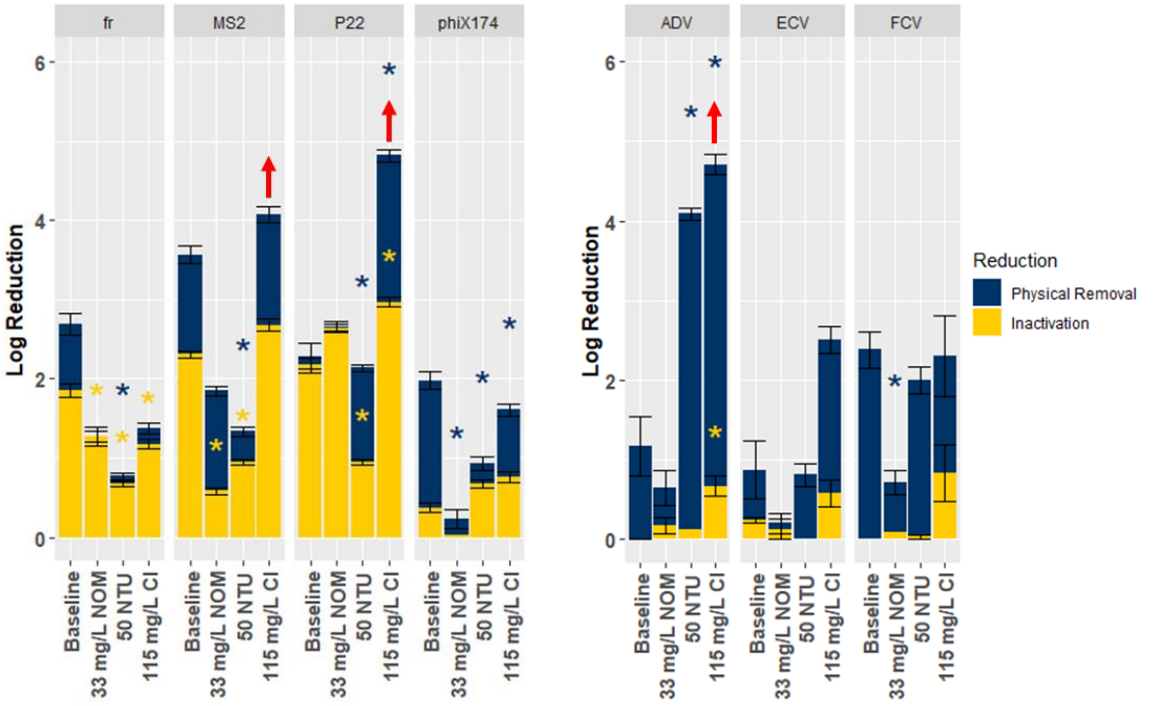

Figure 4-2. Effect of water constituents on inactivation and physical removal of A) bacteriophages and B) mammalian viruses due to electrocoagulation. Asterisks indicate a significant difference in log reduction from the baseline condition (pH 7, simple electrolyte) due to physical removal (blue asterisk) or inactivation (yellow asterisk). Upward arrows indicate log reduction beyond the countable limit, so values shown are the limit of quantification. Error bars represent standard error of the mean of triplicate tests.

Both bacteriophage P22 and ADV had greater removal by physical removal with increased turbidity. As the largest viruses tested (50 – 100 nm diameter), P22 and ADV were likely retained due to internal fouling or formation of a cake layer during filtration of the turbid samples. Using the same filtration technique as in EC experiments, filters fouled with EC flocs and turbidity significantly rejected P22 (1.27 log reduction, $p = 2.01\text{x}10^{-5}$) to a greater degree than MS2 (0.66 log reduction, $p = 0.00014$), as shown in Appendix C.5. The greater degree of rejection for large viruses may override the coagulant demand of the A2 dust. Smaller

bacteriophages like MS2, which saw a small increase in rejection by the fouled filter, may have been adversely affected to a greater degree by the decrease in available coagulant. In Zhu's study,[14] development of a cake layer did not enhance dead-end microfiltration of the smaller MS2 bacteriophage following ferric chloride coagulation.

4.3.1.2. Effect of Chloride

Chloride was expected to increase inactivation through the production of free chlorine at the anode.[25] However, inactivation significantly increased for P22 and ADV, and decreased slightly for bacteriophage fr (Figure 4-2). No other viruses showed significant changes in mitigation with the addition of chloride. In the absence of viruses, the chlorine residual in the bulk solution during EC remained below the detection limit of 0.02 mg/L Cl_2. Most of the chlorine generated by chloride oxidation would likely be scavenged by ferrous iron, which is also produced at the anode surface. Tanneru et al.[25] similarly found poor inactivation of bacteriophage MS2 due to free chlorine generation with aluminum EC. Aluminum EC would be expected to show greater efficiency in producing free chlorine than iron EC, because aluminum ions are oxidized to a stable form at the electrode and would not exert oxidant demand in solution.[46]

The rate of iron generation by EC increased dramatically in the presence of chloride, as shown in Appendix C.6. Carbon steel is susceptible to increased corrosion rates and pitting in the presence of chloride.[47] Therefore, the greater iron generation was likely due to chemical corrosion. The greater iron dose (6.6 mg/L Fe) may have impacted physical removal, increasing mitigation of P22 and ADV by physical removal but decreasing ΦX174 mitigation. Again, the largest viruses (P22 and ADV) showed increased physical removal, possibly indicating retention of viruses due to membrane fouling during filtration. In the case of ΦX174, lower removal at

higher doses may seem paradoxical. However, total removal of ΦX174 was not significantly different from total removal without chloride, so the decrease in physical removal represents only a shift in mechanism of mitigation.

4.3.2. Mechanisms of Virus Mitigation

To determine why some bacteriophages demonstrated inactivation due to EC, the mechanisms of bacteriophage mitigation were investigated. Understanding the reason why some bacteriophages are inactivated by ferrous iron may help choose better virus surrogates or identify more susceptible pathogen targets. As shown in Figure 4-3, ferric chloride coagulation and ferrous chloride coagulation reasonably predicted whether inactivation or physical removal was the predominate bacteriophage fate in EC, whereas adsorption to preformed flocs and electrooxidation were not important mechanisms. Chapter 3 and previous research[13,21] has found a correlation between oxidation of ferrous iron (Fe^{II}) and bacteriophage inactivation. Therefore, chemical coagulation with $FeCl_2$ was expected to achieve inactivation, whereas the already oxidized ferric coagulant ($FeCl_3$) should achieve only physical removal.

Compared to chemical coagulation with $FeCl_3$, EC resulted in significant inactivation for all bacteriophages (*p*-values: fr, 3.69×10^{-6}; MS2, 1.33×10^{-6}; P22, 5.63×10^{-6}; and ΦX174, 1.01×10^{-3}), though ΦX174 mitigation was predominately due to physical removal. Like EC, chemical coagulation with $FeCl_2$ showed substantial inactivation of fr, MS2, and P22, but only slight inactivation of ΦX174. More importantly, chemical coagulation with $FeCl_2$ resulted in an even greater discrepancy in inactivation between ΦX174 and the other bacteriophages than was observed with EC. Inactivation of fr and P22 was greater with $FeCl_2$ than EC, though MS2 inactivation was slightly greater with EC than $FeCl_2$. Greater inactivation with $FeCl_2$ might have occurred because the entire concentration of ferrous iron was added at once and thoroughly

mixed to provide a higher and more homogenous ferrous concentration throughout the reactor. Despite differences in the final log inactivation between $FeCl_2$ and EC, the effect of ferrous iron is sufficient to explain inactivation observed in EC. Conversely, chemical coagulation with $FeCl_3$ achieved only physical removal. For fr, MS2, and P22, EC achieved a similar degree of physical removal as $FeCl_3$ coagulation, and EC outperformed chemical coagulation for ΦX174.

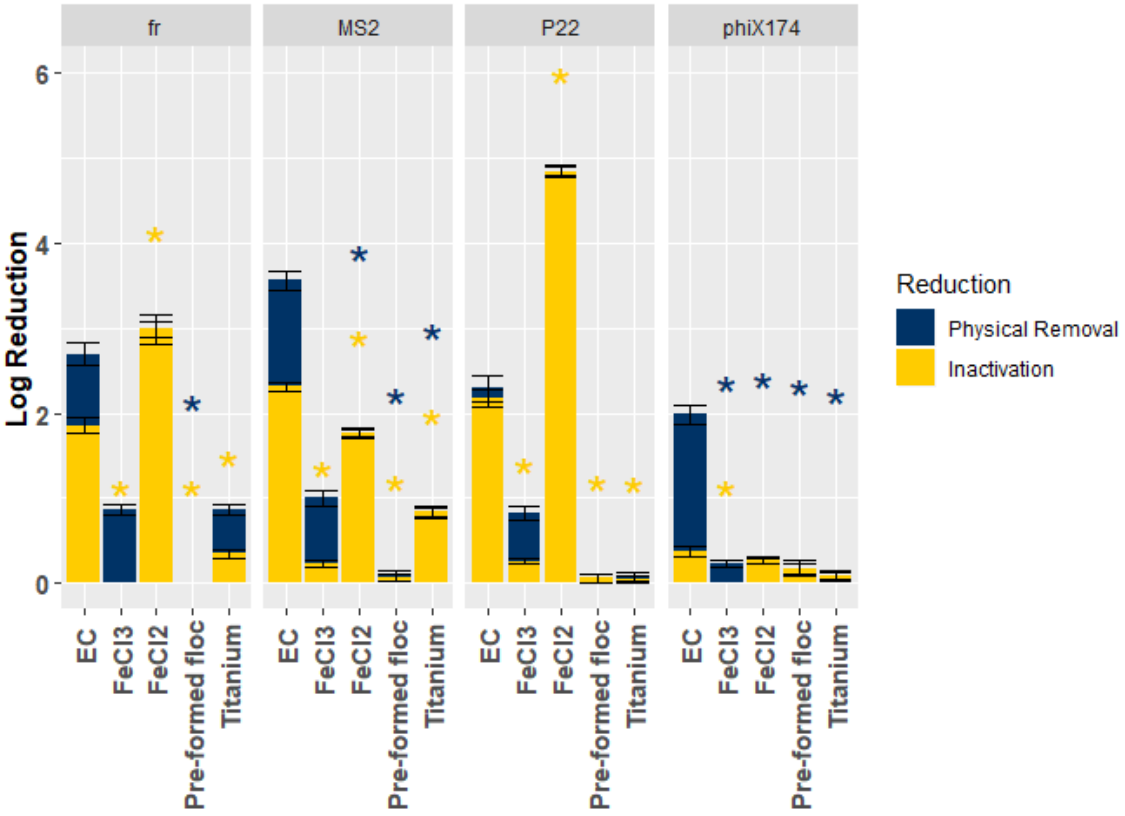

Figure 4-3. Mechanisms of bacteriophage mitigation due to electrocoagulation, chemical coagulation, adsorption and electrooxidation. Inactivation and physical removal were compared between electrocoagulation (EC), chemical coagulation with ferric chloride ($FeCl_3$), chemical coagulation with ferrous chloride ($FeCl_2$), flocs formed by electrocoagulation prior to the addition of bacteriophages (pre-formed floc), and electrooxidation with inert titanium electrodes (Titanium). Asterisks indicate a significant difference in log reduction from electrocoagulation due to physical removal (blue asterisk) or inactivation (yellow asterisk). Error bars represent standard error of the mean of triplicate tests.

4.3.2.1. Pre-formed Flocs

No bacteriophages demonstrated mitigation (neither inactivation nor physical removal) when added to reactors containing flocs pre-formed by EC. Therefore, sorption to flocs was not a significant mechanism of virus mitigation in simple electrolyte solution. Instead, physical removal in EC is due to inclusion of viruses within the developing floc. Other researchers[48–50] have similarly found greater virus mitigation during rapid mixing and floc formation. The importance of inclusion of viruses in the floc may also explain why EC was more effective than $FeCl_3$ chemical coagulation for mitigating ΦX174. In EC, coagulant is gradually added to solution, which typically slows floc formation in comparison to chemical coagulation;[51] thus EC allows longer contact time for virus inclusion within the floc.

4.3.2.2. Titanium Electrodes

Uncoated titanium electrodes were used to evaluate the potential for bacteriophage mitigation due to generation of non-ferrous oxidants (*e.g.*, reactive oxygen species) and/or oxidation at the anode surface. Air-oxidized titanium anodes are stable in aqueous solutions, extracting electrons from species in solution rather than dissolving like iron.[39,52] Titanium electrooxidation mitigated both MS2 and fr, though less than one log total reduction was achieved. No significant mitigation was found for P22 or ΦX174. Titanium electrodes are likely to overestimate the effects of inactivation, because a) ferrous iron may scavenge oxidants, and b) oxidation of the iron electrode competes with other oxidation reactions at the electrode surface. Nevertheless, inactivation with titanium electrodes was far less than with iron electrodes. Therefore, neither anodic oxidation nor generation of non-ferrous oxidants can be considered important mechanisms of virus mitigation under the conditions investigated in this

study. This finding further confirms that ferrous oxidation is the primary determiner of inactivation due to EC.

4.3.3.Virion Properties and Ferrous Susceptibility

4.3.3.1. Isoelectric Point

Of the mechanisms of bacteriophage mitigation discussed in Section 4.3.2, susceptibility to ferrous inactivation was the primary cause of differences in log reduction between bacteriophages fr, MS2, and P22 on the one hand, and bacteriophage ΦX174 and the mammalian viruses on the other. Ferrous cations differ from neutrally- or negatively-charged disinfectants such as free chlorine. Though the positive ferrous charge may enhance disinfection of negatively-charged pathogens, pathogens with a positive charge near neutral pH may be repelled.

In addition, aggregation can shield viruses and reduce the efficacy of disinfection.[41] Since iron-based inactivation is more effective at lower pH,[21] viruses with pIs near pH 6 – 7 would therefore tend to aggregate due to charge neutralization and become shielded under the conditions of greatest disinfection capacity in this study. Thus, electrostatic repulsion and aggregation may explain the poor inactivation of ΦX174 (pI = 6.0 – 7.0) compared to bacteriophages fr, MS2, and P22, which have low pIs (<4, see Table 4-2). Because pI values reported in the literature varied widely for bacteriophage fr (pI = 3.5 to 9.0), the pI for fr was experimentally validated in this study at approximately 2.7, as shown in Appendix C.4. Enteric viruses often enter the water cycle as aggregates,[41] and much of the viral load for drinking water treatment is associated with particles.[53] Therefore, the tendency of viruses to aggregate is similarly an important factor for EC treatment of natural waters.

Bacteriophage ΦX174 may also have been mitigated to a lesser extent than other bacteriophage surrogates due to structural robustness. Whereas F-specific bacteriophages like fr and MS2, as well as tailed bacteriophages like P22, have a single locus of attachment and penetration, ΦX174 can attach to and penetrate host cells at any of 12 spikes occurring at the capsid's 5-fold vertices.[54] However, ΦX174 has not been shown to have similarly high resistance to other disinfectants, and the single maturation protein of F-specific bacteriophages does not appear to be an Achilles heel for chemical disinfection.[15]

While experimental values are not available for ADV and ECV isoelectric points, both viruses are resistant to inactivation and have theoretical isoelectric points close to neutral (5.2 and 6.2, respectively, see Table 4-2). However, FCV is one possible exception to the hypothesis that electrostatic forces determine ferrous disinfection. FCV has a theoretical pI of 4.6, and virus-like particles consisting of FCV capsid proteins have a similar reported pI of 3.9.[55] Therefore, the FCV capsid likely has a negative charge at neutral pH, yet FCV remains resistant to ferrous-based inactivation.

4.3.3.2. Capsid Structure

A review of capsid structure provides some insight into the resistance of mammalian viruses. Protein structures for bacteriophages and viruses were accessed from the VIPERdb database, as summarized in Table 4-3.[56] Structural files for adenovirus 4 were not available, so adenovirus serotypes 5 and 26 were used instead. (Both ADV5 and ADV26 shared similar dimensions, despite representing different species.) Crenulations and protuberances on the capsid surface can result in outer diameter values not representative of actual capsid thickness, and the method of structural analysis influences the degree of detail captured on the capsid surface.[57] To minimize the influence of surface features, "adjusted" capsid thickness was

obtained by subtracting the inside diameter from the average diameter (rather than from the outside diameter).

Capsid thickness increased from bacteriophages to the mammalian viruses: MS2 ≈ fr < P22 < ΦX174 < FCV < ECV < ADV. The three bacteriophages with the thinnest capsids (fr, MS2, and P22) were also the most susceptible to inactivation due to EC. Though ΦX174 has only a slightly thicker capsid than P22 (~13%), electrostatic repulsion and aggregation can still explain the recalcitrance of ΦX174 to iron-based disinfection. On the other hand, the recalcitrance of FCV to iron-based disinfection may be due more to capsid structure, given its theoretically low pI but thicker (9 nm) capsid. The susceptibility of viruses to inactivation due to iron EC may therefore be a combination of electrostatic interactions and capsid structure. Capsid thickness would likely not play as large a role for uncharged disinfectants like hypochlorous acid that could

Table 4-3. Bacteriophage and mammalian virus capsid dimensions based on structural models acquired from VIPERdb [56]. Structural files were not available for adenovirus 4, so adenovirus 5 (ADV 5) and 26 (ADV 26) were compared. Both adenovirus serotypes shared similar dimensions. Color scale indicates low (red) to high (green) capsid thickness.

		Bacteriophage				**Mammalian Virus**			
		fr	**MS2**	**P22**	**ΦX174**	**FCV**	**ECV 12**	**ADV 5**	**ADV 26**
Diameter (Å)	Outer	286	288	686	342	416	404	940	952
	Inner	210	210	534	192	236	212	632	630
	Avg.	276	276	662	336	410	398	906	914
Adjusted capsid thickness (Å)		33	33	64	72	87	93	137	142
Source File	PDB-ID	1FRS	2MS2	5UU5	2BPA	3M8L	2C8I	6CGV	5TX1
	Resolution (Å)	3.50	2.80	3.30	3.00	3.40	14.0	3.80	3.70
	Method	XD	XD	EM	XD	XD	EM	XD	EM
	Primary Citation	[58]	[59]	[60]	[61]	[62]	[57]	[63]	[64]

XD: X-ray diffraction; EM: Electron microscopy

permeate capsid pores more readily. Though thickness may be a rough indicator of capsid durability, a more detailed evaluation of capsid structure and function could provide greater insight into why mammalian viruses are more resistant to inactivation.

4.4. Conclusions

This is the first work to evaluate human virus mitigation and quantitatively assess the fate of viruses in iron EC. Both inactivation and physical removal were important mechanisms of mitigation via EC for three of the four bacteriophages evaluated: fr, MS2, and P22. However, ΦX174 and the three mammalian viruses (ADV, ECV and FCV) showed the greatest mitigation due to physical removal and were less susceptible to ferrous inactivation. In representing virus mitigation, ΦX174 was the only bacteriophage surrogate resistant to ferrous inactivation, possibly due to electrostatic repulsion between ΦX174 and ferrous iron at pH 6 and/or shielding of ΦX174 virions in aggregates near neutral pH. Though electrostatic interactions between ferrous ions and virions likely explains at least some of the differences in inactivation efficacy between viruses, resistant viruses also had thicker capsids. The lack of experimental isoelectric point data for human viruses prevents a full analysis of this hypothesis. However, a detailed theoretical evaluation of capsid structure may provide additional insight where empirical methods are prohibitive.

4.5. References

1. Centers for Disease Control and Prevention. Surveillance reports for drinking water-associated disease & outbreaks. https://www.cdc.gov/healthywater/surveillance/drinking-surveillance-reports.html. Published 2015. Accessed July 7, 2017.

2. Xagoraraki I, Yin Z, Svambayev Z. Fate of Viruses in Water Systems. *J Environ Eng*. 2014;140(7):040140201-18. doi:10.1061/(ASCE)EE.1943-7870.0000827

3. Gall AM, Mariñas BJ, Lu Y, Shisler JL. Waterborne Viruses: A Barrier to Safe Drinking Water. *PLoS Pathog*. 2015;11(6):1-7. doi:10.1371/journal.ppat.1004867

4. Centers for Disease Control and Prevention. Effect of chlorination on inactivating selected pathogens. http://www.cdc.gov/safewater/effectiveness-on-pathogens.html. Published 2012. Accessed January 1, 2015.

5. Tanneru CT, Chellam S. Sweep flocculation and adsorption of viruses on aluminum flocs during electrochemical treatment prior to surface water microfiltration. *Environ Sci Technol*. 2013;47:4612-4618.

6. US Environmental Protection Agency. Microbial contaminants - CCL 4. https://www.epa.gov/ccl/microbial-contaminants-ccl-4. Published 2016.

7. Grabow WOK. Overview of health-related water virology. In: Bosch A, ed. *Human Viruses in Water*. 1st ed. Amstersdam: Elsevier; 2007:1-26.

8. Hall AJ. Noroviruses: The perfect human pathogens? *J Infect Dis*. 2012;205(11):1622-1624. doi:10.1093/infdis/jis251

9. Bae J, Schwab KJ. Evaluation of murine norovirus, feline calicivirus, poliovirus, and MS2 as surrogates for human norovirus in a model of viral persistence in surface water and groundwater. *Appl Environ Microbiol*. 2008;74(2):477-484. doi:10.1128/AEM.02095-06

10. Cannon JL, Papafragkou E, Park GW, Osborne J, Jaykus L-A, Vinjé J. Surrogates for the study of norovirus stability and inactivation in the environment: A comparison of murine norovirus and feline calicivirus. *J Food Prot*. 2006;69(11):2761-2765. doi:10.4315/0362-028X-69.11.2761

11. World Health Organization. *Guidelines for Drinking-Water Quality: Health Criteria and Other Supporting Information*. Vol 2. 2nd ed. Geneva: World Health Organization; 1996.

12. EDR Group. *Failure to Act: The Impact of Current Infrastructure Investment on America's Economic Future*.; 2013. www.asce.org/failuretoact.

13. Tanneru CT, Chellam S. Mechanisms of virus control during iron electrocoagulation--microfiltration of surface water. *Water Res*. 2012;46(7):2111-2120. doi:10.1016/j.watres.2012.01.032

14. Zhu B, Clifford DA, Chellam S. Virus removal by iron coagulation-microfiltration. *Water Res*. 2005;39(20):5153-5161. doi:10.1016/j.watres.2005.09.035

15. Heffron J, Mayer BK. Virus mitigation by coagulation: recent discoveries and future directions. *Environ Sci Water Res Technol*. 2016;2(3):443-459. doi:10.1039/C6EW00060F

16. Zhu B, Clifford DA, Chellam S. Comparison of electrocoagulation and chemical coagulation pretreatment for enhanced virus removal using microfiltration membranes. *Water Res*. 2005;39(13):3098-3108. doi:10.1016/j.watres.2005.05.020

17. Lakshmanan D, Clifford DA. Ferrous and Ferric Ion Generation During Iron Electrocoagulation. *Env Sci Technol*. 2009;43(10):3853-3859.

18. Li L, van Genuchten CM, Addy SEA, Yao J, Gao N, Gadgil AJ. Modeling As(III) oxidation and

removal with iron electrocoagulation in groundwater. *Environ Sci Technol*. 2012;46(21):12038-12045. doi:10.1021/es302456b

19. Delaire C, Van Genuchten CM, Nelson KL, Amrose SE, Gadgil AJ. Escherichia coli attenuation by Fe electrocoagulation in synthetic Bengal groundwater: effect of pH and natural organic matter. *Environ Sci Technol*. 2015;49(16):9945-9953. doi:10.1021/acs.est.5b01696

20. Ndjomgoue-Yossa AC, Nanseu-Njiki CP, Kengne IM, Ngameni E. Effect of electrode material and supporting electrolyte on the treatment of water containing Escherichia coli by electrocoagulation. *Int J Environ Sci Technol*. 2015;12(6):2103-2110. doi:10.1007/s13762-014-0609-9

21. Kim JY, Lee C, Love DC, Sedlak DL, Yoon J, Nelson KL. Inactivation of MS2 coliphage by ferrous ion and zero-valent iron nanoparticles. *Environ Sci Technol*. 2011;45(16):6978-6984. doi:10.1021/es201345y

22. Jeong J, Kim JY, Yoon J. The role of reactive oxygen species in the electrochemical inactivation of microorganisms. *Environ Sci Technol*. 2006;40(19):6117-6122. doi:10.1021/es0604313

23. Amarasiri M, Kitajima M, Nguyen TH, Okabe S, Sano D. Bacteriophage removal efficiency as a validation and operational monitoring tool for virus reduction in wastewater reclamation: Review. *Water Res*. 2017;121:258-269. doi:10.1016/j.watres.2017.05.035

24. Grabow WOK. Bacteriophages: Update on application as models for viruses in water. *Water SA*. 2001;27(2):251-268. doi:10.4314/wsa.v27i2.4999

25. Tanneru CT, Jothikumar N, Hill VR, Chellam S. Relative insignificance of virus inactivation during aluminum electrocoagulation of saline waters. *Environ Sci Technol*. 2014;48(24):14590-14598. doi:10.1021/es504381f

26. Mayer BK, Yang Y, Gerrity DW, Abbaszadegan M. The impact of capsid proteins on virus removal and inactivation during water treatment processes. *Microbiol Insights*. 2015;8(Suppl 2):15-28. doi:10.4137/Mbi.s31441.TYPE

27. Maher EK, O'Malley KN, Heffron J, et al. Analysis of operational parameters, reactor kinetics, and floc characterization for the removal of estrogens via electrocoagulation. *Chemosphere*. 2019;220:1141-1149. doi:10.1016/j.chemosphere.2018.12.161

28. Michen B, Graule T. Isoelectric points of viruses. *J Appl Microbiol*. 2010;109(2):388-397. doi:10.1111/j.1365-2672.2010.04663.x

29. Chen WS, Soucie WG. The ionic modification of the surface charge and isoelectric point of soy protein. *J Am Oil Chem Soc*. 1986;63(10):1346-1350. doi:10.1007/BF02679599

30. Mechenich C, Andrews E. *Interpreting Drinking Water Test Results*.; 2004. https://adams.uwex.edu/files/2013/01/Home-Water-Safety-Interpreting-Drinking-Water-Test-Results.pdf.

31. Armanious A, Aeppli M, Jacak R, et al. Viruses at Solid-Water Interfaces: A Systematic Assessment of Interactions Driving Adsorption. *Environ Sci Technol*. 2015;50(2):732-743. doi:10.1021/acs.est.5b04644

32. Shen C, Phanikumar MS, Fong T-T, et al. Evaluating bacteriophage P22 as a tracer in a complex surface water system: The Grand River, Michigan. *Environ Sci Technol*. 2008;42(7):2426-2431. doi:10.1021/es702317t

33. Fidalgo De Cortalezzi MM, Gallardo M V., Yrazu F, et al. Virus removal by iron oxide ceramic membranes. *J Environ Chem Eng*. 2014;2(3):1831-1840. doi:10.1016/j.jece.2014.08.006

34. Prasad BVV, Matson DO, Smith AW. Three-dimensional Structure of Calicivirus. *J Mol Biol*. 1994;240:256-264. doi:S0022-2836(84)71439-2 [pii]\r10.1006/jmbi.1994.1439

35. Adams MH. *Bacteriophages*. New York: Interscience Publishers; 1959.

36. Mayer BK, Ryu H, Abbaszadegan M. Treatability of U.S. Environmental Protection Agency contaminant candidate list viruses: Removal of coxsackievirus and echovirus using enhanced coagulation. *Environ Sci Technol*. 2008;42(18):6890-6896. doi:10.1021/es801481s

37. Beck NK, Callahan K, Nappier SP, Kim H, Sobsey MD, Meschke JS. Development of a spot-titer culture assay for quantifying bacteria and viral indicators. *J Rapid Methods Autom Microbiol*. 2009;17(4):455-464. doi:10.1111/j.1745-4581.2009.00182.x

38. Reed LJ, Muench H. A simple method of estimating fifty per cent endpoints. *Am J Hyg*. 1938;27(3):493-497. doi:10.1093/OXFORDJOURNALS.AJE.A118408

39. Bagotsky VS. *Fundamentals of Electrochemistry*. 2nd ed. Hoboken, New Jersey: John Wiley & Sons, Inc; 2006.

40. R Core Team. R: A language and environment for statistical computing. 2014.

41. Gerba CP, Betancourt WQ. Viral Aggregation: Impact on Virus Behavior in the Environment. *Environ Sci Technol*. 2017;51(13):7318-7325. doi:10.1021/acs.est.6b05835

42. Averett R, Leenheer J, McKnight D, Thorn K. *Humic Substances in the Suwannee River, Georgia: Interactions, Properties and Proposed Structures*.; 1994. http://scholar.google.com/scholar?hl=en&btnG=Search&q=intitle:Humic+Substances+in+the+Suwannee+River,+Georgia:+Interactions,+Properties,+and+Proposed+Structures#0.

43. Leenheer JA, Wershaw RL, Reddy MM. Strong-Acid, Carboxyl-Group Structures in Fulvic Acid from the Suwannee River, Georgia. 1. Minor Structures. *Environ Sci Technol*. 1995;29(2):393-398. doi:10.1021/es00002a015

44. Crittenden JC, Trussell RR, Hand DW, Howe KJ, Tchobanoglous G. *MWH's Water Treatment: Principles and Design*. 3rd ed. Hoboken, New Jersey: John Wiley & Sons, Inc.; 2012.

45. Powder Technology Inc. *Safety Data Sheet: Arizona Test Dust*.; 2016. https://www.powdertechnologyinc.com/wp-content/uploads/2012/08/SDS.01.Arizona-Test-Dust.4-Feb-2016.pdf.

46. Cañizares P, Jiménez C, Martínez F, Sáez C, Rodrigo MA. Study of the electrocoagulation process using aluminum and iron electrodes. *Ind Eng Chem Res*. 2007;46(19):6189-6195. doi:10.1021/ie070059f

47. Song Y, Jiang G, Chen Y, Zhao P, Tian Y. Effects of chloride ions on corrosion of ductile iron and carbon steel in soil environments. *Sci Rep*. 2017;7(1):1-13. doi:10.1038/s41598-017-07245-1

48. Shirasaki N, Matsushita T, Matsui Y, Urasaki T, Ohno K. Comparison of behaviors of two surrogates for pathogenic waterborne viruses, bacteriophages Qbeta and MS2, during the aluminum coagulation process. *Water Res*. 2009;43(3):605-612. doi:10.1016/j.watres.2008.11.002

49. Shirasaki N, Matsushita T, Matsui Y, Marubayashi T. Effect of aluminum hydrolyte species on human enterovirus removal from water during the coagulation process. *Chem Eng J*. 2016;284(2016):786-793. doi:10.1016/j.cej.2015.09.045

50. Kreißel K, Bösl M, Hügler M, Lipp P, Franzreb M, Hambsch B. Inactivation of F-specific bacteriophages during flocculation with polyaluminum chloride - A mechanistic study. *Water Res*. 2014;51:144-151. doi:10.1016/j.watres.2013.12.026

51. Harif T, Khai M, Adin A. Electrocoagulation versus chemical coagulation: Coagulation/flocculation mechanisms and resulting floc characteristics. *Water Res*. 2012;46(10):3177-3188. doi:10.1016/j.watres.2012.03.034

52. Wilhelmsen W. Passive Behaviour of Titanium in Alkaline. *Electrochim Acta*. 1987;32(1):85-89.

53. Springthorpe S, Sattar SA. Virus removal during drinking water treatment. In: Bosch, ed. *Human Viruses in Water*. 1st ed. Amstersdam: Elsevier; 2007:109-126.

54. Sun L, Young LN, Zhang X, et al. Icosahedral bacteriophage ΦX174 forms a tail for DNA transport during infection. *Nature*. 2013;505(7483):432-435. doi:10.1038/nature12816

55. Samandoulgou I, Fliss I, Jean J. Zeta Potential and Aggregation of Virus-Like Particle of Human Norovirus and Feline Calicivirus Under Different Physicochemical Conditions. *Food Environ Virol*. 2015;7(3):249-260. doi:10.1007/s12560-015-9198-0

56. TSRI. ViperDB. http://viperdb.scripps.edu/. Published 2018. Accessed November 30, 2018.

57. Pettigrew DM, Williams DT, Kerrigan D, Evans DJ, Lea SM, Bhella D. Structural and Functional Insights Into the Interaction of Echoviruses and Decay-Accelerating Factor. *JBiolChem*. 2006;281:5169. doi:10.2210/PDB2C8I/PDB

58. Liljas L, Fridborg K, Valegård K, Bundule M, Pumpens P. Crystal structure of

bacteriophage fr capsids at 3.5 A resolution. *J Mol Biol*. 1994;244(3):279-290. doi:10.1006/jmbi.1994.1729

59. Golmohammadi R, Valegard K, Fridborg K, Liljas L. The refined structure of bacteriophage MS2 at 2.8 A resolution. *JMolBiol*. 1993;234:620-639. doi:10.2210/PDB2MS2/PDB

60. Hryc CF, Chen DH, Afonine PV, et al. Accurate model annotation of a near-atomic resolution cryo-EM map. *Proc Natl Acad Sci USA*. 2017;114:3103-3108. doi:10.2210/PDB5UU5/PDB

61. McKenna R, Xia D, Willingmann P, et al. Atomic structure of single-stranded DNA bacteriophage phi X174 and its functional implications. *Nature*. 1992;355:137-143. doi:10.2210/PDB2BPA/PDB

62. Ossiboff RJ, Zhou Y, Lightfoot PJ, Prasad BV, Parker JS. Conformational changes in the capsid of a calicivirus upon interaction with its functional receptor. *JVirol*. 2010;84:5550-5564. doi:10.2210/PDB3M8L/PDB

63. Kundhavai Natchiar S, Venkataraman S, Mullen TM, Nemerow GR, Reddy VS. Revised Crystal Structure of Human Adenovirus Reveals the Limits on Protein IX Quasi-Equivalence and on Analyzing Large Macromolecular Complexes. *J Mol Biol*. 2018;430(21):4132-4141. doi:10.1016/j.jmb.2018.08.011

64. Yu X, Veesler D, Campbell MG, et al. Cryo-EM structure of human adenovirus D26 reveals the conservation of structural organization among human adenoviruses. *Sci Adv*. 2017;3:e1602670-e1602670. doi:10.2210/PDB5TX1/PDB

5. OBJECTIVE 3: SEQUENTIAL ELECTROCOAGULATION-ELECTROOXIDATION FOR VIRUS MITIGATION IN DRINKING WATER

Abstract

Electrochemical water treatment is a promising alternative for small-scale and remote water systems that lack operational capacity or convenient access to reagents for chemical coagulation and disinfection. In this study, the mitigation of viruses was investigated using electrocoagulation as a pretreatment prior to electrooxidation treatment using boron-doped diamond electrodes. This research is the first to investigate a sequential electrocoagulation-electrooxidation treatment system for virus removal. Bench-scale, batch reactors were used to evaluate mitigation of viruses in variable water quality via: a) electrooxidation, and b) a sequential electrocoagulation-electrooxidation treatment train. Electrooxidation of two bacteriophages, MS2 and ΦX174, was inhibited by natural organic matter and turbidity, indicating the probable need for pretreatment. However, the electrocoagulation-electrooxidation treatment train was beneficial only in the model surface waters employed. In model ground waters, electrocoagulation alone was as good or better than the combined electrocoagulation-electrooxidation treatment train. Reduction of human echovirus was significantly lower than one or both bacteriophages in all model waters, though bacteriophage ΦX174 was a more representative surrogate than MS2 in the presence of organic matter and turbidity. Compared to conventional treatment by ferric salt coagulant and free chlorine disinfection, the electrocoagulation-electrooxidation system was less effective in model surface waters but more effective in model groundwaters. Sequential electrocoagulation-electrooxidation was beneficial for some applications, though practical considerations may currently outweigh the benefits.

5.1. Introduction

Electrochemical water treatment holds promise as a portable option for coagulation and disinfection in small-scale water systems. More than half of the public water systems in the United States (US) serve fewer than 500 people,[1] and approximately 15% of individuals in the US get water from private wells.[2] Many of these public and private water systems draw from groundwater and lack disinfection treatment processes. Between 1971 and 2014, over half of the drinking water outbreaks in the US were due to untreated or inadequately treated groundwater.[3,4]

Electrooxidation (EO) uses inert electrodes to directly oxidize contaminants at the electrode surface and/or generate oxidants in solution. Boron-doped diamond (BDD) electrodes are commonly used in EO research due to BDD's high resistance to chemical and thermal degradation and low tendency to react with solvents.[5,6] BDD EO is capable of disinfecting pathogens through either the production of reactive oxygen species (ROS) from electrochemical water decomposition or free chlorine and chlorine dioxide produced from oxidation of chloride.[7–10] In the absence of chloride, hydroxyl radicals at the electrode surface are the primary oxidant species, and disinfection relies on pathogen transport and sorption to the electrode surface.[11,12] In general, the efficacy of BDD disinfection increases with the concentration of chloride in the water matrix.[7,8,13,14] Increased disinfection in the presence of chloride may indicate that chlorine species are more important to BDD disinfection compared to ROS. Alternatively, chlorine may have a synergistic effect on ROS generation, with more ROS generated in high chloride matrices.[7]

A combined process using EO with BDD followed by electrocoagulation (EC) was used by Cotillas et al.[15] and Llanos et al.[16] for *E. coli* mitigation. EC is the *in situ* formation of coagulant in water due to oxidation of a sacrificial anode, typically aluminum or iron. EC has been considered as a pretreatment process for removal of turbidity and natural organic matter in a variety of

applications.[17–20] EC is also an effective means of virus reduction.[21] The primary mechanism of EC is often considered to be the same as chemical coagulation, *i.e.*, physical removal by charge neutralization or sweep flocculation.[21] However, EC can also inactivate viruses and bacteria via generation of free chlorine or Fenton-like reactive intermediates due to ferrous iron oxidation.[22–25] Iron EC generates ferrous ions (Fe^{2+}) in solution by oxidizing a zero-valent iron electrode.[26,27] The oxidation of ferrous ions to ferric can generate intermediate oxidants capable of inactivating viruses.[25] In Chapter 4, virus inactivation due to iron EC was found to be more prevalent in slightly acidic waters (~pH 6), while physical removal is the dominant fate of viruses in iron EC above pH 7. In a combined EO-EC reactor, Llanos et al.[16] found that iron electrodes were more effective for *E. coli* reduction compared to aluminum electrodes. The team attributed the greater removal observed with iron electrodes to the formation of a passivation layer on aluminum electrodes, though the possibility of *E. coli* inactivation due to iron oxidation was not investigated.

Disinfection by means of EO has been extensively investigated for mitigation of bacteria,[7,11,13,15,28–31] but virus mitigation by EO has received comparatively little attention.[32–34] Both bacteriophage MS2 and recombinant human adenovirus have been found to be more resistant to electrochemical disinfection compared to *E. coli* and *Enterococcus.*[34] Since bacteria may therefore be poor indicators of virus disinfection via EO, the lack of information on virus mitigation by EO is a critical gap in the literature. Moreover, EC pretreatment ahead of EO may offer advantages for virus treatment, but has not yet been thoroughly assessed.

The goal of this study was to evaluate iron EC as a pretreatment for disinfection of waterborne viruses via BDD EO. To accomplish this goal, the effects of pH, natural organic matter, and turbidity on virus mitigation by EO were first evaluated. The impact of ferrous iron on EO was also investigated in order to design an effective treatment train using sequential EC

and EO. Next, a sequential EC-EO treatment train was evaluated for mitigation of two bacteriophage surrogates and echovirus in four synthetic water matrices representing a range of source waters. The EC-EO system was then compared to a more conventional treatment train comprising chemical coagulation and free chlorine disinfection.

Notably, in testing water treatment processes, bacteriophage surrogates are frequently used in place of human viruses for reasons of cost, ease, and safety.[35–38] However, surrogates should be compared to human viruses of interest in any novel application. Echovirus is a ubiquitous pathogen in human-impacted water systems and among the smallest viruses, with diameters typically smaller than 30 nm.[39,40] The results from Chapter 4 determined that echovirus 12 is resistant to inactivation by EC and is therefore a conservative indicator of virus mitigation.

5.2. Materials and Methods

5.2.1. Batch Electrocoagulation and Electrooxidation Process Operation

All EC and EO tests were conducted in 200-mL polypropylene batch reactors. EC reactors utilized four 1020 steel electrodes (VMetals, Milwaukee, WI). EO reactors used a single BDD/Si anode (NeoCoat SA, La Chaux-de-Fonds, France) and commercially available pure Grade 2 titanium as an inert cathode (Performance Titanium Group, San Diego CA). Similar disinfection performance may be possible with lower cost electrodes, for example graphite.[28,41] However, BDD electrodes were used in this study as a representative EO treatment because of the prevalence of BDD usage in electrochemical disinfection research. The BDD coating was 3 µm thick and p-doped with 700 – 800 ppm boron. All electrodes had a submerged working surface area of 15 cm^2 (5 cm x 3 cm).

Prior to use, iron EC electrodes were wet-polished with 400 grit Si-C sandpaper, triple-rinsed with PureLab ultrapure water (ELGA LabWater, UK), and then disinfected under UV light for 30 minutes per side in a biosafety cabinet. EC electrodes were polarized at 100 mA in 3 mM sodium bicarbonate solution for 10 minutes to mimic conditions of continual use in drinking water, then thoroughly rinsed with ultrapure water to remove residual iron. The BDD anode and titanium cathode were polarized at 100 mA for 10 minutes in 0.1 M H_2SO_4 to rehydrogenize the electrode surface before each test in order to provide consistent electrode conditions.[6,12]

5.2.2.Virus Propagation and Quantification

Two bacteriophages were used as human virus surrogates: MS2 (ATCC #15597-B1) and ΦX174 (ATCC #13706-B1). MS2 is an F-specific coliphage with a single-stranded RNA genome (Baltimore group IV), while ΦX174 is a somatic coliphage with a single-stranded DNA genome (Baltimore group II).[38] These bacteriophages are standard laboratory surrogates for enteric viruses.[21] To evaluate the suitability of these bacteriophage surrogates for indicating human virus mitigation during electrochemical treatment, human echovirus 12 (ATCC #VR-1563) was used to verify a subset of tests.

Bacteriophages were propagated using the double-agar layer (DAL) method. *E. coli* ATCC #15597 and #13706 were used to propagate and quantify MS2 and ΦX174, respectively. Echovirus was propagated in Buffalo Green Monkey Kidney cell culture (ATCC CCL-161) until cell monolayers were reduced to approximately 10 - 20% confluence, then subjected to three freeze-thaw cycles at -20^{o}C. All viruses were purified by two cycles of polyethylene glycol (PEG) precipitation followed by a Vertrel XF (DuPont, Wilmington, DE) purification, as described by Mayer et al.[42] Bacteriophages were quantified using the spot titer plaque assay method, as described by Beck et al.[43] Echovirus was quantified using the Reed & Muench $TCID_{50}$ method.[44]

Bacteriophages were stored at 4^{o} C. Even at low concentrations, dimethyl sulfoxide (DMSO) inhibited bacteriophage inactivation due to EO, as shown in Appendix E.1. DMSO exerts a high demand for hydroxyl radicals at concentrations as low as 0.25 mM.[45] For this reason, echovirus was stored at -20^{o} C without cryopreservant and was used within 2 months of propagation.

Bacteriophages were spiked at concentrations of approximately 10^7 PFU/mL, while echovirus was spiked at approximately 10^4 $TCID_{50}$/mL due to limitations in virus propagation. After treatment, the reactor was briefly homogenized by rapid stirring (600 rpm for 15 s), and a 20-mL sample was taken for virus elution. Elution was performed 15 minutes after EO treatment to allow the same reaction time as EC. Elution was performed by adding an equal volume of 6% beef broth to homogenized samples and vortexing for approximately 10 s. Samples containing bacteriophages were diluted in tenfold series in pH 7.0 buffered demand free (BDF) water, and ten 10-µL drops of each dilution were plated. Samples containing echovirus were also diluted in BDF. Aliquots of 100 µL from each echovirus dilution series were added to 6 wells in a 24-well tray of 1-day-old BGM cells. BGM cultures were observed under magnification for the appearance of cytopathic effects over the following 10 days, and were quantified using the Reed & Muench $TCID_{50}$ method.[44]

5.2.3.Impact of Water Constituents on Electrooxidation

To test the impact of NOM, turbidity, pH, and ferrous iron on EO with BDD electrodes, batch EO tests were performed at a constant current of 20 mA (i = 1.3 mA/cm^2) for 5 minutes. Sodium bicarbonate (2.1 mM) was added to ultrapure water for a background electrolyte solution, and pH was adjusted with 1 M H_2SO_4 or NaOH. NOM, turbidity, and ferrous iron tests were conducted at pH 7; pH tests were conducted at pH 6, 7, and 8. NOM was added as humic acid sodium salt (Sigma Aldrich, St. Louis, MO) at concentrations of 0.1 to 15 mg/L total organic

carbon (TOC). Turbidity was increased by adding A2 test dust (Powder Technology Inc., Arden Hills, MN) to approximately 1 to 30 NTU. Contributions of NOM to TOC were measured using a TOC-V CSN total organic carbon analyser (Shimadzu, Kyoto, Japan) following sample acidification with analytical grade hydrochloric acid. Though NOM contributes to turbidity, tests were performed by adding enough A2 dust to provide the target turbidity (see Appendix E.2) independent of NOM. Turbidity was measured using a Hach 2100AN Turbidimeter (Hach, Loveland, CO).

5.2.4.Sequential Electrocoagulation-Electrooxidation Process Operation

A treatment train schematic for sequential EC-EO treatment is shown in Figure 5-1. Preliminary testing determined that a particle separation step between the EC and EO stages provided greater bacteriophage reduction, as shown in Appendix E.3. For this reason, the entire volume of the reactor was filtered before EO treatment with a Whatman 114 filter to remove coarse precipitates (> 25 µm) without affecting turbidity or NOM. Due to potential formation of iron flocs from dissolved iron during EO treatment, an additional filtration step was performed after EO as well. After final filtration, 5-mL samples were diluted into 5 mL 6% beef broth (pH 9.5) to elute viruses from any remaining floc and promote monodispersion.

Untreated controls were performed along with every EC-EO treatment test. All untreated controls were retained in reactors for the same amount of time as treated replicates (but without electrochemical treatment) and underwent the same filtration and elution procedures. Log reduction of viruses was calculated by comparing eluted virus concentrations

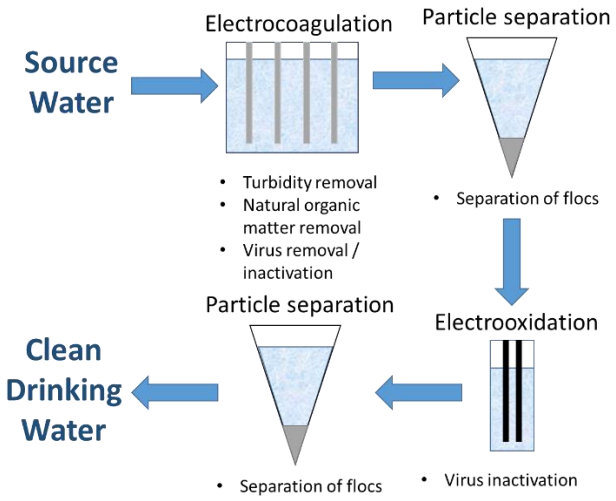

Figure 5-1. Schematic of electrocoagulation-electrooxidation treatment train and hypothesized treatment effects for each stage.

after EC-EO to these untreated controls. Therefore, these controls accounted for any minor losses of virus due to sorption to the coarse filters or elution. The data indicated that virus concentrations remained at approximately the spiked concentration in the untreated controls (10^7 PFU/mL for bacteriophages and 10^4 $TCID_{50}$/mL for echovirus), indicating that any virus loss due to experimental artifact was minor. In combination with floc formation, some fraction of viruses was expected to be retained with the floc on the coarse filter. In any coagulation process, some method of floc separation is required, whether settling, centrifugation or filtration. In this case, a coarse filter was used for expediency compared to gravitational separation and to provide a more conservative account of physical separation compared to microfiltration.

A constant charge loading of 150 C/L was divided between the EC and EO processes by varying current over a constant retention time of 5 minutes per treatment process. The charge loading of 150 C/L (50 mA applied over 10 minutes total reaction time in a 200-mL reactor, i_{EC} = 1.1 mA/cm^2, i_{EO} = 3.3 mA/cm^2) was chosen in order to establish a curve that demonstrated

differences between charge allocations and virus log reduction without exceeding the measurable limit of virus reduction (~5 log reduction), as explained in Appendix E.4. Total and ferrous iron concentrations were measured using Hach FerroVer Total Iron and Ferrous Iron Reagent (Hach, Loveland, CO). Absorbance was measured at 510 nm using a Genesys 20 spectrophotometer (Thermo Fisher Scientific, Waltham, MA).

5.2.5.Preparation of Synthetic Waters for Sequential EC-EO Process

Removal of the two bacteriophage surrogates (MS2 and ΦX174) and echovirus was evaluated in synthetic waters modeled after a range of environmental source waters. Four model waters were synthesized by adding reagent-grade chemicals to ultrapure water and adjusting pH, NOM, and turbidity, as shown in Table 5-1. Model water parameters were based on water quality data for the Mississippi River at Brooklyn Park, MN, Lake Michigan at Milwaukee, WI, and shallow (dolomite), and deep (sandstone) aquifers near Lincoln township and Waukesha, WI, as detailed in Appendix E.2. To represent the anoxic conditions of groundwater, Dolomite and Sandstone Aquifer model waters were degassed using argon for 15 minutes prior to pH adjustment and virus addition.

5.2.6.Comparison of Sequential EC-EO to Conventional Coagulation/Disinfection

Ferric chloride was added to match the iron dose achieved by 50 mA EC with a 5-minute retention time (22 mg Fe/L) to represent a 50/50 allocation of charge for EC-EO. Reactors were rapidly stirred (600 rpm) for 30 s, followed by a slower stir rate (200 rpm, as used in EC) for 270 s (total reaction time of 5 minutes). Consistent with EC-EO treatment tests, reactors were allowed to settle for 15 minutes without stirring, and then the total volume was passed through a Whatman 114 filter. Sodium hypochlorite was added (1.2 mg/L as Cl_2, 5 min retention) to meet

Table 5-1. Model water parameters

	Alkalinity (mg/L as $CaCO_3$)	Chloride (mg/L)	Added Turbidity (NTU)	Total Organic Carbon (mg/L)	pH	Conductivity (µS/cm)	Dissolved Oxygen (mg/L)
Lake Michigan	118	13	0	2	8.3	340	9
Mississippi River	162	11	30	8.7	8.1	400	9
Sandstone (deep) Aquifer	220	4	0	0	7.5	550	0.3
Dolomite (shallow) Aquifer	320	70	10	0	7.5	1000	0.4

the recommended 6 mg-min/L chlorine dose for small water treatment systems.[46] After 5 minutes retention time, an excess of sodium thiosulfate (0.03 mM) was added to the reactor to quench residual chlorine.

5.2.7.Data Analysis

All statistical analyses were performed in the R statistical language using the stats package.[47] Bacteriophage inactivation was correlated to charge allocation between EC and EO by linear regression. Models were evaluated for residual distribution, normality, and leverage points (Cook's distance) using the plot.lm() function, and significance of variables was evaluated by analysis of variance with the anova() function.[47] Akaike's 'An Information Criterion' was used to evaluate the goodness-of-fit and parsimony of competing linear models.[47,48]

Echovirus tests were performed in triplicate at 0, 50, and 100% charge allocations to EC and compared to MS2 and ΦX174 reduction in the same waters at all charge allocations. One-way ANOVA was performed to assess differences in mean removal between viruses within each

model water. Post-hoc comparison of means was performed using Tukey's HSD using the aov() and TukeyHSD()functions.[47]

The electrical energy per order of magnitude (EEO) [49] virus reduction was calculated for the sequential EC-EO treatment in the four model waters. This parameter provides a benchmark for comparing the energy costs of virus mitigation in different treatment scenarios.

5.3. Results and Discussion

5.3.1. Effect of Water Constituents on BDD Electrooxidation

To evaluate the impact of water quality on virus inactivation via EO, BDD EO was performed under conditions of varying NOM, turbidity, and pH. Both NOM and turbidity impeded EO, as shown in Figure 5-2. NOM increases oxidant demand, resulting in poorer disinfection of target pathogens.[50] NOM is particularly effective at quenching hydroxyl radicals, with a rate constant near 10^8 $M^{-1}s^{-1}$.[51] Hydrophobic virions may also sorb to, and be shielded by, NOM. The A2 test dust used to increase turbidity consists of silica, alumina, and various metal oxides.[52] The presence of metal oxides in A2 test dust likely provides oxidant demand, leading to the poor inactivation shown in Figure 5-2B. Therefore, a pretreatment stage prior to EO is needed to mitigate the negative influence of NOM and turbidity on virus inactivation during EO.

Reduction of both MS2 and ΦX174 was greater at pH 6 and 7 compared to pH 8, as shown in Figure 5-2C. Generation of ROS (primarily hydroxyl radicals) due to EO is greater at lower pH.[12] Inactivation of either bacteriophage was not statistically different between triplicate tests at pH 6 and 7. Therefore, virus reduction above pH 7 should be a conservative indicator of reduction in slightly acidic waters as well. For this reason, model waters below pH 7 were not investigated in later experiments. In all tests, pH increased slightly during the EO process by an average of 0.20 ± 0.05 pH units.

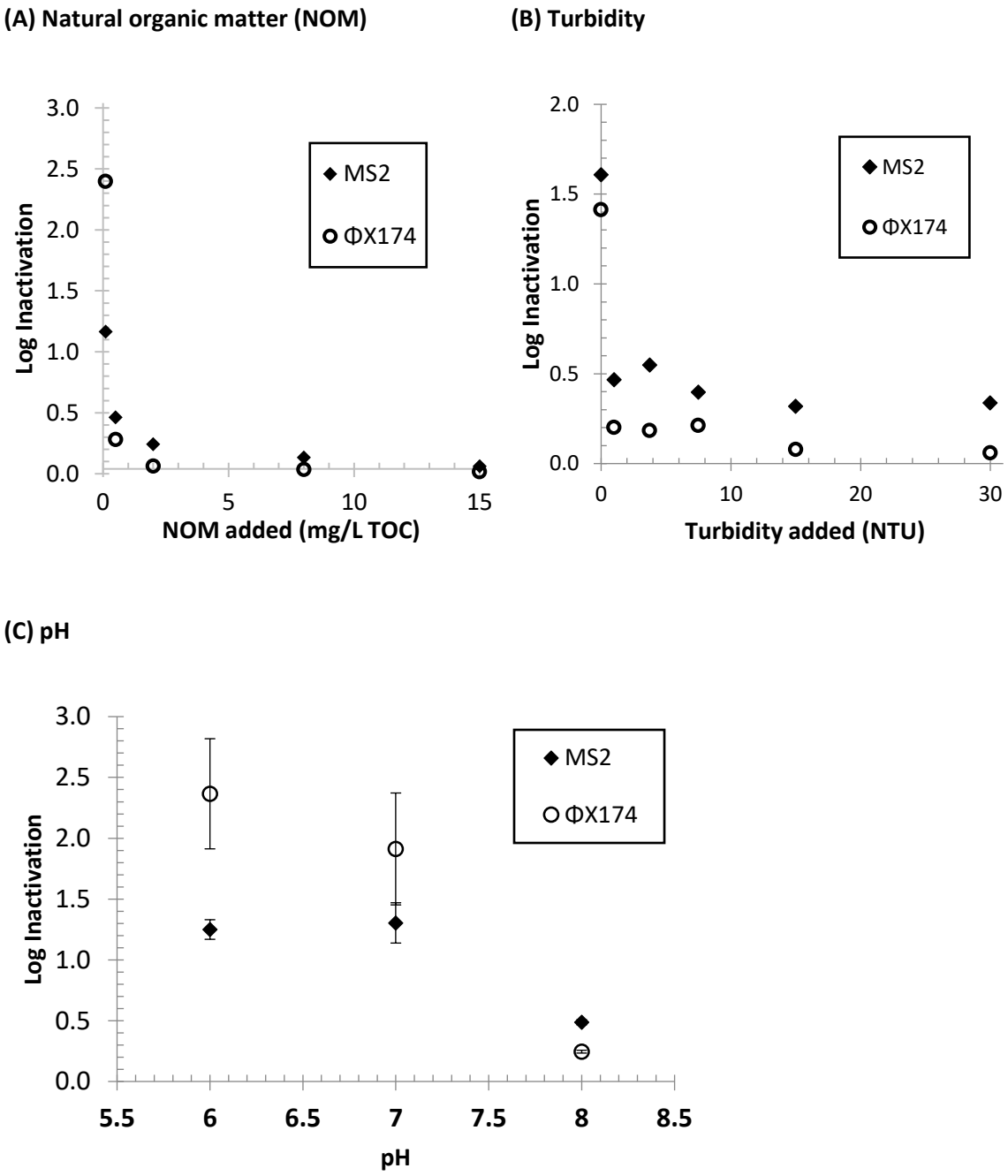

Figure 5-2. Impact of water quality, (A) natural organic matter, (B) turbidity, and (C) pH, on bacteriophage MS2 and ΦX174 reduction by electrooxidation using boron-doped diamond (BDD) electrodes (20 mA, 5 min). Tests were conducted in 2.1 mM $NaHCO_3$. Both NOM and turbidity inhibited inactivation, and inactivation was significantly lower at pH 8. Points in (A) and (B) represent single tests (mean of 10 counts). Points in (C) represent mean values of triplicate tests with ±1 standard error shown by the error bars.

5.3.2.Impact of Ferrous Iron on BDD Electrooxidation

In addition to directly oxidizing contaminants, ferrous iron can enhance other oxidation treatment processes. Iron-enhanced oxidation has been demonstrated for many contaminants. Ferrous-catalyzed ozonation has been found to be more effective than ozonation alone in oxidizing organic pollutants and COD.[53–55] Researchers have found that ferric iron has similar, albeit possibly lesser, catalytic effects for ozonation of organic pollutants.[54,56] Though disinfection studies using iron-enhanced oxidation are scarce, Sjogren and Sierka[57] found that 2 µM ferrous sulfate-augmented TiO_2 photocatalysis achieved an additional 2 $\log_{10}$ reduction of MS2 over TiO_2 photocatalysis alone. Although the mechanisms for enhancing oxidation are likely different between these treatment processes and BDD EO, iron enhancement is common among these processes. To the author's knowledge, iron-enhanced BDD EO has not previously been investigated. Using an oxidation method like EO could also regulate iron oxidation to maximize disinfection and minimize soluble iron residuals. Conversely, EO may benefit EC by further oxidizing iron species to form more floc.

For this reason, the possible synergistic effects of ferrous iron generated by EC and EO performance was investigated. As shown in Appendix E.3, inclusion of a filtration step between EC and EO improved virus reduction beyond EC alone. Thus, ferrous iron from EC likely created an oxidant demand rather than enhancing EO. To confirm the effect of ferrous iron as an oxidant scavenger, a follow up experiment was performed using ferrous chloride to demonstrate the effect of ferrous iron dose on EO inactivation. Samples of the bulk solution after EO were homogenized and eluted (6% beef broth, pH 9.5) to show the effect of inactivation only, without considering removal due to coagulation/destabilization. As shown in Figure 5-3, the oxidant demand of ferrous iron inhibited virus inactivation at low doses. At higher doses of ferrous iron, virus inactivation eventually met or exceeded the level achieved by EO without ferrous addition.

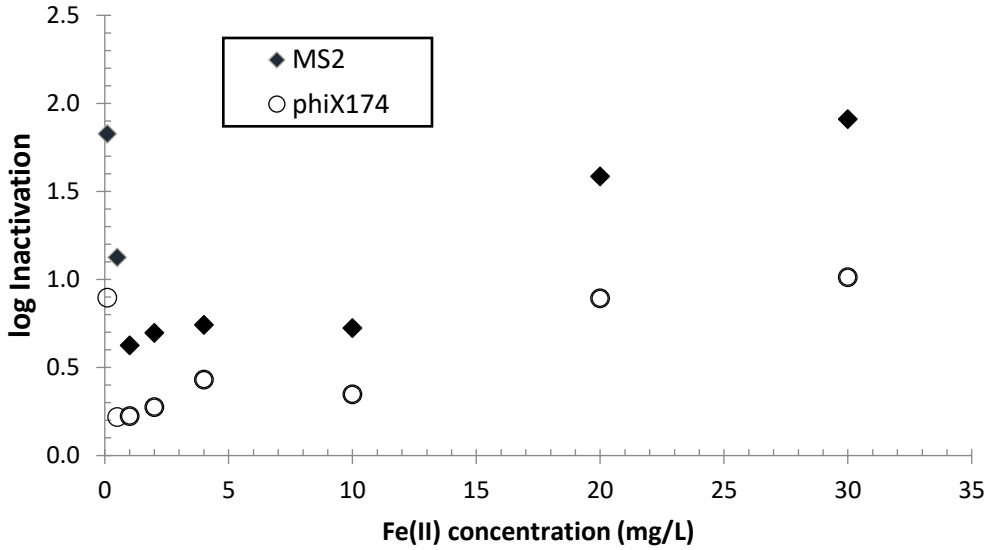

Figure 5-3. Combined effect of ferrous chloride coagulation and subsequent boron-doped diamond electrooxidation on the reduction of bacteriophages MS2 and ΦX174. Inactivation was inhibited by low doses of ferrous iron and returned to iron-free inactivation levels only at very high doses (~ 30 mg/L Fe). Tests were conducted in 2.1 mM $NaHCO_3$, pH 7. Points represent single tests (mean of 10 counts).

Therefore, ferrous iron may catalyze virus inactivation, but the concentration of iron needed (> 30 mg/L Fe) to do so may be cost-prohibitive and introduce high concentrations of residual iron.

5.3.3.Sequential EC-EO Treatment of Model Waters

5.3.3.1. Charge Allocation for Optimal EC-EO Virus Mitigation

The impact of energy allocation between EC and EO in the EC-EO treatment train was evaluated to determine how the two processes might be balanced for enhanced virus reduction. The total charge loading of 150 C/L for EC-EO treatment and retention time of 5 minutes per process were held constant while current allocated to each treatment varied. Increased charge allocation to EC from 0% to 100% (0 to 100 mA) was approximately equal to the increase in energy density (kJ/L, or energy normalized to the reactor volume) for EC and EO, as shown in Appendix E.5. Here, virus mitigation was related to charge allocation so that the results could be

generalized to other EC and EO reactors. These charge allocation tests were conducted in each of the four model waters representing a wide range of environmental source waters (summarized in Table 5-1).

The effect of charge allocation on MS2 and ΦX174 bacteriophage removal is shown in Figure 5-4 for the four model waters. Charge allocation was arbitrarily represented as a percentage of the total charge loading allocated to EC. Regression models expressing log reduction in terms of percent charge allocated to EC are summarized in Table 5-2, including estimated optimal charge allocation in each source water. Both surface waters (Lake Michigan and Mississippi River) tended to favor the dual process of EC-EO, with optimal charge allocated to EC of 47% (both MS2 and ΦX174) in Lake Michigan model water and 60% (MS2) or 26% (ΦX174) in Mississippi River model water. Sandstone Aquifer model groundwater favored EC alone, while Dolomite Aquifer model groundwater showed no significant trend, with similar removal across the charge allocation range. The main difference in formulation between these two waters was the chloride concentration (see Table 5-1), with Sandstone Aquifer comprising very little chloride (4 mg/L Cl^-) and Dolomite an excess of chloride (70 mg/L Cl^-). Evolution of free chlorine was therefore likely to have improved disinfection by EO, as previous researchers have also reported.[7,8,13,14] Nevertheless, EO still did not surpass EC in Dolomite Aquifer model water.

This trend was somewhat surprising, because model groundwaters had a lower pH (pH 7.5) than surface waters (pH 8.1 – 8.25). During the EC-EO process, pH increased slightly in all model waters but did not increase disproportionately for surface waters, as shown in Appendix

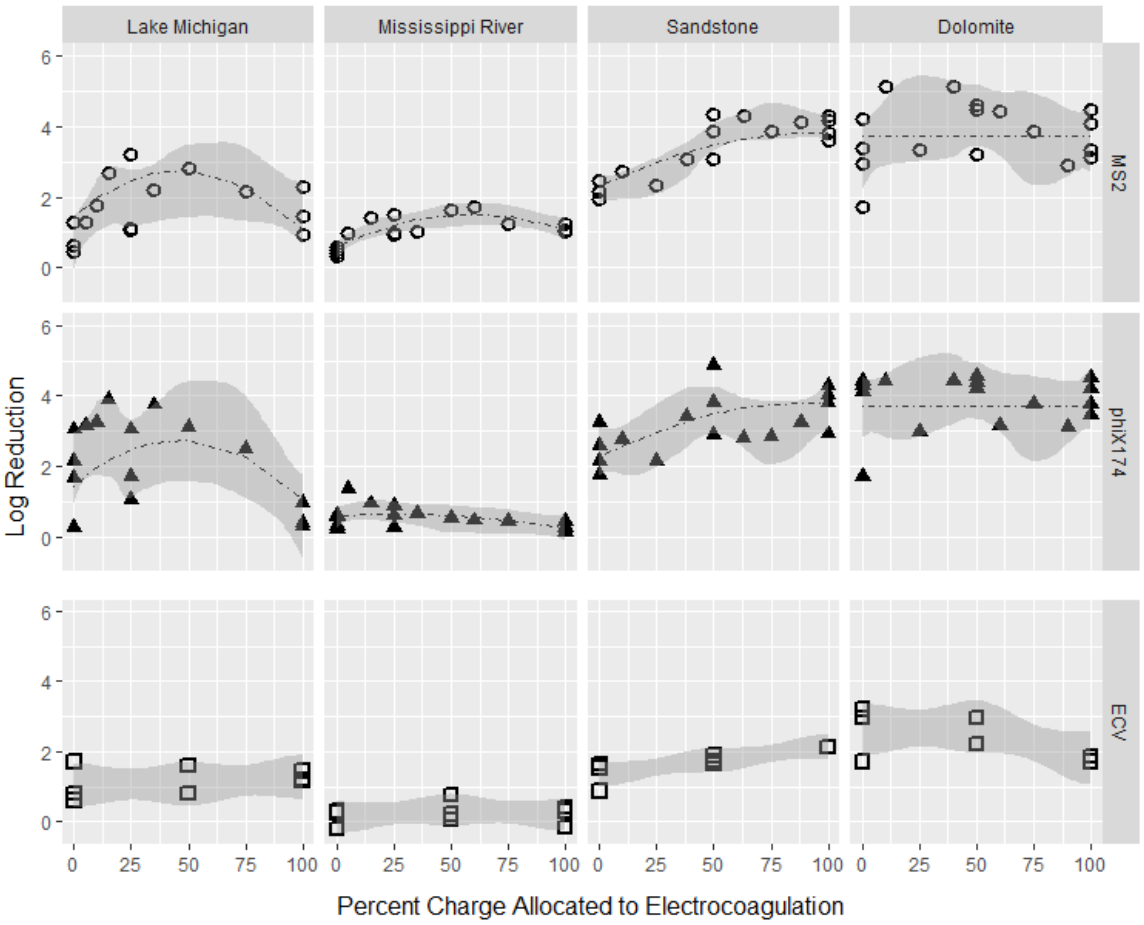

Figure 5-4. The effect of charge allocation between iron electrocoagulation and boron-doped diamond electrooxidation on the reduction of bacteriophages MS2 and ΦX174 and human echovirus 12 (ECV) in four model waters. Poorest removal occurred in Mississippi River water (the highest in NOM and turbidity), while greatest average removal occurred in Dolomite Aquifer (the highest in conductivity and chloride). Points represent single tests (mean of 10 counts for bacteriophages, single well plates for ECV); lines represent predicted values based on regression models. ECV data was insufficient to characterize over the entire range of charge allocation.

E.5. Therefore, EO was expected to be more effective in groundwaters than surface waters. In fact, log reduction was overall greater in groundwaters. This indicates that low pH improved virus mitigation via EC to an even greater extent than EO. The results from Chapter 4 demonstrated that inactivation via iron EC increases at lower pH levels and may even become the dominant fate of viruses. In Chapter 3, bacteriophage inactivation was found to be a

Table 5-2. Summary of linear regression models for log reduction of bacteriophage MS2 and ΦX174 as a function of the percent of the total charge used in the EC-EO treatment process (150 C/L) that was allocated to EC ("% EC"). Estimated optimal charge allocation based on the regression models ranged from 26% to 100% EC. A single model described log reduction of both MS2 and ΦX174 for all waters except Mississippi River. Log reduction in the Dolomite Aquifer model water was independent of charge allocation, so there was no optimal % EC.

		Lake Michigan		Mississippi River		Sandstone Aquifer		Dolomite Aquifer	
		MS2	ΦX174	MS2	ΦX174	MS2	ΦX174	MS2	ΦX174
Intercept	β	1.46		0.584	0.584	2.28		3.53	
	p-value	2.04E-05		1.50E-07	1.50E-07	2.24E-13		<2e-16	
% EC	β	0.0557		0.0313	0.00438	0.0329		n.s	
	p-value	5.21E-03		1.49E-05	5.72E-04	1.39E-03		n.s	
$(\% EC)^2$	β	-5.96E-04		-2.63E-04	-7.62E-05	-1.74E-04		n.s	
	p-value	2.24E-03		2.00E-04	2.39E-02	6.32E-02 *		n.s	
Estimated optimal % EC		47%		60%	26%	100%		N/A	
F statistic (degrees of freedom)		6.047 (2,29)		14.28 (4, 27)		20.15 (2,31)		N/A	
R^2adj		0.25		0.63		0.54		N/A	

n.s: Not significant

* Variable was not strictly significant (α = 0.05) but was determined to be beneficial to the model by Aikake's An Information Criterion (AIC).

function of both the amount of iron oxidation and the iron oxidation rate. Because the groundwaters had low initial pH and dissolved oxygen concentrations, greater ferrous concentrations were maintained in solution, as shown in Appendix E.6. In low-oxygen conditions, ferrous iron requires a longer time to oxidize.[58] Therefore, model groundwaters offered a more favorable environment for virus inactivation due to ferrous iron.

As anticipated, the high NOM, high turbidity, and high pH Mississippi River water was the most challenging for virus reduction. Ferrous iron binds with NOM, thereby becoming resistant to oxidation.[59] Accordingly, ferrous iron residual remained high after EO only in the high-NOM

Mississippi River water (see Appendix E.6). Therefore, NOM impairs not only the EO stage (Figure 5-3), but also EC. The failure of EC to dramatically improve virus mitigation in Mississippi River water is testament to the fact that EC did not substantially improve water quality prior to EO (in contrast to the original hypothesis). In Mississippi River water, total organic carbon did not significantly change between the initial concentration and post-EO filtration (p = 0.175). Decreasing pH prior to EC to achieve enhanced coagulation can improve NOM removal.[18] However, the tendency of EC to increase solution pH could counteract enhanced coagulation.

The electrical energy per order (EEO) for virus reduction further highlighted the efficacy of the overall treatment in model groundwaters over model surface waters, as shown in Figure 5-5. In a sequential treatment evenly divided between EC and EO (50 mA for 5 min in each stage), log virus reduction required approximately 2 to 10 times greater energy input in model surface waters compared to groundwaters. The greater energy density requirements are due not only to poorer virus mitigation in surface waters, but also the higher potentials needed to overcome resistance due to low conductivity (see Table 5-1). Though EEO provides a benchmark for comparing virus mitigation in the different model water matrices used in this study, using EEO to compare to other technologies is potentially problematic. The batch EC and EO reactors used in this study were not optimized for energy efficiency, so comparisons to established technologies are not possible. In addition, a lack of standard experimental conditions for assessing EEO makes comparisons between even studies using the same technology problematic.[60] With these caveats in mind, it is still possible to compare the order of magnitude of EEOs in this study to other values. An EEO of <0.265 kW/m^3 is generally recommended, although higher values have been used in cases where there are no treatment alternatives.[59] Figure 5-5 shows that groundwater treatment using EC-EO for virus mitigation falls within the recommended range, even without any attempt to optimize the process for power efficiency.

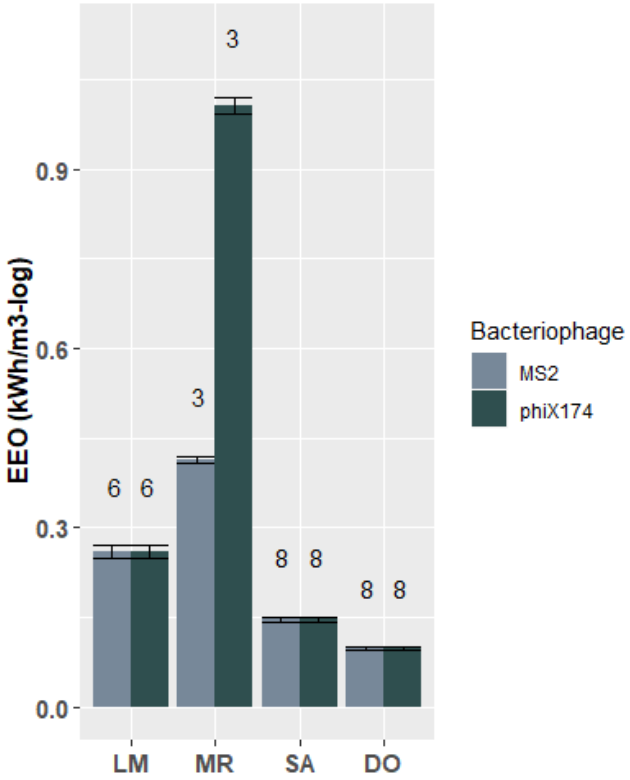

Figure 5-5. Electrical energy per order (EEO) for sequential electrocoagulation – electrooxidation treatment train in four model waters. Though the batch reactors used in this study were not optimized for energy efficiency, EEO provides a benchmark for comparing the energy cost of virus mitigation between different water matrices. Log reduction was estimated in each water for an even distribution of charge between electrocoagulation and electrooxidation (50 mA for 5 min, or 75 C/L, per process) using the regression models shown in Table 5-2. LM = Lake Michigan, MR = Mississippi River, SA = Sandstone Aquifer , and DO = Dolomite Aquifer model waters. Each column represents the mean values of replicate tests (n shown above bars) with ±1 standard error shown by the error bars.

Though the trends modeled in Figure 5-4 were significant, triplicate tests of virus mitigation did not significantly differ between a balance of EC-EO and EC alone. These results indicated that EC alone was nearly as effective as the sequential EC-EO treatment. Ferrous iron concentrations entering the EO stage were low (0.02 – 0.17 mg/L Fe, see Appendix E.6), but still in the inhibitory range for EO (Figure 5-3). Therefore, a more effective particle separation stage, *e.g.,* microfiltration, could lead to greater disinfection in the EO stage. Given the relative cost of iron and BDD electrodes, a one-stage EC treatment would be far preferable for virus mitigation

from a practical standpoint. In addition, the combination of ROS and chlorine species formed by BDD electrodes can give rise to disinfection byproducts (DBPs) like chlorate and perchlorate unless operating conditions are carefully controlled.[7,8] However, EO may still offer benefits for oxidizing other contaminants, such as organic micropollutants. EO also oxidized residual ferrous iron after EC for most waters (see Appendix E.6). EO can therefore act as a polishing step to oxidize residual iron for improved precipitation and removal in order to meet aesthetic standards for iron in drinking water.

5.3.3.2. Comparison of Bacteriophage Surrogates to Human Echovirus

Reduction of echovirus by the EC-EO treatment train was also evaluated in the four model waters, as shown in Figure 5-4. Echovirus mitigation followed the same pattern as bacteriophages, in order of increasing reduction: Mississippi River < Lake Michigan < Sandstone Aquifer ≈ Dolomite Aquifer (as summarized in Appendix E.2). However, the mean reduction of echovirus was significantly less than one or both bacteriophage surrogates in all model waters by a factor of 0.9 to 1.5 logs, as summarized in Table 5-3. By contrast, the two bacteriophages significantly differed only in Mississippi River model water, where removal followed the pattern of echovirus ≈ ΦX174 < MS2.

Mitigation of bacteriophage MS2 was significantly higher in Mississippi River model water than either ΦX174 or echovirus, which indicates that bacteriophage ΦX174 mitigation is impaired to a greater degree by NOM and turbidity. As discussed in Section 5.3.1, NOM and turbidity can dramatically impact the efficacy of EO. As seen in Chapter 4 and previous research, [61] NOM also impairs virus mitigation by iron EC. Though neither phage was a conservative surrogate, the lack of a significant difference in echovirus and ΦX174 mitigation in Mississippi River model water indicates that ΦX174 should be considered the more conservative surrogate

Table 5-3. Comparison of bacteriophage surrogates MS2 and ΦX174 and human echovirus 12 (ECV) reduction due to sequential electrocoagulation-electrooxidation treatment. Mean reduction from all tests in each model water was compared by Tukey's HSD. Cells in gray indicate non-significant differences (α = 0.05).

Mean Difference in Log Reduction and Significance

	MS2 - ECV	ΦX174 - ECV	MS2 - ΦX174
Lake Michigan	0.660 *p =2.53E-01*	1.266 *p =9.73E-03*	-0.606 *p =1.69E-01*
Mississippi River	0.876 *p =1.76E-05*	0.420 *p =4.59E-02*	0.457 *p =4.72E-03*
Sandstone Aquifer	1.503 *p =2.58E-05*	1.334 *p =1.64E-04*	0.169 *p =7.57E-01*
Dolomite Aquifer	1.092 *p =2.27E-02*	1.213 *p =1.02E-02*	-0.122 *p =9.20E-01*

for human viruses across a range of waters. In addition, the difference in mean log reduction between bacteriophage ΦX174 and echovirus was consistent across model waters (between 2 – 3 times greater log reduction). Until a better surrogate is identified, correcting bacteriophage ΦX174 inactivation results by a safety factor of 2-log reduction could provide a reasonable indicator of echovirus mitigation.

5.3.3.3. Comparison to Conventional Coagulation/Disinfection

The EC-EO treatment train was compared to a conventional treatment train of chemical coagulation with ferric chloride salt (22 mg Fe/L, equivalent to the iron generated by EC at 50 mA for 5 min) and free chlorine (1.2 mg/L Cl_2). The purpose of this comparison was to evaluate the relative efficacy of EC-EO compared to typical treatment processes under identical water quality conditions. Although the iron dose was equivalent to the EC dose for Dolomite Aquifer and Sandstone Aquifer model groundwaters, these tests did not provide a mechanistic comparison to the conventional treatment train as they did not account for ferrous oxidation, generation of ROS, or anodic oxidation.

In the Lake Michigan and Mississippi River model surface waters, the conventional treatment system outperformed the EC-EO system, as shown in Figure 5-6. However, in the model Sandstone and Dolomite Aquifer groundwaters, EC-EO dramatically outperformed the conventional system. This discrepancy may be due to iron-based disinfection in low-oxygen waters, as discussed in Section 5.3.3.1. In addition, the two surface waters were above pH 8, leading to poor conditions for disinfection by either free chlorine or hydroxyl radicals. Addition

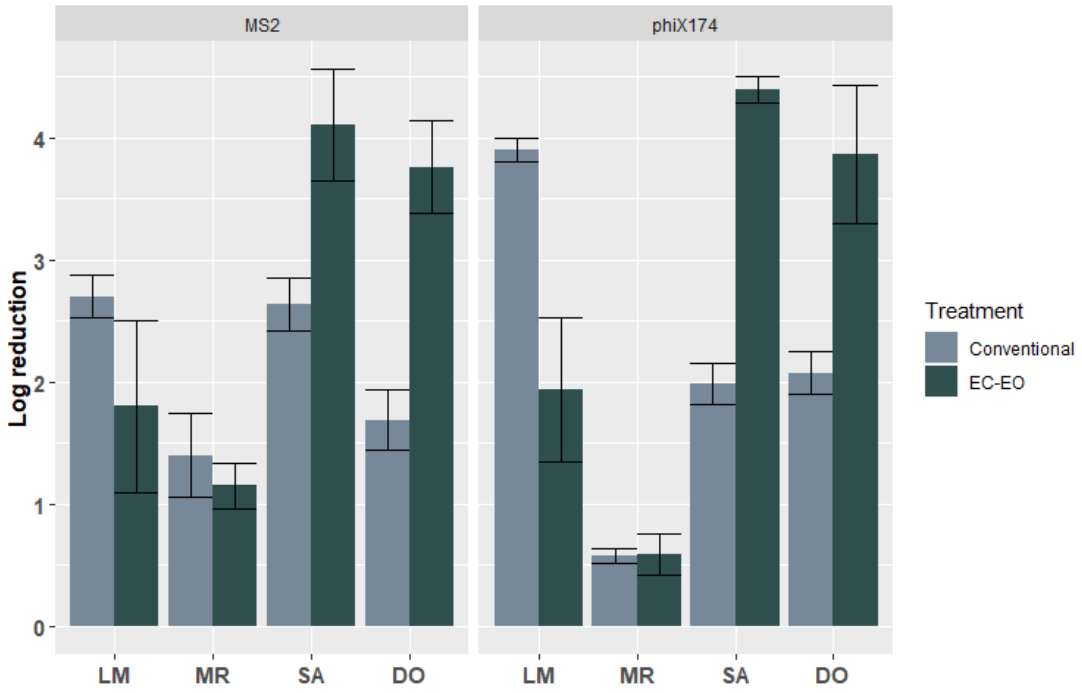

Figure 5-6. Comparison of conventional coagulation/chlorination treatment train to the electrocoagulation-electrooxidation (EC-EO) treatment train for the reduction of bacteriophages MS2 and ΦX174. "Conventional" treatment consisted of $FeCl_3$ chemical coagulation (22 mg/L Fe) followed by NaOCl disinfection (6 mg-min/L Cl_2). EC-EO was conducted near the optimal division of 150 C/L in the EC-EO treatment train (25% EC for LM and MR, 50% EC for DO and SA). LM = Lake Michigan, MR = Mississippi River, SA = Sandstone Aquifer , and DO = Dolomite Aquifer model waters. Each column represents the mean values of triplicate tests with ±1 standard error shown by the error bars.

of chemical coagulant decreased the pH to 7.0 or less in all waters, which likely improved disinfection by ensuring free chlorine was predominately in the hypochlorous acid, rather than the hypochlorite, form.

5.4. Conclusions

Few studies have assessed at EC and EO individually for virus mitigation, and no previous research has investigated an EC-EO process for virus mitigation. Previous attempts to combine EC and EO processes have used a simultaneous EC/EO reactor that would likely be inhibited by the oxidant demand of ferrous iron (Cotillas et al., 2013; Llanos et al., 2014). This study both establishes a basis for using a novel, sequential EC-EO treatment train for drinking water and thoroughly evaluates treatment performance for two bacteriophages and a human waterborne virus.

The improved virus mitigation achieved by the EC-EO treatment system proposed in this study warrants further attention. In model surface waters, the EC-EO treatment train exhibited removal greater than either technology operated alone. However, EC alone achieved comparable or greater virus removal in model groundwaters. Experiments evaluating the effect of ferrous iron on EO indicated that the benefit of EC-EO was probably not due to iron-enhanced oxidation. Instead, greater virus reduction observed in the EC-EO treatment train was likely achieved not by a synergistic mechanism, but rather the additive effects of physical removal via coagulation/filtration, ferrous iron-based disinfection, and EO disinfection. In evaluating mitigation via EC-EO, neither bacteriophage was a conservative surrogate for human echovirus 12. However, ΦX174 mitigation was impaired in the high-NOM, high-turbidity model water to a similar degree as echovirus and was therefore a better predictor of echovirus mitigation.

The cost of BDD electrodes is a major hurdle to implementing an EC-EO treatment process. The comparable removal found by EC alone under many conditions in this study make EC an attractive alternative to a two-step treatment train. However, EO may provide other benefits not considered here, e.g., the oxidation of organic micropollutants or residual iron from EC treatment. As new, more cost-effective EO electrodes are developed, the combined EC-EO process will become more attractive as an alternative to conventional drinking water treatment.

5.5. References

1. EDR Group. *Failure to Act: The Impact of Current Infrastructure Investment on America's Economic Future*.; 2013. www.asce.org/failuretoact.

2. DeSimone LA. *Quality of Water from Domestic Wells in Principal Aquifers of the United States, 1991–2004*. Vol 5227.; 2008. doi:9781411323506

3. Craun GF, Brunkard JM, Yoder JS, et al. Causes of outbreaks associated with drinking water in the United States from 1971 to 2006. *Clin Microbiol Rev*. 2010;23(3):507-528. doi:10.1128/CMR.00077-09

4. Centers for Disease Control and Prevention. Waterborne Disease & Outbreak Surveillance Reports. https://www.cdc.gov/healthywater/surveillance/surveillance-reports.html. Published 2017.

5. Radjenovic J, Sedlak DL. Challenges and Opportunities for Electrochemical Processes as Next-Generation Technologies for the Treatment of Contaminated Water. *Environ Sci Technol*. 2015;49(19):11292-11302. doi:10.1021/acs.est.5b02414

6. Macpherson J V. A practical guide to using boron doped diamond in electrochemical research. *Phys Chem Chem Phys*. 2015;17(5):2935-2949. doi:10.1039/c4cp04022h

7. Rajab M, Heim C, Letzel T, Drewes JE, Helmreich B. Electrochemical disinfection using boron-doped diamond electrode - The synergetic effects of in situ ozone and free chlorine generation. *Chemosphere*. 2015;121:47-53. doi:10.1016/j.chemosphere.2014.10.075

8. Polcaro AM, Vacca A, Mascia M, Palmas S, Rodiguez Ruiz J. Electrochemical treatment of waters with BDD anodes: Kinetics of the reactions involving chlorides. *J Appl Electrochem*. 2009;39(11):2083-2092. doi:10.1007/s10800-009-9870-x

9. Palmas S, Polcaro AM, Vacca A, Mascia M, Ferrara F. Influence of the operating conditions on the electrochemical disinfection process of natural waters at BDD electrodes. *J Appl Electrochem*. 2007;37(11):1357-1365. doi:10.1007/s10800-007-9368-3

10. He Y, Lin H, Guo Z, Zhang W, Li H, Huang W. Recent developments and advances in boron-doped diamond electrodes for electrochemical oxidation of organic pollutants. *Sep Purif Technol*. 2019;212(December 2017):802-821. doi:10.1016/j.seppur.2018.11.056

11. Bruguera-Casamada C, Sirés I, Brillas E, Araujo RM. Effect of electrogenerated hydroxyl radicals, active chlorine and organic matter on the electrochemical inactivation of Pseudomonas aeruginosa using BDD and dimensionally stable anodes. *Sep Purif Technol*. 2017;178:224-231. doi:10.1016/j.seppur.2017.01.042

12. Jeong J, Kim JY, Yoon J. The role of reactive oxygen species in the electrochemical inactivation of microorganisms. *Environ Sci Technol*. 2006;40(19):6117-6122. doi:10.1021/es0604313

13. Lacasa E, Tsolaki E, Sbokou Z, Rodrigo MA, Mantzavinos D, Diamadopoulos E. Electrochemical disinfection of simulated ballast water on conductive diamond electrodes. *Chem Eng J*. 2013;223:516-523. doi:10.1016/j.cej.2013.03.003

14. Mascia M, Vacca A, Palmas S. Electrochemical treatment as a pre-oxidative step for algae removal using Chlorella vulgaris as a model organism and BDD anodes. *Chem Eng J*. 2013;219:512-519. doi:10.1016/j.cej.2012.12.097

15. Cotillas S, Llanos J, Cañizares P, Mateo S, Rodrigo MA. Optimization of an integrated electrodisinfection/electrocoagulation process with Al bipolar electrodes for urban wastewater reclamation. *Water Res*. 2013;47(5):1741-1750. doi:10.1016/j.watres.2012.12.029

16. Llanos J, Cotillas S, Can˜izares P, Rodrigo MA. Effect of bipolar electrode material on the reclamation of urban wastewater by an integrated electrodisinfection/electrocoagulation process. *Water Res*. 2014;53:329-338. doi:10.1016/j.watres.2014.01.041

17. Dubrawski KL, Fauvel M, Mohseni M. Metal type and natural organic matter source for direct filtration electrocoagulation of drinking water. *J Hazard Mater*. 2013;244-245:135-141. doi:10.1016/j.jhazmat.2012.11.027

18. Vepsäläinen M, Ghiasvand M, Selin J, et al. Investigations of the effects of temperature and initial sample pH on natural organic matter (NOM) removal with electrocoagulation using response surface method (RSM). *Sep Purif Technol*. 2009;69(3):255-261. doi:10.1016/j.seppur.2009.08.001

19. Bagga A, Chellam S, Clifford DA. Evaluation of iron chemical coagulation and electrocoagulation pretreatment for surface water microfiltration. *J Memb Sci*. 2008;309(1-2):82-93. doi:10.1016/j.memsci.2007.10.009

20. Ben-Sasson M, Lin YM, Adin a. Electrocoagulation-membrane filtration hybrid system for colloidal fouling mitigation of secondary-effluent. *Sep Purif Technol*. 2011;82:63-70. doi:10.1016/j.seppur.2011.08.020

21. Heffron J, Mayer BK. Virus mitigation by coagulation: recent discoveries and future directions. *Environ Sci Water Res Technol*. 2016;2(3):443-459. doi:10.1039/C6EW00060F

22. Zhu B, Clifford DA, Chellam S. Virus removal by iron coagulation-microfiltration. *Water Res*. 2005;39(20):5153-5161. doi:10.1016/j.watres.2005.09.035

23. Delaire C, Van Genuchten CM, Nelson KL, Amrose SE, Gadgil AJ. Escherichia coli attenuation by Fe electrocoagulation in synthetic Bengal groundwater: effect of pH and natural organic matter. *Environ Sci Technol*. 2015;49(16):9945-9953. doi:10.1021/acs.est.5b01696

24. Tanneru CT, Jothikumar N, Hill VR, Chellam S. Relative insignificance of virus inactivation during aluminum electrocoagulation of saline waters. *Environ Sci Technol*. 2014;48(24):14590-14598. doi:10.1021/es504381f

25. Kim JY, Lee C, Love DC, Sedlak DL, Yoon J, Nelson KL. Inactivation of MS2 coliphage by ferrous ion and zero-valent iron nanoparticles. *Environ Sci Technol*. 2011;45(16):6978-6984. doi:10.1021/es201345y

26. Lakshmanan D, Clifford DA. Ferrous and Ferric Ion Generation During Iron Electrocoagulation. *Env Sci Technol*. 2009;43(10):3853-3859.

27. Li L, van Genuchten CM, Addy SEA, Yao J, Gao N, Gadgil AJ. Modeling As(III) oxidation and removal with iron electrocoagulation in groundwater. *Environ Sci Technol*. 2012;46(21):12038-12045. doi:10.1021/es302456b

28. Hussain SN, de las Heras N, Asghar HMA, Brown NW, Roberts EPL. Disinfection of water by adsorption combined with electrochemical treatment. *Water Res*. 2014;54:170-178. doi:10.1016/j.watres.2014.01.043

29. Ahmadi A, Wu T. Inactivation of E. coli using a novel TiO2 nanotube electrode. *Environ Sci Water Res Technol*. 2017;3:534-545. doi:10.1039/C6EW00319B

30. Bruguera-Casamada C, Sires I, Prieto MJ, Brillas E, Araujo RM. The ability of electrochemical oxidation with a BDD anode to inactivate Gram-negative and Gram-positive bacteria in low conductivity sulfate medium. *Chemosphere*. 2016;163:516-524. doi:10.1016/j.chemosphere.2016.08.042

31. Cossali G, Routledge EJ, Ratcliffe MS, Blakes H, Karayiannis TG. Inactivation of E . coli , Legionella and Pseudomonas in Tap Water Using Electrochemical Disinfection. *J Environ Eng*. 2016;142(12):04016063. doi:10.1061/(ASCE)EE.1943-7870.0001134.

32. Fang Q, Shang C, Chen G. MS2 Inactivation by Chloride-Assisted Electrochemical Disinfection. *J Environ Eng*. 2006;132(1):13-22. doi:10.1061/(ASCE)0733-9372(2006)132:1(13)

33. Drees KP, Abbaszadegan M, Maier RM. Comparative electrochemical inactivation of bacteria and bacteriophage. *Water Res*. 2003;37:2291-2300. doi:10.1016/S0043-1354(03)00009-5

34. Huang X, Qu Y, Cid CA, et al. Electrochemical disinfection of toilet wastewater using wastewater electrolysis cell. *Water Res*. 2016;92:164-172. doi:10.1016/j.watres.2016.01.040

35. Boudaud N, Machinal C, David F, et al. Removal of MS2, Qβ and GA bacteriophages during drinking water treatment at pilot scale. *Water Res*. 2012;46(8):2651-2664. doi:10.1016/j.watres.2012.02.020

36. Ferrer O, Casas R, Galvañ C, et al. Challenge tests with virus surrogates: an accurate membrane integrity evaluation system? *Desalin Water Treat*. 2013;51(1):4947-4957. doi:10.1080/19443994.2013.795339

37. Amarasiri M, Kitajima M, Nguyen TH, Okabe S, Sano D. Bacteriophage removal efficiency as a validation and operational monitoring tool for virus reduction in wastewater reclamation: Review. *Water Res*. 2017;121:258-269. doi:10.1016/j.watres.2017.05.035

38. Grabow WOK. Bacteriophages: Update on application as models for viruses in water. *Water SA*. 2001;27(2):251-268. doi:10.4314/wsa.v27i2.4999

39. Grabow WOK. Overview of health-related water virology. In: Bosch A, ed. *Human Viruses in Water*. 1st ed. Amstersdam: Elsevier; 2007:1-26.

40. World Health Organization. *Guidelines for Drinking-Water Quality: Health Criteria and Other Supporting Information*. Vol 2. 2nd ed. Geneva: World Health Organization; 1996.

41. Saha J, Gupta SK. A novel electro-chlorinator using low cost graphite electrode for drinking water disinfection. *Ionics (Kiel)*. 2017;23(7):1903-1913.

42. Mayer BK, Ryu H, Abbaszadegan M. Treatability of U.S. Environmental Protection Agency contaminant candidate list viruses: Removal of coxsackievirus and echovirus using enhanced coagulation. *Environ Sci Technol*. 2008;42(18):6890-6896. doi:10.1021/es801481s

43. Beck NK, Callahan K, Nappier SP, Kim H, Sobsey MD, Meschke JS. Development of a spot-titer culture assay for quantifying bacteria and viral indicators. *J Rapid Methods Autom Microbiol*. 2009;17(4):455-464. doi:10.1111/j.1745-4581.2009.00182.x

44. Reed LJ, Muench H. A simple method of estimating fifty per cent endpoints. *Am J Hyg*. 1938;27(3):493-497. doi:10.1093/OXFORDJOURNALS.AJE.A118408

45. Tai C, Peng JF, Liu JF, Jiang G Bin, Zou H. Determination of hydroxyl radicals in advanced oxidation processes with dimethyl sulfoxide trapping and liquid chromatography. *Anal Chim Acta*. 2004;527(1):73-80. doi:10.1016/j.aca.2004.08.019

46. Washington Administrative Code. *WAC 246-290-451, Disinfection of Drinking Water*.; 2017.

47. R Core Team. R: A language and environment for statistical computing. 2014.

48. Sakamoto Y, Ishiguro M, Kitagawa G. *Akaike Information Criterion Statistics*. Springer Netherlands; 1986.

49. Bolton JR, Bircher KG, Tumas W, Tolman CA. Figures of Merit for the Technical Development and Application of Advanced Oxidation Processes. *J Adv Oxid Technol*.

1996;1(1):1-11. doi:10.1515/jaots-1996-0104

50. Haselow JS, Siegrist RL, Crimi M, Jarosch T. Estimating the total oxidant demand for in situ chemical oxidation design. *Remediation*. 2003;13(4):5-16. doi:10.1002/rem.10080

51. Westerhoff P, Mezyk SP, Cooper WJ, Minakata D. Electron pulse radiolysis determination of hydroxyl radical rate constants with Suwannee river fulvic acid and other dissolved organic matter isolates. *Environ Sci Technol*. 2007;41(13):4640-4646. doi:10.1021/es062529n

52. Powder Technology Inc. *Safety Data Sheet: Arizona Test Dust*.; 2016. https://www.powdertechnologyinc.com/wp-content/uploads/2012/08/SDS.01.Arizona-Test-Dust.4-Feb-2016.pdf.

53. Arslan-Alaton I. Treatability of a simulated disperse dye-bath by ferrous iron coagulation, ozonation, and ferrous iron-catalyzed ozonation. *J Hazard Mater*. 2001;85(3):229-241. doi:10.1016/S0304-3894(01)00232-1

54. Beltrán FJ, Rivas FJ, Montero-De-Espinosa R. Iron type catalysts for the ozonation of oxalic acid in water. *Water Res*. 2005;39(15):3553-3564. doi:10.1016/j.watres.2005.06.018

55. Legube B, Karpel Vel Leitner N. Catalytic ozonation: a promising advanced oxidation technology for water treatment. *Catal Today*. 1999;53(1):61-72. doi:10.1016/S0920-5861(99)00103-0

56. Sreethawong T, Chavadej S. Color removal of distillery wastewater by ozonation in the absence and presence of immobilized iron oxide catalyst. *J Hazard Mater*. 2008;155(3):486-493. doi:10.1016/j.jhazmat.2007.11.091

57. Sjogren JC, Sierka RA. Inactivation of phage MS2 by iron-aided titanium dioxide photocatalysis. *Appl Environ Microbiol*. 1994;60(1):344-347.

58. Stumm W, Lee FG. Oxygenation of ferrous iron. *Ind Eng Chem*. 1961;53(2):143-146. doi:10.1021/ie50614a030

59. Crittenden JC, Trussell RR, Hand DW, Howe KJ, Tchobanoglous G. *MWH's Water Treatment: Principles and Design*. 3rd ed. Hoboken, New Jersey: John Wiley & Sons, Inc.; 2012.

60. Litter M, Bircher K, Oppenländer T, Bolton J, Keen O. Standard reporting of Electrical Energy per Order (EEO) for UV/H2O2 reactors (IUPAC Technical Report). *Pure Appl Chem*. 2018;90(9):1487-1499. doi:10.1515/pac-2017-0603

61. Tanneru CT, Chellam S. Mechanisms of virus control during iron electrocoagulation--microfiltration of surface water. *Water Res*. 2012;46(7):2111-2120. doi:10.1016/j.watres.2012.01.032

6. CONCLUSIONS

Waterborne viruses are a pervasive threat to public health. Their low infectious doses and high persistence in the environment make viruses particularly relevant in small-scale public and private water systems lacking disinfection and/or particle separation.[1,2] A trend in virus mitigation research has emerged of treatment technologies featuring zero- or mixed-valent iron, such as iron-amended sand and membrane filters, iron particles and iron electrocoagulation. Much of this research has relied on bacteriophages as virus surrogates for reasons of ease, cost and safety. Bacteriophage inactivation due to iron oxidation has recently been demonstrated, suggesting a novel mechanism for virus mitigation by zero-valent and ferrous iron. However, the relevance of ferrous inactivation to human viruses in actual water treatment processes has yet to be established.

The goal of this research was to explore the mechanisms and applications of iron-based virus mitigation. This goal was accomplished by first elucidating the relationship of iron oxidation and virus inactivation in ferrous chloride jar tests. Then the importance of ferrous inactivation in relation to physical removal was evaluated for iron EC. Finally, an electrochemical water treatment process, sequential EC-EO, was evaluated for enhanced iron-based mitigation. Bacteriophage inactivation strongly correlated to ferrous oxidation. However, these promising initial results of ferrous inactivation were not borne out with human viruses, raising concerns for the use of bacteriophage surrogates in research of any water treatment technology featuring zero-valent or ferrous iron. Iron-enhanced oxidation was also not observed in the EC-EO treatment train. Nevertheless, both EC and sequential EC-EO were effective means of mitigating viruses in drinking water.

6.1. Key Findings

The first objective of this research was to establish the relationship between ferrous iron and bacteriophage inactivation. Inactivation was determined to be proportional to the extent of iron oxidation, but did not follow classical disinfection kinetics. Inactivation was inversely proportional to the hydroxide and dissolved oxygen concentrations, which was interpreted in terms of ferrous iron oxidation kinetics. This finding predicts that a slower rate of iron oxidation leads to greater chance of contact between reactive ferrous iron and viruses. However, iron oxidation becomes a self-limiting process because the oxidation responsible for inactivation also leads to enmeshment of viruses in floc and precipitation of ferrous iron.

The second objective was to determine the mechanisms of virus mitigation via EC, as well as the suitability of bacteriophages as surrogates. Bacteriophages fr, MS2, and P22 were far more susceptible to inactivation than bacteriophage ΦX174 and the three mammalian viruses. For the latter group, physical removal was the dominant fate. The difference in inactivation was determined to be due to ferrous iron, rather than anodic oxidation, and physical removal was determined to be primarily due to inclusion in flocs. Susceptibility to ferrous-based inactivation was correlated to electrostatic attraction and thin capsid structure.

The third objective was to evaluate sequential EC-EO for virus mitigation. As expected, both NOM and turbidity inhibited EO. Iron-enhanced oxidation was not observed; ferrous iron impaired, rather than enhanced, electrooxidation. Nevertheless, sequential EC-EO was beneficial for virus mitigation of surface waters. EC alone was preferable for groundwaters. High chloride concentrations increased the effectiveness of EO. Lower pH/DO improved the effectiveness of both EC and EO. In assessing virus mitigation via the EC-EO treatment train, mitigation of both bacteriophage MS2 and ΦX174 was significantly greater than mitigation of

echovirus. ΦX174 was slightly preferable as a surrogate for echovirus, because ΦX174 mitigation remained proportional to that of echovirus in high-NOM, high-turbidity water.

6.2. Recommendations for Future Research

The most evident lesson for future research is that bacteriophages have the potential to behave radically differently than the viruses they are intended to mimic. This lesson applies especially, but not exclusively, to treatment processes using some form of zero- or mixed-valent iron. Only one bacteriophage (ΦX174) was a conservative estimator of virus mitigation due to EC. Three of the four bacteriophages (fr, MS2, and P22) showed dramatic susceptibility to ferrous-based inactivation, whereas physical removal far surpassed inactivation for mammalian viruses in EC. In the sequential EC-EO process, even ΦX174 overestimated human virus mitigation – though in an apparently predictable way, unlike bacteriophage MS2. Therefore, researchers must continue to compare human viruses and their surrogates in any new application.

However, this research is not merely a cautionary tale about inappropriate surrogates, nor is it the death knell for iron-based inactivation. Inactivation was observed, though to a small degree, for bacteriophage ΦX174 and two human viruses at the lowest pH tested (pH 6). Therefore, iron-based inactivation is not a quirk of some bacteriophages. However, since the ferrous inactivation step is self-limiting, engineering controls are needed to ensure optimal conditions. Acidifying pH to an even greater degree prior to iron-based inactivation, as is common in enhanced coagulation, could enhance inactivation by decreasing the oxidation rate of ferrous oxidation. In addition, though a synergistic relationship between EC and EO was not determined, the sequential EC-EO process showed greater efficacy for treating surface waters

than either process alone. Considering the inhibition of EO by NOM, enhanced EC for NOM removal could also dramatically improve disinfection by EO.

Further research into how capsids interact with the environment outside the host could lead to important advances in water treatment and virus transport. A better understanding of how capsid structure, surface charge, and hydrophobicity contribute to susceptibility could better identify both resistant surrogates and potential targets for ferrous-based disinfection. Furthermore, the high variation in virus susceptibility to ferrous iron suggests a potentially novel aspect of virus capsid function. Much attention has been justly paid to capsid function in the context of the infectious cycle, but research into capsid function in the environment could also be productive. Iron and other transition metals are ubiquitous in the environment, so it is not unreasonable to suggest that such oxidizers have exerted a selective influence on viruses. Even a virus' isoelectric point has likely been selected for by both its replication cycle and the external environment.

6.3. References

1. Bosch A, Pintó RM, Abad FX. Survival and Transport of Enteric Viruses in the Environment. *Viruses in foods*. 2003;(Springer US):151-187. doi:10.1007/0-387-29251-9_6

2. Xagoraraki I, Yin Z, Svambayev Z. Fate of Viruses in Water Systems. *J Environ Eng*. 2014;140(7):040140201-18. doi:10.1061/(ASCE)EE.1943-7870.0000827

APPENDICES

SUPPORTING INFORMATION FOR CHAPTER 3

A.1 Verification of Phage Recovery Using the Beef Broth Elution Method

Virus recovery was compared after coagulation with ferric chloride and ferrous chloride (8.5 mg/L Fe). After coagulation, bacteriophage concentration was compared in filtered (0.45 µm PTFE filter) water (indicating the sum of physical removal and inactivation) and in a sample eluted with an equal volume of 6% beef broth (pH 9.5) (indicting the degree of inactivation). As shown in Figure B-1, the majority of the spiked MS2 and P22 (~10^7 PFU/mL) were recovered by beef broth elution after ferric chloride coagulation, demonstrating the validity of this recovery

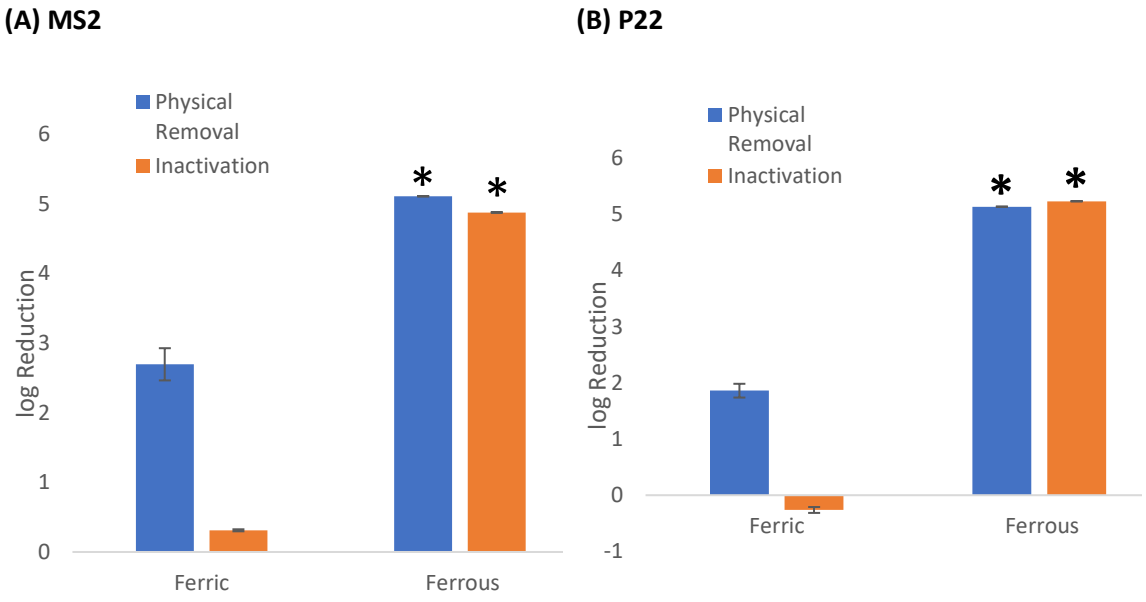

Figure B-1. Confirmation of the beef broth elution method using ferric and ferrous chloride (8.5 mg/L Fe) for bacteriophages (A) MS2, and (B) P22. Error bars represent standard error of triplicate experiments. Asterisks (*) indicate removal beyond the detection limit (plaques were too few to quantify at the lowest dilution).

method. However, no recovery was observed in the ferrous chloride test, demonstrating virus inactivation.

A.2 Calculation of Apparent k Values

Ferrous concentration was measured after addition of $FeCl_2$ (2.5 mg/L Fe) to 3 mM bicarbonate solution at pH levels ranging from 5.99 to 8.06. An exponential trendline was fitted in Excel using the following formula:

$$C_{ferrous} = C_0 \exp[-\beta t] \tag{A-1}$$

To calculate apparent rate constant values (*k'*), the Stumm and Lee model for ferrous oxidation (Equation 3-1) was first integrated:

$$\int_{C_0}^{C} \frac{dC_{ferrous}}{C_{ferrous}} = \int_0^t -k[O_2][OH^-]^2 dt \tag{A-2}$$

$$\ln(C_{ferrous}) - \ln(C_0) = -k[O_2][OH^-]^2\, t \tag{A-3}$$

$$C_{ferrous} = C_0 \exp[-k[O_2][OH^-]^2\, t] \tag{A-4}$$

Then *k'* was calculated based on empirical β values from Equation A-1:

$$k' = \frac{\beta}{[O_2][OH^-]^2} \tag{A-5}$$

Table B-1. Calculated k’ values based on iron oxidation rates from pH 6 to 8

pH	β	[OH]	[O2]	k'	1/k'
5.99	0.005	9.77E-09	2.71E-04	1.93E+17	5.17E-18
6.31	0.003	2.04E-08	2.61E-04	2.76E+16	3.62E-17
6.46	0.023	2.88E-08	2.71E-04	1.02E+17	9.80E-18
6.54	0.013	3.47E-08	2.61E-04	4.15E+16	2.41E-17
6.82	0.036	6.61E-08	2.61E-04	3.16E+16	3.16E-17
6.96	0.099	9.12E-08	2.71E-04	4.39E+16	2.28E-17
7.2	0.11	1.58E-07	2.61E-04	1.68E+16	5.95E-17
7.47	0.52	2.95E-07	2.71E-04	2.20E+16	4.54E-17
7.66	0.297	4.57E-07	2.61E-04	5.45E+15	1.83E-16
7.75	0.363	5.62E-07	2.61E-04	4.40E+15	2.27E-16
7.96	0.821	9.12E-07	2.61E-04	3.79E+15	2.64E-16
8.06	1.192	1.15E-06	2.71E-04	3.34E+15	3.00E-16

A.3 R Script for Linear Regression Analyses

The R scripts used for linear regression analyses are provided at:

github.com/JoeHeffron/BacteriophageFerrousOxidation

A.4 Summary of Regression Models

Table B-2. Summary of regression model variables and statistics for bacteriophage inactivation as a function of iron oxidation (controlled by time or sodium thiosulfate addition), ferrous iron dose, hydroxide concentration, and dissolved oxygen concentration. Independent variable transformations were used to test the hypothetical relation between log inactivation and ferrous iron oxidation. Models were evaluated by goodness-of-fit and distribution of residuals, in addition to using ANOVA to identify significant variables.

	Percent iron oxidation (timed test)		Percent iron oxidation (sodium thiosulfate test)		Ferrous dose (mg/L Fe)		Hydroxide concentration ($[OH^-]$, mol/L)		Dissolved oxygen (mg/L)	
	MS2	P22	MS2	P22	MS2	P22	MS2	P22	MS2	P22
Independent variable transform	None	None	None	None	None	None	Inverse	Inverse	Inverse	Inverse
p-value	6.95 E-10	3.60 E-09	1.15 E-02	5.64 E-07	6.49 E-07	2.13 E-04	1.93 E-07	3.42 E-06	9.58 E-04	5.98 E-04
β coefficient/ slope	0.0104	0.0463	0.00847	0.378	0.228	1.14	1.34 E-07	1.73 E-07	0.719	0.894
F statistic (degrees of freedom)	128 (1,19)	104.8 (1,19)	10.65 (1,8)	294 (1,7)	965 (1,5)	91.3 (1,5)	130 (1,11)	101 (1,9)	21.3 (1, 10)	16.03 (1,22)
R^2_{adj}	0.864	0.839	0.517	0.973	0.994	0.938	0.915	0.909	0.649	0.395

Table B-3. Summary of regression model variables and statistics for floc size as a function of flocculation time and ferrous dose. Separate models were developed for low ferrous doses (< 3 mg/L Fe) and high ferrous doses (> 3 mg/L Fe). Beyond 3 mg/L Fe, floc size was not significantly affected by increasing the ferrous dose. The estimated slope of the time variable (β) was also nearly twice as great at higher ferrous doses, indicating that flocs form more slowly at low doses than at high doses.

	Flocculation time (min)				Ferrous dose (mg/L Fe)				
	transform	β	p-value	F statistic (degrees of freedom)	transform	β	p-value	F statistic (degrees of freedom)	R^2_{adj}
< 3 mg/L Fe	Square root	196	< 2E-16	415 (1, 48)	None	310	< 2E-16	167 (1, 48)	0.921
> 3 mg/L Fe	Square root	370	< 2E-16	1656 (1, 30)	None	16.8	0.246	1.40 (1, 30)	0.981

A.5 Floc Formation at Varying Ferrous Iron Doses

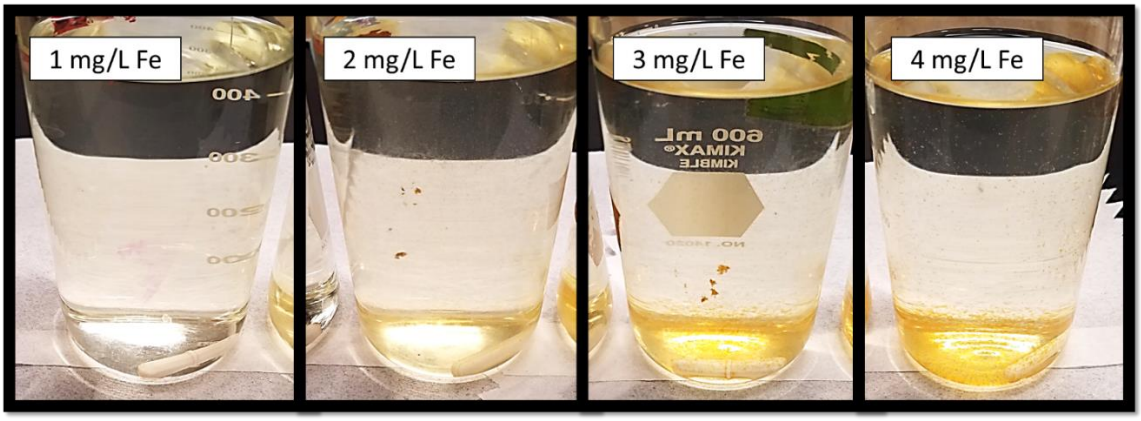

Figure B-2. Floc formation at varying ferrous iron doses. Iron was spiked as $FeCl_2 \bullet 4H_2O$ and allowed to form at slow mixing (60 rpm) for 90 min. By visual evaluation, abundant, large flocs formed at 3 mg/L Fe and above, while few settleable flocs formed at lower concentrations. These results support the floc formation trends observed via dynamic light scattering.

A.6 Impact of Ferrous Iron Oxidation on Floc Formation

Floc formation was measured after addition of $FeCl_2$ (2.5 mg/L Fe) to 3 mM bicarbonate solution at pH levels ranging from 5.99 to 8.06. Ferrous concentration was measured using Hach Ferrous Iron Reagent (Hach, Loveland, CO) and a Genesys 20 spectrophotometer (510 nm, Thermo Fisher Scientific, Waltham, MA). Particle size was measured by dynamic light scattering. Both ferrous oxidation and floc growth was far more rapid at higher pH. Maximum floc size also increased with pH.

(A) Ferrous oxidation **(B) Particle formation**

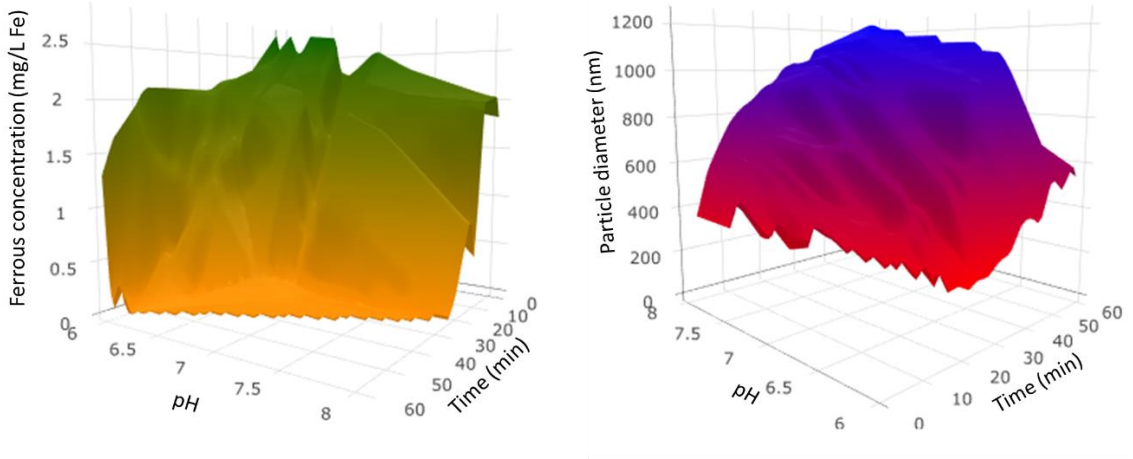

Figure B-3. Ferrous oxidation (A) and growth of iron flocs (B) over time as a function of pH. Ferrous oxidation (A) is presented here in addition to Error! Reference source not found. for the s ake of easy comparison. Note that x- and y-axes are reversed in (A) and (B) in order to show the contour of each plot. Iron was spiked as $FeCl_2$ (2.5 mg/L Fe) into 3 mM $NaHCO_3$. Surfaces were interpolated from more than 100 data measurements across the ranges shown.

An equilibrium model of ferrous iron speciation over a range of ferric iron concentrations was developed using MINEQL+ software (Environmental Research Software, Hallowell, ME). Experimental conditions were replicated in the model (pH 7, 3 mM bicarbonate solution, $9x10^{-6}$ M Fe^{II}, $1.8x10^{-5}$ M Cl^-). Results are shown in Figure B-4.

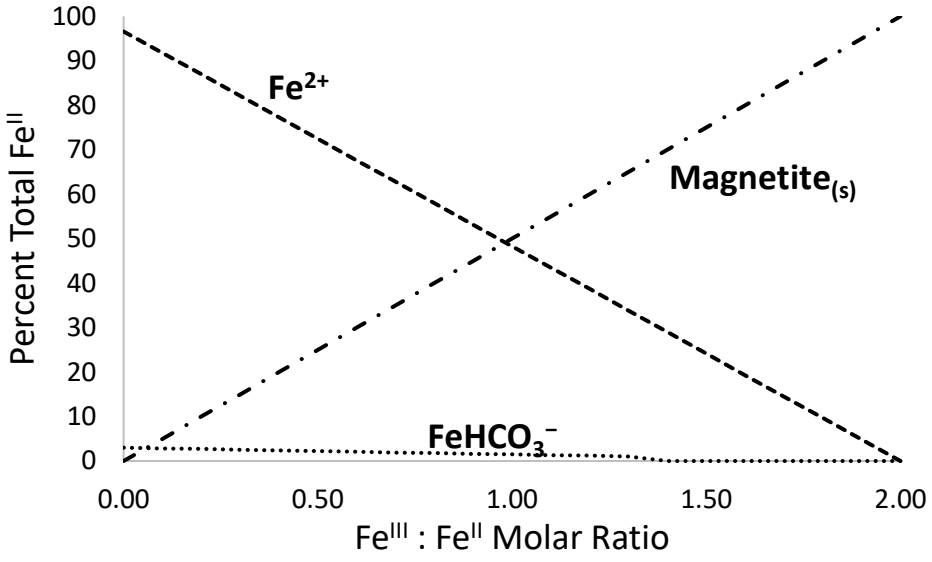

Figure B-4. Theoretical ferrous iron speciation as a function of ferric iron concentration. As ferric iron concentration approached the stoichiometric ratio for magnetite ($Fe^{II}Fe^{III}_2O_4$), magnetite replaced ferrous ions as the dominant species.

APPENDIX B DETERMINATION OF ELECTROCOAGULATION OPERATING PARAMETERS

To determine operational parameters for electrocoagulation (EC) experiments for the experiments described in Chapters 4 and 5, a screening test was performed to evaluate the effect of basic operational parameters on MS2 bacteriophage reduction. Parameters considered included electrode material, current density, retention time, stir rate, and rate of current alteration. In EC, electrode material determines the type of coagulant ions released into solution. By Faraday's laws of electrolysis, the coagulant dose is proportional to the charge, *i.e.*, the current integrated over time. Here, current is held constant, so the coagulant dose is therefore proportional to the product of current and time. Because batch EC reactors do not necessarily have separate stages for rapid mixing (coagulation) and slow mixing (flocculation), the stir rate has the potential to both accelerate coagulant dispersion and increase shear forces, preventing floc formation. Finally, the direction of the current was alternated at regular intervals to prevent the accumulation of oxidized species on the surface of the anode (passivation). The rate of current alternation may also affect the concentration of reactive species within the diffusion layer around each electrode.

B.1 Materials and Methods

EC tests were conducted in a 500 mL glass beaker with two plate electrodes (60 cm^2 submerged facial area, 1 cm inter-electrode distance) consisting of either aluminum (6061 alloy) or iron (mild steel). The reactor was stirred with a magnetic stir bar. Constant current was supplied by a Sorensen XEL 60-1.5 variable DC power supply (AMETEK, San Diego, CA). Current polarity was alternated at regular intervals to prevent passivation. The electrodes and polarity-alternating controller were kindly provided by A.O. Smith Corporation. Electrodes were polished with 400 Si-C sandpaper, washed with Milli-Q water and sterilized with UV light in a biological

safety cabinet before each test. The effects of electrode material, current density, retention time, stir rate, and current alternation were tested using a ¼ factorial experimental design, as shown in Table B-1. Neither of the confounded variables (stir rate and current alternation period) proved to have significant main effects.

MS2 bacteriophage (ATCC 15597-B1) was used as a model virus. Bacteriophages were propagated using the double-agar layer (DAL) method and purified by polyethylene glycol (PEG) precipitation followed by a Vertrel XF (DuPont, Wilmington, DE) purification, as described by Mayer et al.[1] *E. coli* C-3000 (ATCC 15597) was used as the host bacterium. MS2 bacteriophage was spiked at a concentration of approximately 10^7 PFU/mL into Milli-Q water with ACS-grade Na_2SO_4 as a background electrolyte (pH = 6.5, conductivity = 1000 µS/cm). Conductivity was measured using a "Pure H_2O" conductivity meter (VWR, Radnor, PA), and pH was measured using an Orion 4-star pH meter (Thermo Scientific, Waltham, MA). Bulk pH did not change significantly during the EC process. After EC treatment, a 25-mL sample was taken from the full height of the water column while the reactor continued to stir. Samples were centrifuged at 1700xg, 4° C, for 20 minutes. The supernatant was then serially diluted in 0.01 M buffered-demand-free (BDF) Milli-Q water for quantification. Bacteriophages were quantified using the spot titer plaque assay method, as described by Beck et al.[2] At least 2 viable replicates were performed for each test, with a minimum of 8 countable, 10 µL 'spots' per replicate. Log_{10} reduction efficiencies were analyzed by multiple linear regression to identify significant main effects and interactions using the *stats* package in *R*.[3]

B.2 Results and Discussion

Virus mitigation results for the experiment are shown in Table B-1. Maximum reduction was observed during tests with iron electrodes, 10-minute retention time and 60 rpm stir rate.

The plaques observed in these tests were below the countable range and were recorded as a minimum 5.1 $\log_{10}$ reduction. Significant parameters are summarized in

Table B-2. Retention time was a significant parameter, with greater reduction after 10 minutes than after 5 minutes. A long retention time not only increases the coagulant dose (current being constant), but also allows more time for sweep flocculation and diffusion. In addition, a lower stir rate (60 rpm) was preferable when using iron electrodes. The significance of stir rate for iron but not aluminum may indicate that iron flocs have a greater tendency to shear at high stir rates. Xiao et al.[4] also found that iron hydroxide flocs have a greater tendency to decrease in size than aluminum hydroxide flocs when mixing rates are increased. However, reduction with aluminum electrodes was in all cases less than 2 $\log_{10}$ reduction and may have been too low to distinguish the effect of stir rate given experimental variability.

Of the conditions tested, electrode material had the greatest effect. Virus reduction with iron electrodes was far greater than with aluminum electrodes. Though both aluminum and iron electrodes have been used in virus mitigation studies,[5–8] the effectiveness of the two materials for virus mitigation has never been directly compared.

Table B-1. Experimental design and results for log_{10} reduction in bacteriophage MS2 concentrations. Variables are labelled A through E, with confounded variables D and E. Shading is used to differentiate between the two conditions tested for each variable (SD = standard deviation).

A	**B**	**C**	**D = AB**	**E = BC**	**Log_{10} reduction**		
Current density (mA/cm^2)	Retention time (s)	Electrode material	Stir rate (rpm)	Current alternation period (s)	**Mean**	**SD**	**n**
1.25	300	Al	120	120	1.1	0.07	3
2.50	300	Al	60	120	1.1	0.18	3
1.25	600	Al	60	30	0.94	0.07	2
1.25	300	Fe	120	30	3.2	0.96	3
2.50	600	Al	120	30	1.8	0.66	3
2.50	300	Fe	60	30	4.1	0.21	2
1.25	600	Fe	60	120	>5.1	--	2
2.50	600	Fe	120	120	3.9	0.49	3

Table B-2. Summary of linear regression of significant ($\alpha = 0.05$) operational parameters (adjusted $R^2 = 0.89$).

	β (log_{10} reduction)	t value	p value
(Intercept)	2.6	23.5	5.9E-15
Electrode material (Iron)	1.4	12.3	3.6E-10
Time (s)	0.25	2.26	0.037
Electrode material (Iron) x stir rate (rpm)	-0.33	-2.91	0.0093

Some researchers prefer aluminum to iron electrodes, because soluble ferrous ions released at the anode may not be fully oxidized to form insoluble coagulant.[5,6] In light of these results, the tendency to form soluble iron may be inconsequential given the far greater virus

mitigation achieved using iron electrodes. The superior performance of iron may be due to greater affinity of the virions to iron flocs near neutral pH or virus inactivation. With longer contact times, zero-valent iron has also been shown to mitigate viruses through the slow formation of iron oxy-hydroxides.[9] In addition, studies evaluating EC for arsenite removal have found that the process of iron oxidation can also oxidize other species in solution,[10] though the same has not been found for aluminum. The oxidants generated during iron EC could potentially result in virus inactivation.

Surprisingly, current density did not affect virus reduction. Charge loading, the product of current and time, is directly proportional to the coagulant dose. However, analyzing the data based on charge loading rather than time and current independently did not better explain the data than time alone (data not shown). The insignificance of current density and charge loading indicates that virus reduction was not limited by coagulant concentration under the tested conditions, but instead by a kinetic process like diffusion, disinfection or flocculation.

As expected, the rate of current alternation also did not significantly directly affect virus reduction. The longer current alternation period (120 s) maintained a more constant voltage over time with slightly greater energy consumption, as shown in Figure B-1. While the current alternation rate could affect passivation and the corrosion patterns on the electrode, the higher power consumption between current alternations likely indicates a higher concentration overpotential as charge carrying species are depleted near the electrode surface. For this reason, shorter current alternation periods may be preferable to reduce power consumption.

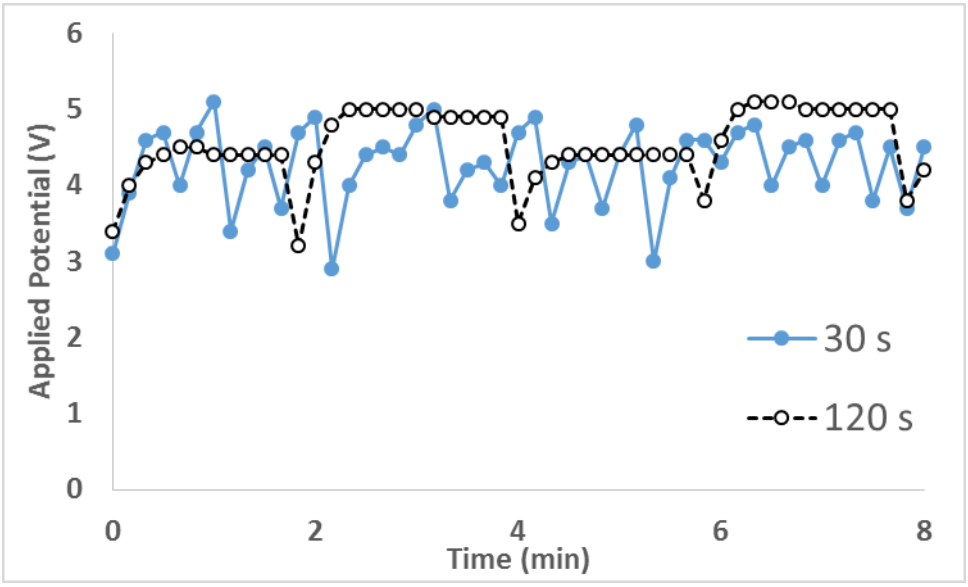

Figure B-1. Applied voltage profile for 30 s and 120 s current alternation periods (I = 150 mA).

B.3 Conclusions

Operational parameters can have a dramatic effect on virus mitigation during electrocoagulation. In this study, electrode material was the greatest determining factor for virus reduction efficiency. Iron electrodes were more effective for virus mitigation than aluminum. However, future research is required to determine if iron continues to be beneficial in more complex water matrices. For the values tested in this experiment, retention time had a comparatively minor impact on virus reductions, while current density had no significant effect. The rate of current alternation affected applied voltage, but not virus reduction efficiency.

B.4 References

1. Mayer BK, Ryu H, Abbaszadegan M. Treatability of U.S. Environmental Protection Agency contaminant candidate list viruses: Removal of coxsackievirus and echovirus using enhanced coagulation. *Environ Sci Technol*. 2008;42(18):6890-6896. doi:10.1021/es801481s

2. Beck NK, Callahan K, Nappier SP, Kim H, Sobsey MD, Meschke JS. Development of a spot-titer culture assay for quantifying bacteria and viral indicators. *J Rapid Methods Autom Microbiol*. 2009;17(4):455-464. doi:10.1111/j.1745-4581.2009.00182.x

3. R Core Team. R: A language and environment for statistical computing. 2014.

4. Xiao F, Yi P, Pan XR, Zhang BJ, Lee C. Comparative study of the effects of experimental variables on growth rates of aluminum and iron hydroxide flocs during coagulation and their structural characteristics. *Desalination*. 2010;250(3):902-907. doi:10.1016/j.desal.2008.12.050

5. Tanneru CT, Jothikumar N, Hill VR, Chellam S. Relative insignificance of virus inactivation during aluminum electrocoagulation of saline waters. *Environ Sci Technol*. 2014;48(24):14590-14598. doi:10.1021/es504381f

6. Tanneru CT, Chellam S. Sweep flocculation and adsorption of viruses on aluminum flocs during electrochemical treatment prior to surface water microfiltration. *Environ Sci Technol*. 2013;47:4612-4618.

7. Tanneru CT, Chellam S. Mechanisms of virus control during iron electrocoagulation--microfiltration of surface water. *Water Res*. 2012;46(7):2111-2120. doi:10.1016/j.watres.2012.01.032

8. Zhu B, Clifford DA, Chellam S. Comparison of electrocoagulation and chemical coagulation pretreatment for enhanced virus removal using microfiltration membranes. *Water Res*. 2005;39(13):3098-3108. doi:10.1016/j.watres.2005.05.020

9. You Y, Han J, Chiu PC, Jin Y. Removal and inactivation of waterborne viruses using zerovalent iron. *Environ Sci Technol*. 2005;39(23):9263-9269. doi:10.1021/es050829j

10. Li L, van Genuchten CM, Addy SEA, Yao J, Gao N, Gadgil AJ. Modeling As(III) oxidation and removal with iron electrocoagulation in groundwater. *Environ Sci Technol*. 2012;46(21):12038-12045. doi:10.1021/es302456b

APPENDIX C SUPPORTING INFORMATION FOR CHAPTER 4

C.1 Virus Propagation and Quantification Cultures

The hosts and cell culture media used for virus propagation and quantification are given in Table C-1. In addition to minimal essential medium and the sera listed, cell culture media also contained 25 mM HEPES buffer, 18 mM sodium bicarbonate, 0.1 mM non-essential amino acids, 2 mM L-glutamate, 1x antimycotic-antibiotic, and 100 mg/L kanamycin sulfate (Thermo Fisher, Waltham, MA). 10% serum solutions also contained 1 mM sodium pyruvate.

Table C-1. Host and culture medium for viruses in this study

Virus	**Host/Cell Culture**	**Culture Medium**
fr	*Escherichia coli* (ATCC 19853)	Tryptic Soy Agar
MS2	*Escherichia coli* (ATCC 15597)	Tryptic Soy Agar
P22	*Salmonella enterica* subsp. *typhimurium* LT2 (ATCC 19585)	Tryptic Soy Agar
ΦX174	*Escherichia coli* (ATCC 13706)	Tryptic Soy Agar
Adenovirus 4 (ADV)	Primary liver cancer (ATCC CRL-8024)	MEM + 10% Fetal Bovine Serum
Echovirus 12 (ECV)	Buffalo green monkey kidney (ATCC CCL-161)	MEM + 5% Fetal Bovine Serum
Feline calicivirus (FCV)	Crandall-Reese feline kidney (ATCC CCL-94)	MEM +10% Equine Serum

MEM: Minimal Essential Medium

C.2 R Script for Data Visualization and Analysis

The R scripts used for linear regression analyses are provided at:

http://github.com/JoeHeffron/MechanismVirusEC

C.3 Summary of Regression Models for Log Inactivation as a Function of pH

Log inactivation was significantly correlated to pH and pH^2 for all bacteriophages. This relationship confirms the impact of pH on log inactivation. However, the model is not predictive, as MS2 and P22 inactivation was greater than the quantifiable limit of approximately 5 – 6 logs (depending on initial titer), as shown in Figure 4-1.

Table C-2. Summary of regression model variables and statistics for log inactivation as a function of pH.

		Bacteriophage			
Variable		fr	MS2	P22	ΦX147
pH	β	-4.66	-14.0	-15.8	-1.61
	p-value	0.000577	<2e-16	<2e-16	0.00250
pH^2	β	0.224	0.894	0.960	0.104
	p-value	0.01811	<2e-16	<2e-16	0.00569
F statistic		404	5000	1380	27.3
(degrees of freedom)		(2,87)	(2,87)	(2,87)	(2,87)
R^2_{adj}		0.901	0.991	0.965	0.371

C.4 Zeta Potential of Bacteriophage fr and A2 Test Dust

Isoelectric point values for bacteriophage fr vary widely in the literature,[1,2] though experimental validation of pI values of 8.9 – 9.0 could not be found by the author. For this reason, bacteriophage fr zeta potential was analyzed by dynamic light scattering. Evaluation of zeta potential showed that fr zeta potential was strongly negative (-35 ± 10 mV) over the range of pH 6 to 8, and that fr had an experimentally determined isoelectric point of approximately 2.7, as shown in Figure C-1.

The zeta potential for A2 test dust (used to increase turbidity in this study) was also determined, as shown in Figure C-2. A2 test dust was negatively charged at all pH values tested

(pH 1.0 – 8.2). This data trend agrees with literature values for the surface charge of silica (the primary constituent of A2 test dust).[3]

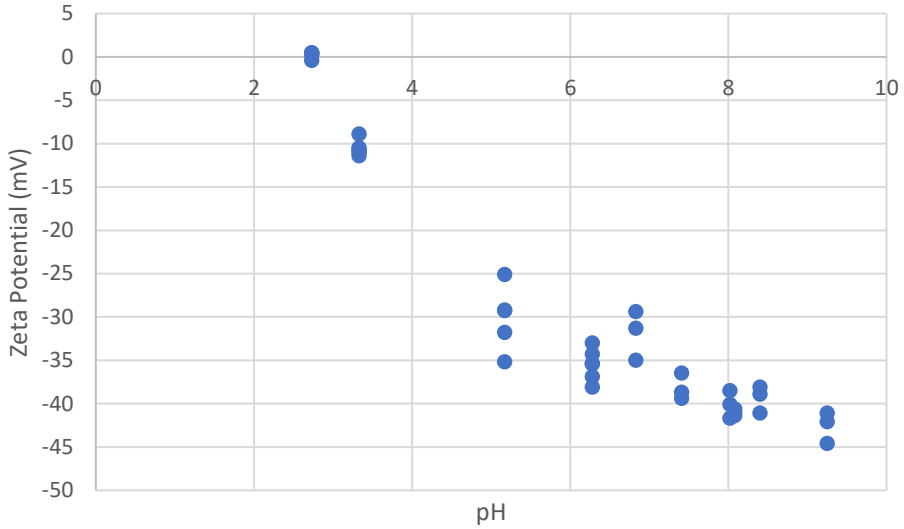

Figure C-1. Zeta potential of bacteriophage fr measured by dynamic light scattering.

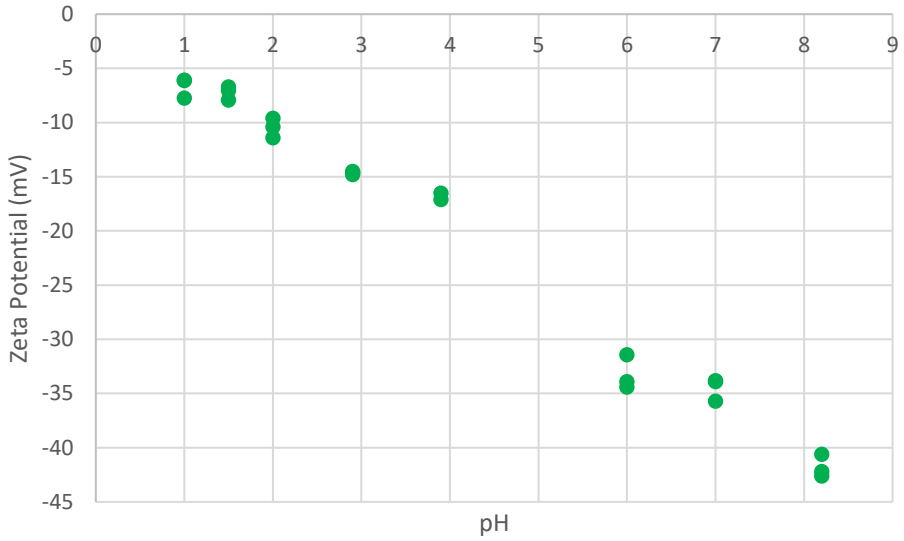

Figure C-2. Zeta potential of A2 test dust measured by dynamic light scattering.

C.5 Phage Rejection on Fouled Microfilters

Phage rejection from 0.45 µm filters fouled with turbid water and ferric iron flocs was significantly greater for both P22 ($p = 2.01x10-5$) and MS2 ($p = 0.00014$), as shown in Figure C-3. Filters fouled with turbid water alone did not reject either bacteriophage. Log removal of P22 (1.27 log) due to rejection in filters with floc and turbidity was approximately double that of MS2 (0.66 log).

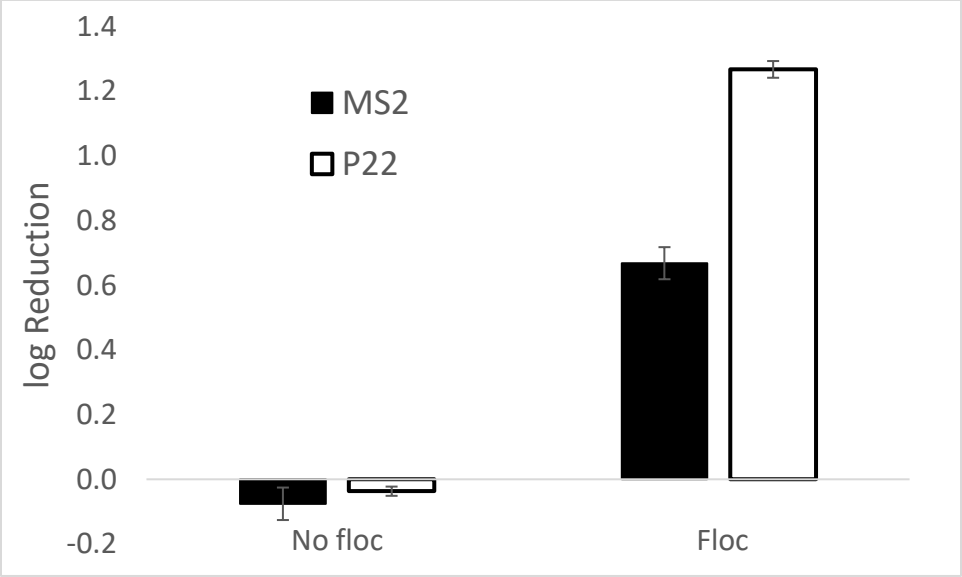

Figure C-3. Phage rejection on fouled microfilters. Bacteriophage MS2 and P22 were filtered through 0.45 µm syringe filters fouled with 15 mL of turbid (110 mg/L A2 dust, ~50 NTU) water with and without preformed electrocoagulation floc (2.3 mg/L Fe). Neither phage was removed by filters fouled with A2 dust alone. In water containing preformed floc, both phages were rejected by the filter. However, P22, the larger phage, exhibited log removal approximately double that of MS2.

C.6 Iron generation with and without chloride

The generation of iron via EC was measured in “baseline” electrolyte (3.3 mM $NaNO_3$, 1 mM HCO_3) and an electrolyte with chloride (3.2 mM NaCl, 1 mM HCO_3). As shown in Figure C-4, iron generation was approximately twice as efficient in electrolyte with chloride.

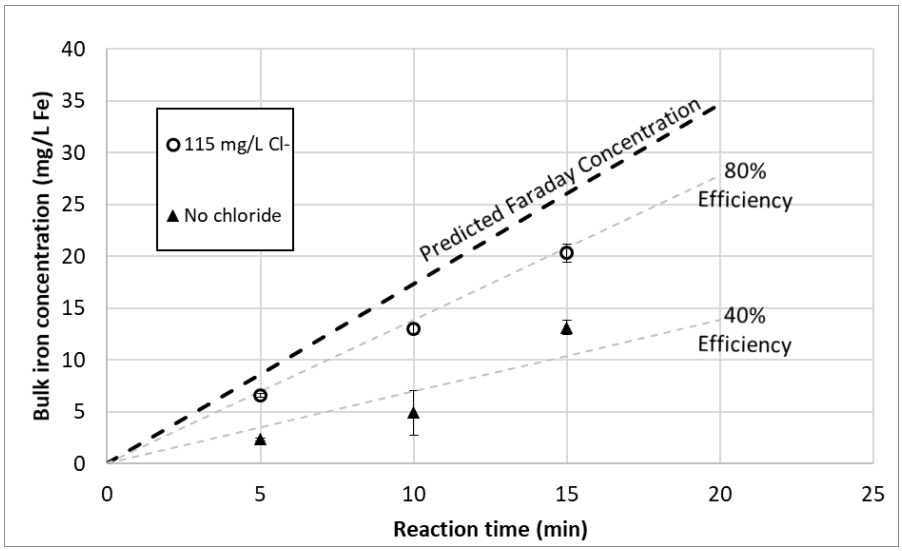

Figure C-4. Iron generation with and without chloride added. The presence of chloride dramatically increased iron corrosion to near the predicted concentration based on Faraday's Laws of Electrolysis.

C.7 References

1 A. Armanious, M. Aeppli, R. Jacak, D. Refardt, T. Sigstam, T. Kohn and M. Sander, *Environ. Sci. Technol.*, 2015, **50**, 732–743.

2 B. K. Mayer, Y. Yang, D. W. Gerrity and M. Abbaszadegan, *Microbiol. Insights*, 2015, **8**, 15–28.

3 M. Kosmulski, *Adv. Colloid Interface Sci.*, 2016, **238**, 1–61.

APPENDIX D SUPPORTING INFORMATION FOR CHAPTER 5

D.1 Effect of DMSO Cryopreservant on Electrooxidation

As shown in Figure D-1, dimethyl sulfoxide (DMSO) inhibited bacteriophage inactivation due to boron-doped diamond (BDD) electrooxidation (EO). For this reason, viruses were not stored with cryopreservant. Viruses were stored at -20° C and used within 2 months of propagation to prevent significant loss of titer.

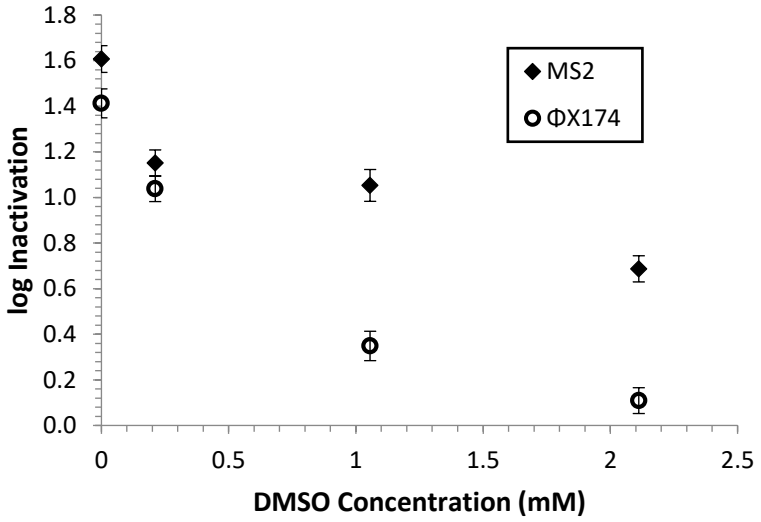

Figure D-1. Effect of DMSO on removal of bacteriophages MS2 and ΦX174 due to electrooxidation (100 mA, 5 min) in 2.1 mM $NaHCO_3$. Error bars represent standard error of mean plaque count (n = 10) for single tests.

D.2 Basis for Model Water Matrices

The four model waters used in this study (Table D-1) were based on empirical values for water at four sites. Lake Michigan model water was based on median water parameters of Milwaukee Water Works source water in 2016 [1]. For Mississippi River model water, water quality data for United States Geological Survey (USGS) site 05288500 (Mississippi River at Hwy.

610 in Brooklyn Park, MN), was accessed via the USGS (United States Geological Survey) National Water Information System (NWIS) web interface [2]. This sampling site was chosen based on breadth of water quality data and location in the upper Midwest US, similar to the other waters evaluated. Median values of water quality data ranging from 1996 to 2006 were used as the basis for Mississippi River model water. Dolomite Aquifer model water was a composite of shallow aquifer data from Kewaunee and Waukesha Counties, WI [3,4]. Sandstone Aquifer model water was based on deep aquifer data from Waukesha, WI [3].

Reagent-grade KCl was added to achieve target chloride levels. Reagent-grade $NaHCO_3$ was then added to achieve target conductivity and approximate alkalinity. Test water pH was adjusted with H_2SO_4 to add sulfates found at the ppm level in environmental waters. A2 test dust and humic acid sodium salt were added to increase turbidity and natural organic matter (NOM), respectively. Hardness was not included in test water formulations because adding soluble $CaCl_2$ or $MgCl_2$ salt would often result in chloride concentrations many times greater than target levels.

Table D-1. Empirical water quality data used to formulate model waters used in this study. Mississippi River data represents the median of water quality measurements between 1996 and 2006. Kewaunee groundwater data represents the median of water quality measurements in 10 wells in Lincoln Township, Kewaunee County.

Water Source	Associated Model Water	Conductivity (µS/cm)	Alkalinity (mg/L as $CaCO_3$)	Hardness (mg/L as $CaCO_3$)	Total Organic Carbon (mg/L)	Chloride (mg/L)	Sodium (mg/L)	pH	Turbidity (NTU)	Sulfate (mg/L)	Source
Lake Michigan	Lake Michigan	303	118	137	1.9	12.6	8.65	8.25	1	21.9	[1]
Mississippi River	Mississippi River	359	162	180	8.65	11	7.7	8.1	30	13	[2]
Waukesha groundwater	Sandstone Aquifer	484 (300 mg/L TDS)	220	250		4.1	40	7.5			[3]
Kewaunee groundwater	Dolomite Aquifer	774.5	323	413		28.25		7.82		28.25	[4]
Waukesha groundwater	Dolomite Aquifer	871 - 758 (540 - 470 mg/L TDS)	320	420		115	41.5	7.3			[3]

D.3 Contribution of Particle Separation to the EC-EO Treatment Train

Figure D-2 shows the contribution of three different treatment processes on the reduction of the bacteriophages using boron-doped diamond (BDD) electrodes for electrooxidation (EO): EO only without electrocoagulation (EC) pretreatment, EC with a post-particle filtration step, and 3) EC pretreatment without particle separation.

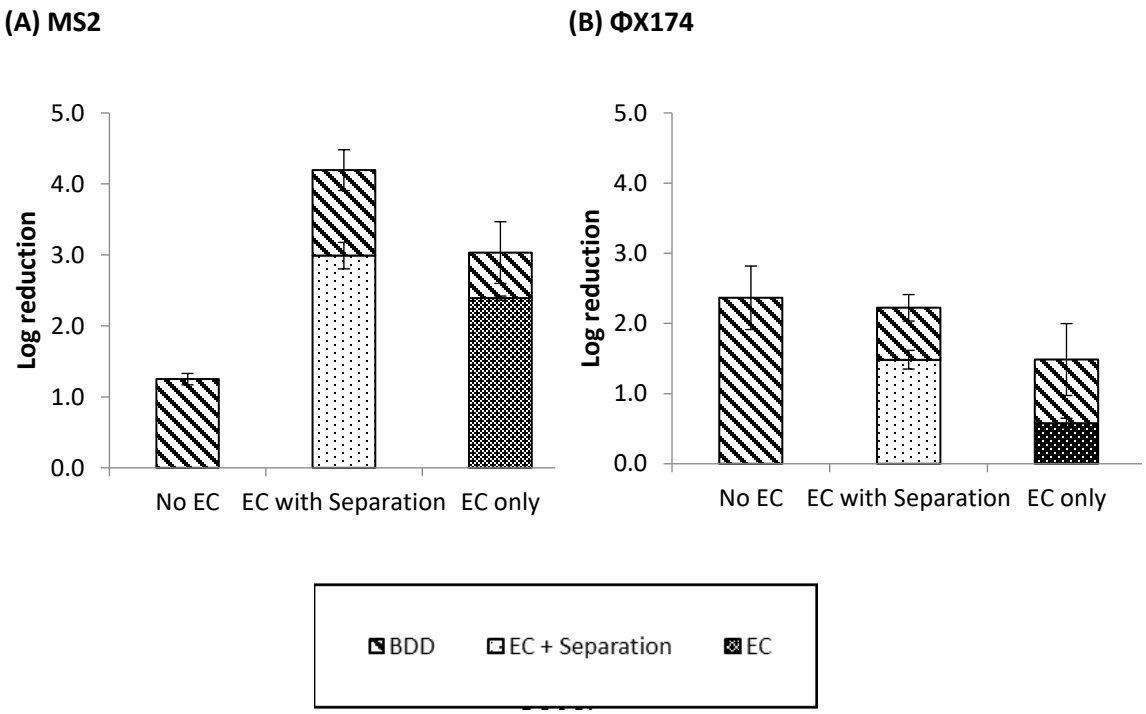

Figure D-2. The effect of three treatment processes on the reduction of bacteriophages (A) MS2 and (B) ΦX174 by boron-doped diamond (BDD) electrooxidation: EO only (No EC), iron electrocoagulation followed by particle separation using a Whatman 114 filter (EC with Separation), and iron electrocoagulation with no particle separation (EC only). Particle separation after electrocoagulation improved overall virus reduction compared to electrocoagulation alone. Tests were conducted in 2.1 mM $NaHCO_3$, pH 7. Each data point represents the mean values of triplicate tests with ±1 standard error shown by the error bars.

D.4 Effect of Total Charge Loading on Bacteriophage Removal

Three charge loadings (300, 150, and 90 C/L) were tested in Lake Michigan model water to determine an appropriate operating current for charge distribution tests in various model waters (Figure D-3). Bacteriophage reduction using the 300 C/L electrocoagulation-electrooxidation (EC-EO) process exceeded the 4-log removal requirement set by the U.S. Environmental Protection Agency's (EPA) Surface Water Treatment Rule, and was thus used for all subsequent tests.

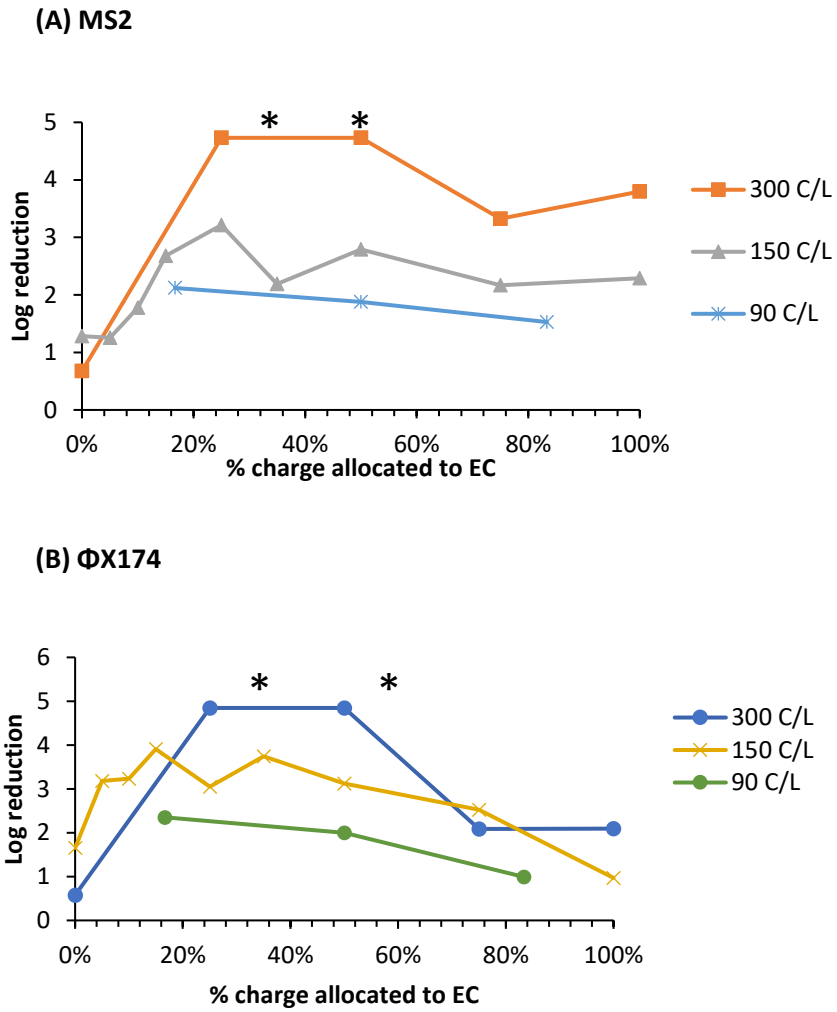

Figure D-3. Reduction of bacteriophages (A) MS2 and (B) ΦX174 showing the effect of total charge on charge distribution between electrocoagulation (EC) and electrooxidation. Tests were performed in the Lake Michigan model water. The * symbol indicates virus removal beyond the countable limit.

D.5 Reactor Performance During the EC-EO Process

During sequential EC-EO treatment, pH increased on average 0.41 ± 0.25 pH units, as shown in Figure D-4. For Lake Michigan and Mississippi River model surface waters, the change in pH was positively correlated ($p = 8.2 \times 10^{-5}$; $p = 1.9 \times 10^{-5}$, respectively) with increasing charge allocation to EC rather than EO. EC can increase the pH of solution due to the reduction of water at the cathode producing more hydroxide ions than are incorporated into iron precipitates [5]. Sandstone Aquifer and Dolomite Aquifer model groundwaters were not significantly correlated with charge allocation to one process over another.

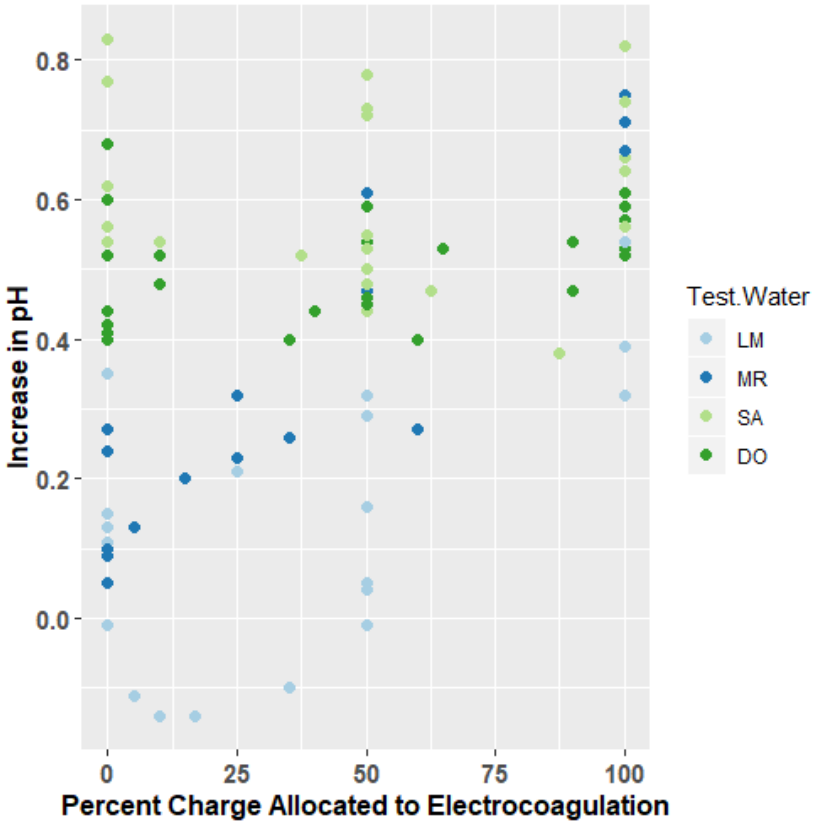

Figure D-4. Increase in pH as a function of the percent of a constant charge loading (150 C/L) allocated between electrocoagulation (EC) and electrooxidation (EO). LM = Lake Michigan, MR = Mississippi River, SA = Sandstone Aquifer, and DO = Dolomite Aquifer model waters.

Figure D-5 shows the energy density (kWh/m^3, or energy input normalized to the reactor volume) required by each of the individual processes in the EC-EO treatment train. For the batch reactors used in this study, the energy required at a given current was approximately the same for EC and EO. Therefore, the percent of charge allocated to each process roughly mapped to the percent energy allocated. However, virus mitigation was related to charge allocation so that the results could be generalized to other EC and EO reactors. At 50% charge allocation, applied potentials were lowest due to even distribution of current; greater allocation to either EC or EO resulted in greater energy density due to exponentially increasing potential with increased current. Energy density at 50% charge allocation ranged from 0.12 to 0.41 kWh/m^3 per process (or 0.31 to 0.79 kWh/m^3 for the entire train). For perspective, most conventional drinking water treatment processes operate at ≤ 0.1 kWh/m^3 (for example, the energy consumption to provide a typical UV dose of 40 mJ/cm^2 ranges from approximately 0.003 to 0.025 kWh/m^3, Crittenden et al., 2012; Howe et al., 2012).

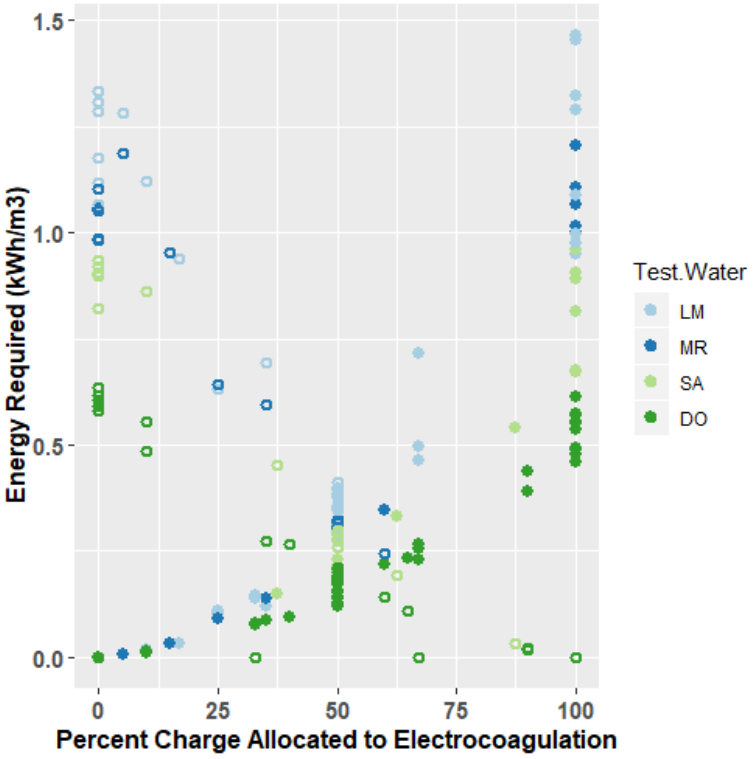

Figure D-5. Energy required for electrocoagulation (filled circles) and electrooxidation (hollow circles) in a sequential electrocoagulation-electrooxidation treatment train. Energy usage was approximately symmetrical as a constant charge loading (150 C/L) was allocated from 100% electrooxidation (0% electrocoagulation) to 100% electrocoagulation. Energy requirements were inversely related to the conductivity of the model water, with decreasing energy from LM < MR < SA < DO. LM = Lake Michigan, MR = Mississippi River, SA = Sandstone Aquifer , and DO = Dolomite Aquifer model waters.

D.6 Iron Generation and Residuals Through the EC-EO Process

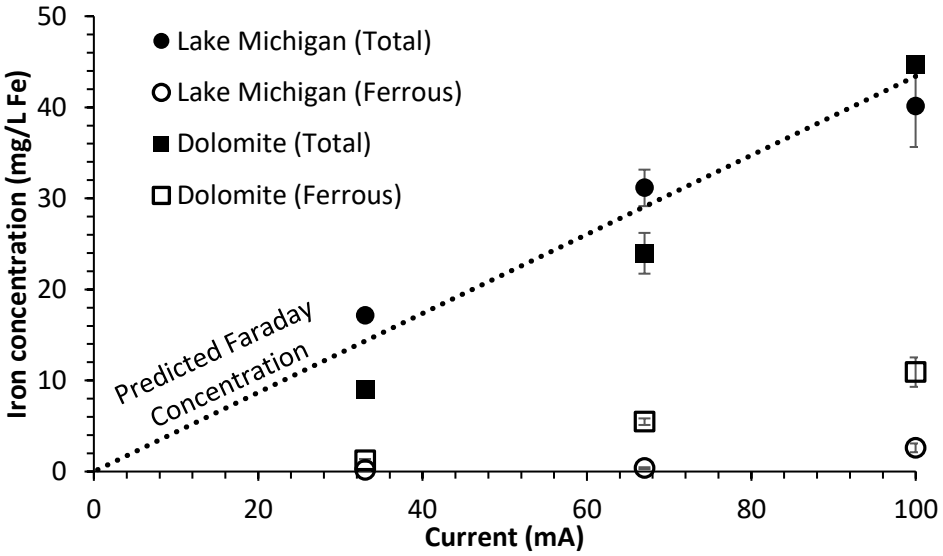

Figure D-6. Total and ferrous iron generation by electrocoagulation (EC) as a function of current. Iron was generated by EC for 5 minutes in low-chloride, high-dissolved oxygen (DO) Lake Michigan model water and high-chloride, low-DO Dolomite Aquifer model water. In both model waters, total iron was generated at high (94-99%) Faraday efficiency. Ferrous iron residual increased with current and was greater in the low-DO Dolomite Aquifer water. The rate of ferrous iron oxidation is proportional to the DO concentration.[8]

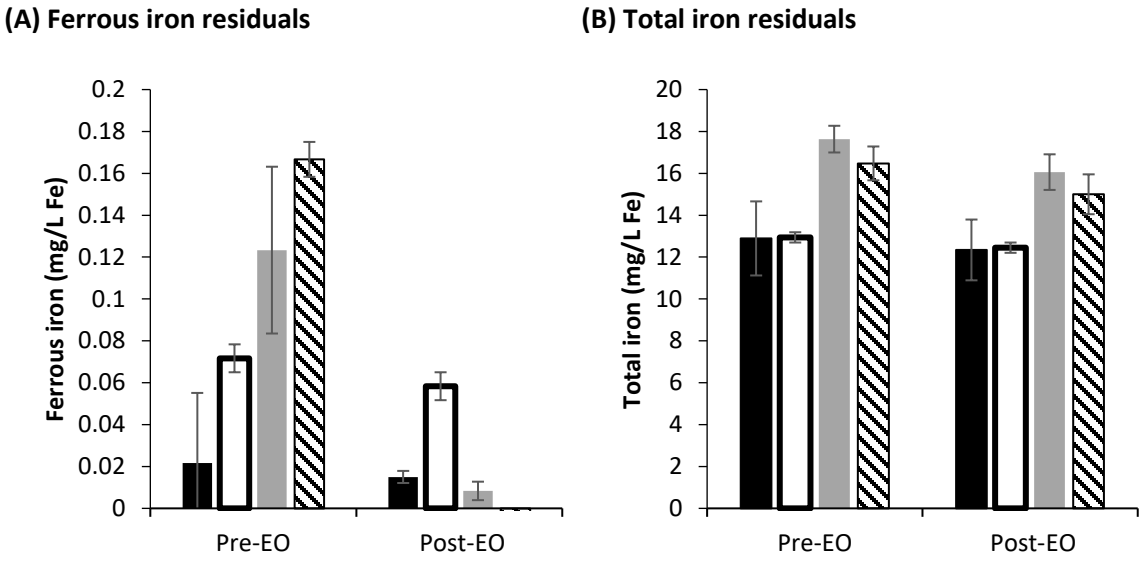

Figure D-7. Total (A) and ferrous (B) iron residuals before and after electrooxidation (EO). Note the different scales of the y-axes. Iron concentrations were measured after coarse filtration with Whatman 114 filters. Pre-EO ferrous iron residuals were in the inhibitory range for EO, as shown in Figure 5-4. While total iron residuals remained high (~12 – 16 mg/L Fe) after final filtration (post-EO), post-EO ferrous iron concentrations were less than 0.02 mg/L Fe in all model waters except Mississippi River water. Natural organic matter binds ferrous iron and prevents oxidation to the ferric state. These results indicate that a post-treatment stage is required for decreasing iron residuals, and EO may increase the effectiveness of iron removal by oxidizing ferrous iron to less soluble ferric iron.

D.7 References

1. Milwaukee Water Works. *2016 Quality of Lake Michigan Source Water*.; 2017. http://city.milwaukee.gov/ImageLibrary/Groups/WaterWorks/files/LakeMichiganSourceWaterQuality2015.pdf.

2. USGS. NWIS Water Quality Samples (USGS 05288500). https://nwis.waterdata.usgs.gov/usa/nwis/qwdata/?site_no=05288500. Published 2006. Accessed July 1, 2018.

3. Waukesha Water Utility. *Waukesha Water Diversion Application, Appendix C: Future Water Supply Study*.; 2002. https://dnr.wi.gov/topic/EIA/documents/waukesha/Appendix_C.pdf.

4. Bonness D, Masarik K. *Investigating Intra-Annual Variability of Well Water Quality in Lincoln Township*.; 2014. http://www.cleanwisconsin.org/wp-content/uploads/2015/01/Ex1_Lincoln_FinalReport.pdf.

5. Dubrawski KL, Mohseni M. In-situ identification of iron electrocoagulation speciation and application for natural organic matter (NOM) removal. *Water Res*. 2013;47(14):5371-5380. doi:10.1016/j.watres.2013.06.021

6. Crittenden JC, Trussell RR, Hand DW, Howe KJ, Tchobanoglous G. *MWH's Water Treatment: Principles and Design*. 3rd ed. Hoboken, New Jersey: John Wiley & Sons, Inc.; 2012.

7. Howe KJ, Hand DW, Crittenden JC, Trussell RR, Tchobanoglous G. *Principles of Water Treatment*. 1st ed. Hoboken, New Jersey: John Wiley & Sons, Inc; 2012.

8. Stumm W, Lee FG. Oxygenation of ferrous iron. *Ind Eng Chem*. 1961;53(2):143-146. doi:10.1021/ie50614a030